Volume 10, No. 1
November, 1961

THE SOVIET JOURNAL OF

ATOMIC ENERGY

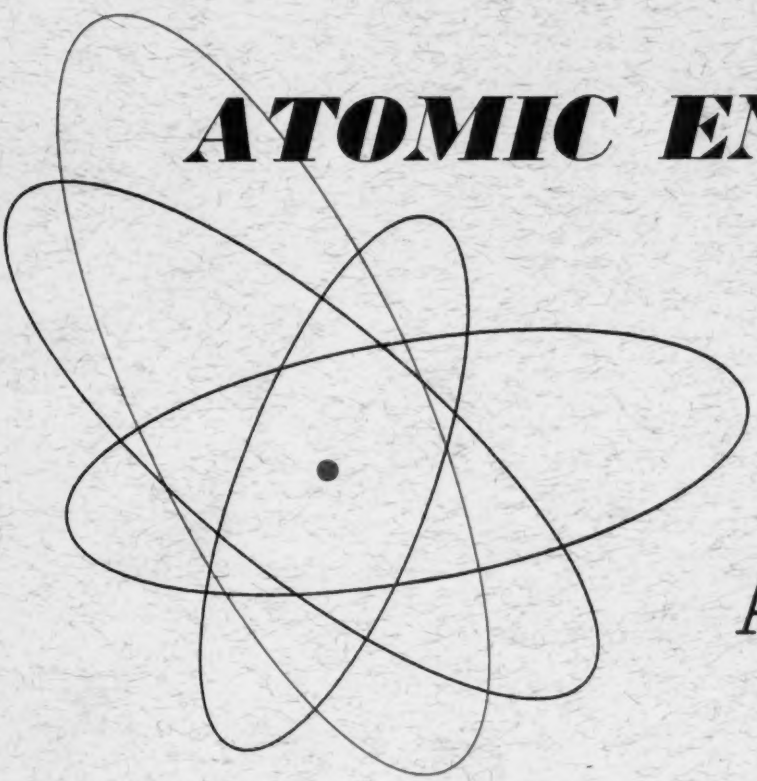

Атомная энергия

TRANSLATED FROM RUSSIAN

CONSULTANTS BUREAU

RESEARCH BY SOVIET EXPERTS

Translated by Western Scientists

RADIATION CHEMISTRY
PROCEEDINGS OF THE FIRST ALL-UNION CONFERENCE
MOSCOW 1957

More than 700 of the Soviet Union's outstanding research scientists participated in this conference sponsored by the Academy of Sciences and the Ministry of the Chemical Industry. Each of the 56 reports read in the various sessions covers either the theoretical or practical aspects of radiation chemistry, and special attention is given to radiation sources used in radiation-chemical investigations. The general discussions which followed each report and reflected various points of view on the problem under analysis are also included.

PRIMARY ACTS IN RADIATION CHEMICAL PROCESSES	$25.00
RADIATION CHEMISTRY OF AQUEOUS SOLUTIONS (Inorganic and Organic Systems)	$50.00
RADIATION ELECTROCHEMICAL PROCESSES	$15.00
THE EFFECT OF RADIATION ON MATERIALS INVOLVED IN BIOCHEMICAL PROCESSES	$12.00
RADIATION CHEMISTRY OF SIMPLE ORGANIC SYSTEMS	$30.00
THE EFFECT OF RADIATION ON POLYMERS	$25.00
RADIATION SOURCES	$10.00

Individual volumes may be purchased separately

Special price for the 7-volume set **$125.00**

Tables of contents upon request.

CONTEMPORARY EQUIPMENT
FOR WORK WITH RADIOACTIVE ISOTOPES

Of the 110 isotopes produced in the USSR during 1958, 92 were obtained by neutron irradiation. The methods and technological procedures used in the production of isotopes and the preparation of labeled compounds from them are reviewed in detail. Shielding and manipulative devices for work with radioactive isotopes are illustrated as well as described fully. These collected reports are of interest to all scientits and technologists concerned with radioactive isotopes.

Tables of contents upon request.

Durable paper covers **66 pp.** **illus.** **$15.00**

PRODUCTION OF ISOTOPES

The eighteen papers which comprise this volume were originally read at the All-Union Scientific and Technical Conference on the Application of Radioactive Isotopes, Moscow, 1957. The reports consider the problems and achievements of Soviet scientists in the production of radioactive isotopes by irradiation of targets in Soviet reactors and cyclotrons. Not only is this work of significance to producers of isotopes, but many of the papers will prove useful to isotope users as well.

Tables of contents upon request.

Durable paper covers **136 pp.** **illus.** **$50.00**

Payment in sterling may be made to Barclay's Bank in London, England.

CONSULTANTS BUREAU

227 West 17th Street • New York 11, N.Y. • U.S.A.

EDITORIAL BOARD OF
ATOMNAYA ÉNERGIYA
A. I. Alikhanov
A. A. Bochvar
N. A. Dollezhal'
D. V. Efremov
V. S. Emel'yanov
V. S. Fursov
V. F. Kalinin
A. K. Krasin
A. V. Lebedinskii
A. I. Leipunskii
I. I. Novikov
(Editor-in-Chief)
B. V. Semenov
V. I. Veksler
A. P. Vinogradov
N. A. Vlasov
(Assistant Editor)
A. P. Zefirov

THE SOVIET JOURNAL OF

ATOMIC ENERGY

A translation of ATOMNAYA ÉNERGIYA,
a publication of the Academy of Sciences of the USSR

(Russian original dated January, 1961)

Vol. 10, No. 1 November, 1961

CONTENTS

Annual subscription $75.00
Single issue 20.00
Single article 12.50

© 1961 Consultants Bureau Enterprises, Inc., 227 West 17th St., New York 11, N. Y.
Note: The sale of photostatic copies of any portion of this copyright translation is expressly prohibited by the copyright owners.

CONTENTS (continued)

Note. The Table of Contents lists all materials that appears in Atomnaya Énergiya. Those items that originated in the English language are not included in the translation and are shown enclosed in brackets. Whenever possible, the English-language source containing the omitted reports will be given. Consultants Bureau Enterprises, Inc.

ERRATA

VOL. 9, NO. 2

Page		Reads	Should Read
655	First equation	$C = C_0 1 + \left[\frac{E(o) + E(d)}{2E_0}\right]$	$C = C_0\left[1 + \frac{E(o) + E(d)}{2E_0}\right]$
620	Table 5, 1st column, 8th row	Charge in grams of elementary boron per 1 cm^2 of column cross section per 1 hr receiver	Charge in grams of elementary boron per 1 cm^2 of column cross section per 1 hr
	Table 5, 1st column, 10th row	Temperature in receiver of column, °C	Temperature at top of column, °C

TIME VARIATION OF SPATIAL AND ENERGY DISTRIBUTION OF NEUTRONS FROM A PULSED SOURCE

I. G. Dyad'kin and É. P. Batalina

Translated from Atomnaya Énergiya Vol. 10, No. 1,
pp. 5-12, January, 1961
Original article submitted February 29, 1960

The present paper is concerned with the time dependence of the spatial and energy distribution of neutrons from a pulsed source. Time-dependent problems of this type are encountered, for example, in geophysical methods of prospecting for oil.

It is shown that the time distribution of neutrons of a given energy can be described by the Poisson probability distribution in practically the entire time interval. A space-energy-time relation is derived from which it follows that the space-energy and energy-time distributions are independent in a certain range of distances and times. Outside this range there is a correlation between these relationships, and the correlation can be taken into account. An expression is obtained for the mean square slowing-down length as a function of time. All these relationships are given in the form of simple formulas having a clear physical interpretation.

Formulation of the problem

The time-dependent transport equation for the slowing-down of neutrons is of the form

$$\left(\frac{l}{v}\frac{\partial}{\partial t}+l\Omega\,\mathrm{grad}+1\right)G(1,\,0,\,t_1,\,t)-\int_0^u du'\int d^2\Omega' f(\Omega\Omega',\,u-u')G(1,\,\mathbf{r},\,\Omega' u',\,t_1,\,t)=$$

$$=\delta(\Omega-\Omega_1)\,\delta(\mathbf{r}-\mathbf{r}_1)\,\delta(u-u_1)\,\delta(t-t_1)\equiv\delta^6(1-0)\,\delta(t-t_1), \tag{1}$$

$$G(1,\,0,\,t_1<t)\equiv 0,$$

where l is the mean free path, Ω is the unit momentum vector; $u=\ln(\varepsilon_0/\varepsilon)=2\ln(v_0/v)$ is the logarithmic neutron energy (ε, v is the neutron energy and velocity, ε_0, v_0 are the initial values of the energy and velocity); 0 represents $\mathbf{r}$, Ω, u; $1\to\mathbf{r}_1$, Ω_1, u_1, etc.; and $G(1,\,0,\,t_1,\,t)\equiv G(\mathbf{r}_1,\,\Omega_1 u_1,\,\mathbf{r},\,\Omega,\,u,\,t_1,\,t)$ is the Green function for the neutron collision density. Furthermore,

$$f(\Omega\Omega',\,u-u')=\sum_M\frac{(M+1)^2}{8\pi M}\frac{l}{l_M}e^{-(u-u'}\times\delta\left(\Omega\Omega'-\frac{M+1}{2}e^{-\frac{u-u'}{2}}+\frac{M-1}{2}e^{\frac{u-u'}{2}}\right), \tag{2}$$

where l_M is the mean free path relative to nuclei of mass M. The operators in Eq. (1) act on $\mathbf{r}$, Ω, t only.

The scattering is assumed to be symmetric in the center of mass system and l is taken to be independent of energy.

An exact solution of Eq. (1) was given in [1] in the form of multiple integrals. In the present paper an approximate solution of Eq. (1) is derived, using the solution obtained in [2, 3] for the stationary case. Using the method described in [1] and [3], and regarding the term $(l/v)(\partial/\partial t)$ as a perturbation, we shall write the new integral equation equivalent to Eq. (1) in the form

$$G(1,\ 0,\ t_1,\ t) = G_{st}(1,\ 0)\,\delta(t_1 - t) - \int d^6 2\, G_{st}\ (2,\ 0)\,\frac{l}{v_2}\,\frac{\partial}{\partial t}\,G(1,\ 2,\ t_1,\ t),$$

where $G_{st}(1, 0)$ is the solution of the stationary equation.

It was shown in [1] that

$$G_{st}(1,\ 0) = \sum_{a,\ b=0}^{\infty} \frac{(2a+1)(2b+1)}{l^3\, 4\pi\, (2\pi)^3} \int d^3\mathbf{k} e^{i\mathbf{k}(\mathbf{r}-\mathbf{r}_1)} \times \Phi_{ab}(k,\ u-u_1)\, P_a(\mathbf{k}_0\Omega)\, P_b(\mathbf{k}_0\Omega_1); \tag{3}$$

$$\Phi_{ab}(k,\ u < u_1) \equiv 0, \tag{4}$$

where $\mathbf{k}_0 = \mathbf{k}/k$, $\Phi_{ab}(k, u)$ are the elements of the matrix fully discussed in [2, 3], and $\mathbf{r}$ and $\mathbf{r}_1$ are in units of l.

On expanding Eq. (2) into a Fourier integral in $(\mathbf{r}\text{-}\mathbf{r}_1)$ and a double Legendre series in $P_a(\mathbf{k}_0\Omega)$ and $P_b(\mathbf{k}_0\Omega_1)$, and carrying out the Laplace transformation $\int_0^{\infty} e^{-\sigma(t-t_1)} d(t-t_1)$, we obtain the following matrix integral equation which is fully equivalent to Eq. (1).

$$\overline{G}(k,\ \sigma,\ u_1,\ u) = \Phi(k,\ u-u_1) - \int_{u_1}^{u} du_2 \frac{\sigma l}{v_2} \times \Phi(k,\ u-u_2)\, C\overline{G}(k,\ \sigma,\ u_1,\ u_2), \tag{5}$$

where

$$G(1,\ 0,\ t_1,\ t) = \sum_{a,\ b=0}^{\infty} \frac{(2a+1)(2b+1)}{l^3\, 4\pi\, (2\pi)^3} \int d^3\mathbf{k} \times \frac{1}{2\pi i} \int_{c-i\infty}^{c+i\infty} d\sigma \exp\left[i\mathbf{k}(\mathbf{r}-\mathbf{r}_1) + \sigma(t-t_1)\right] \times \tag{6}$$

$$\times \left[\overline{G}(k,\ \sigma,\ u_1,\ u)\right]_{ab} P_a(\mathbf{k}_0\Omega)\, P_b(\mathbf{k}_0\Omega_1);$$

and C is a matrix with the following elements:

$$(C)_{ab} = (2a+1)\,\delta_{ab}. \tag{7}$$

Let us now replace the exact matrix Φ by the approximate expression [3]

$$\Phi(k,\ u-u_1) = \exp\left[(u-u_1)\,\beta\,(\alpha - \sqrt{k^2+\alpha^2})\right] \times T(k) + T_0(k)\,\delta(u-u_1), \tag{8}$$

where the matrices T and T_0 have the elements

$$(T_0)_{ab} = (T_0)_{ba} = \frac{i}{k} P_a\left(\frac{i}{k}\right) Q_b\left(\frac{i}{k}\right);\ b \geqslant a, \tag{9}$$

and

$$(T)_{ab} \simeq \frac{(-ik)^{a+b}\,\alpha\gamma_{ab}}{\sqrt{k^2+\alpha^2}}. \tag{10}$$

The first element with the Legendre polynomial can be put equal to zero for convenience.

Equation (8) holds both for $u = u_1$ and for $u - u_1 > \xi$, i.e., in the whole range of values of u except for a small region near u_1. Moreover, it was shown in [3] that α is practically independent of u, a and b.

Substituting Eqs. (9) and (10) into Eq. (8) we have

$$\left[E+\frac{\sigma l}{v}T_0(k)C\right]\bar{G}(k,\sigma,u_1,u)=T(k)+T_0(k)\delta(u-u_1)- \tag{11}$$

$$-\int_{u_1}^{u}\frac{\sigma l}{v_2}\exp\left[(u-u_2)\beta\left(\alpha-\sqrt{k^2+\alpha^2}\right)\right]\times T(k)C\bar{G}(k,\sigma,u_1,u_2)\,du_2.$$

This equation is the final integral-matrix equation which we have to solve.

Thus, the problem is reduced to the solution of Eq. (11), which is equivalent to Eq. (1) for $\underline{u}$ not too close to u_1. The solution will therefore be distorted only for the first few collisions.

Solution of the time-dependent transport equation

Equation (11) can be solved by the method of successive integration:

$$\bar{G}(\mathbf{k},\sigma,u-u_1)=\exp\left[(u-u_1)\beta\left(\alpha-\sqrt{k^2+\alpha^2}\right)\right]\left[E+\frac{\sigma l}{v}T_0(k)C\right]^{-1}\times$$
$$\times\exp\left[-2T(k)T_0^{-1}(k)\ln\frac{E+\sigma l v^{-1}T_0(k)C}{E+\sigma l v_1^{-1}T_0(k)C}\right]T(k)\left[E+\frac{\sigma l}{v_1}CT_0(k)\right]^{-1}+ \tag{12}$$
$$+\left[E+\frac{\sigma l}{v}T_0(k)C\right]^{-1}T_0(k)\delta(u-u_1),$$

where E is the unit matrix. This solution is not formal. It can be computed by taking logarithms and multiplying the obtained matrix from the left by $2TT_0^{-1}$.

By taking the rank of the matrices successively as 1, 2, etc., one can use the Lagrange-Sylvester formula to express Eq. (12) in terms of functions of numbers rather than matrices.

The limitation of matrix T to unit rank does not mean the limitation of the scattering function $f(\Omega\Omega', u-u')$ to the first term in the expansion in the Legendre polynomials. It was shown in [2] that the first element of the matrix includes contributions due to all the coefficients of this expansion. There exist other, simpler methods of evaluating Eq. (12), and these will be analyzed below. They are based on the use of certain specific properties of the matrices T(k) and $T_0(k)$.

Neutron energy distribution

If one integrates Eq. (6) over all the configuation space and velocity directions, all the sums and integrals will vanish and only the function (12) with k = 0 will remain.

Using the results of [1-3] it is easy to verify that the matrix T becomes diagonal with the first element equal to ξ^{-1} where ξ is the average logarithmic energy loss, and the matrix T_0C becomes a unit matrix. They can therefore be regarded as numbers and Eq. (12) will assume the form

$$\bar{G}(k=0,\sigma,u_1,u)=\frac{1}{\xi}\frac{\left(1+\frac{\sigma l}{v_1}\right)^{\frac{2}{\xi}-1}}{\left(1+\frac{\sigma l}{v}\right)^{\frac{2}{\xi}+1}}+\frac{\delta(u-u_1)}{1+\frac{\sigma l}{v}}. \tag{13}$$

Assuming $u_1 = 0$, $t_1 = 0$, $v_1 = v_0$, and transforming Eq. (13) with the aid of the formulas given in [4], we find that the neutron energy distribution is

$$N_0(u,t)=\frac{v_0^2}{\xi(v-v_0)v}\left(\frac{v}{v_0}\right)^{\frac{2}{\xi}+1}e^{-\frac{(v+v_0)t}{2l}}\times M_{\frac{2}{\xi};\frac{1}{2}}\left(\frac{(v-v_0)t}{l}\right)=\frac{v_0^2t}{\xi lv}\left(\frac{v}{v_0}\right)^{\frac{2}{\xi}+1}$$
$$\times\,{}_1F_1\left(1-\frac{2}{\xi};\,2;\,\frac{v-v_0}{l}t\right)\exp\left(-\frac{vt}{l}\right), \tag{14}$$

where $M_{ab}(x)$ is the Whittaker function and ${}_1F_1(\mu, \nu, x)$ is the degenerate hypergeometric series.

When $t > l/(v_0-v)$, i.e., for large t, it is necessary for the first few collisions (for neutrons with initial energy of 1 Mev, $t > \sim 10^{-9}$ sec) to use the asymptotic expression for ${}_1F_1$ (cf., for example [5]):

$$ {}_1F_1(-\alpha,\beta,-z)\simeq\frac{\Gamma(\beta)z^{\alpha}}{\Gamma(\beta+\alpha)}\left(1+\frac{1}{z}+\dots\right);$$
$$z>0,\quad \alpha>0. \tag{15}$$

We then obtain the following formula:

$$N_0(u,t)=\frac{\left(1-\frac{v}{v_0}\right)^{\frac{2}{\xi}-1}}{\xi}\frac{\left(\frac{vt}{l}\right)^{\frac{2}{\xi}}e^{-\frac{vt}{l}}}{\Gamma\left(1+\frac{2}{\xi}\right)}. \tag{16}$$

We have thus reached a surprising result, namely, if one ignores time intervals which are small compared with $t = l/v_0$, then the time distribution is exactly the same as the well-known Poisson probability distribution for the appearance of $2/\xi$ neutrons during a time t, subject to the condition that the probability of appearance of neutrons is the same for all instants of time and is equal to $(v/l)dt$. The time distribution is quite independent of the initial energy [to within the time independent factor $\left(1-\frac{v}{v_0}\right)^{\frac{2}{\xi}-1}$] and is entirely determined by the neutron parameters of the medium.

Marshak was very close to this result in [6]. He guessed the existence of the formula $\exp(-b/x-x)x^{(M+1)^2/4M}$ for large $x = vt/l \gg 1$. However, since he did not succeed in obtaining a formula of the form of Eq. (14), he also did not obtain the simpler formula given by Eq. (16), which is already correct for $v_0t/l > 1$, i.e., for $vt/l > v/v_0$. The latter is a very much less stringent limitation.

Kazarnovskii [7] has obtained a numerical solution of the differential equation for the neutron density for large M. Numerical calculations based on our formula are in good agreement with his data. He also missed the relation given by Eq. (16) which has a clear probabilistic interpretation.

Integrating Eq. (16) with respect to t between 0 and ∞ (which is equivalent to integration with respect to t, between $-\infty$ and t) we obtain the stationary neutron energy distribution

$$\int_0^{\infty}N_0(u,t)\,dt=\left(1-\frac{v}{v_0}\right)^{\frac{2}{\xi}-1}\frac{l}{v\xi}\simeq\frac{l}{v\xi}. \tag{17}$$

Character of time changes in the spatial and energy distribution; mean square slowing-down length

Equation (12) can be used to determine the space-energy distribution of neutrons. The properties of the matrices T and T_0 which enter into this formula have been described in detail in [1-3]. The matrix T_0C is not very different from the unit matrix $q_0(k)E$ for any k. The only large element in the matrix T is the element in the top left corner. We can therefore write these matrices down in the form of a main matrix and a small addition. Thus, for example, second-rank matrices can be written down in the following form:

$$T_0(k)\,C = q_0(k)\,E + \begin{vmatrix} 0 & -3ikq_1(k) \\ -ikq_1(k) & -4k^2q_2(k) \end{vmatrix} \simeq q_0(k)\,E - ikq_1 \begin{vmatrix} 0 & 3 \\ 1 & 0 \end{vmatrix};$$

$$T(k) = \frac{\alpha}{\sqrt{k^2+\alpha^2}} \begin{vmatrix} \gamma_{00}; & -ik\gamma_{01} \\ -ik\gamma_{01}; & -k^2\gamma_{11} \end{vmatrix} \simeq \frac{\alpha\gamma_{00}}{\sqrt{k^2+\alpha^2}} \begin{vmatrix} 1 & 0 \\ 0 & 0 \end{vmatrix} + \frac{-\alpha ik\gamma_{01}}{\sqrt{k^2+\alpha^2}} \begin{vmatrix} 0 & 1 \\ 1 & 0 \end{vmatrix}; \tag{18}$$

$$T_0(k)^{-1} = \begin{vmatrix} 1 & ik \\ ik & 3 \end{vmatrix} = C + ik \begin{vmatrix} 0 & 1 \\ 1 & 0 \end{vmatrix},$$

where

$$q_0(k) = \frac{\operatorname{arctg} k}{k};\quad q_1(k) = \frac{1}{k^2}\,[1 - q_0(k)];\quad q_2(k) = \frac{1}{4k^2}\,[q_0(k) - 3q_1(k)];\quad q_0(0) = 1;\quad q_1(0) = \frac{1}{3};\quad q_2(0) = \frac{1}{15}.$$

If we now substitute these expressions into the matrix functions and expand them into the corresponding series (bearing in mind the noncommutative property), we shall obtain in the zero-order and first approximations

$$\overline{G}(k, \sigma, u_1, u) = \frac{\alpha\gamma_{00}\exp[(u-u_1)\,\beta\,(\alpha - \sqrt{k^2+\alpha^2})]}{\sqrt{k^2+\alpha^2}} \times$$

$$\times \left\{ \begin{vmatrix} 1 & 0 \\ 0 & 0 \end{vmatrix} + ik \begin{vmatrix} 0 & \dfrac{\sigma l v_1^{-1}}{1+\sigma l v_1^{-1} q_0(k)} + \dfrac{\alpha(\gamma_{00}-3\gamma_{01})}{\sqrt{k^2+\alpha^2}} \\ \dfrac{\sigma l v^{-1}}{1+\sigma l v_1^{-1} q_0(k)} + \dfrac{\gamma_{01}\alpha}{\sqrt{k^2+\alpha^2}} & 0 \end{vmatrix} \right\} \times \tag{19}$$

$$\times \frac{\left[1+\dfrac{\sigma l}{v_1}\,q_0(k)\right]^{\frac{2\alpha\gamma_{00}}{\sqrt{k^2+\alpha^2}}-1}}{\left[1+\dfrac{\sigma l}{v}\,q_0(k)\right]^{\frac{2\alpha\gamma_{00}}{\sqrt{k^2+\alpha^2}}+1}}.$$

Inverting the integrals as in the preceding section we obtain the zero-order Green function harmonic

$$\frac{l}{v}\,G(\mathbf{r}_1, u_1, r, u, t_1, t) = \frac{v_1^2(t-t_1)\,\alpha}{\xi 2\pi^2 l^4 v} \int_0^\infty k\,dk\,\frac{\sin k\,|\mathbf{r}-\mathbf{r}_1|}{|\mathbf{r}-\mathbf{r}_1|}\,\frac{\exp[(u-u_1)\,\beta\,(\alpha-\sqrt{k^2+\alpha^2})]}{q_0^2(k)\sqrt{k^2+\alpha^2}} \tag{20}$$

$$\times \left(\frac{v}{v_1}\right)^{\frac{2\alpha}{\xi\sqrt{k^2+\alpha^2}}+1} {}_1F_1\left[1 - \frac{2\alpha}{\xi\sqrt{k^2+\alpha^2}};\ 2;\ \frac{(v-v_1)(t-t_1)}{lq_0(k)}\right].$$

For larger instants of time one can again use the asymptotic expansion for ${}_1F_1$ and Eq. (19) can be integrated numerically. However, in order to obtain a clearer insight into the basic regularities, and to investigate the existence of correlation between the space and time distributions (if any), we shall compute it approximately for $t > l/(v_0 - v)$ and $v \ll v_0$.

We shall take into account the zero-order harmonic only, since the angular distribution has been discussed in detail in [3].

Assuming $t_1 = 0$, $r_1 = 0$, $v_1 = v_0 (u_1 = 0)$; $t > l/v_0 (\approx 10^{-9}$ sec) we find that

$$N(\mathbf{r}, u, t) = \frac{\alpha}{2\pi^2 l^3 \xi} \int_0^\infty k\,dk\,\frac{\sin kr}{r}\,\frac{\exp\left[\beta u\,(\alpha - \sqrt{k^2+\alpha^2}) - \dfrac{vt}{lq_0(k)}\right]}{q_0(k)\sqrt{k^2+\alpha^2}\,\Gamma\left(1+\dfrac{2\alpha}{\xi\sqrt{k^2+\alpha^2}}\right)}\left(\frac{vt}{lq_0(k)}\right)^{\frac{2\alpha}{\xi\sqrt{k^2+\alpha^2}}} \tag{21}$$

The time-dependent factor reaches a maximum when $t \approx 2lq_0(k)/\xi v$ and then falls off exponentially. Therefore, for all values of t for which the integrand is practically different from zero we have

$$\beta u\,(\alpha - \sqrt{k^2+\alpha^2}) \gg \frac{vt}{lq_0(k)}, \quad k > \alpha\,(\approx 0.5).$$

Conversely, for very small k the time-dependent factor varies more rapidly than the energy term. We shall use this in the following way. We shall replace the Γ-function by the Stirling formula and rewrite the argument of the exponential in the form

$$\alpha\beta u\left(1-\sqrt{1+\frac{k^2}{\alpha^2}}\right) - \ln q_0(k) + \frac{2\alpha}{\xi\sqrt{k^2+\alpha^2}} \times$$
$$\times \ln\frac{vt}{lq_0(k)} - \frac{vt}{lq_0(k)} + \frac{2\alpha}{\xi\sqrt{k^2+\alpha^2}} - \left(\frac{1}{2}+\frac{2\alpha}{\sqrt{k^2+\alpha^2}}\right)\ln\frac{2\alpha}{\xi\sqrt{k^2+\alpha^2}}. \tag{22}$$

Let us rewrite this in the form

$$B - A\sqrt{k^2+\alpha^2}, \tag{23}$$

where

$$B = \alpha\beta u + \frac{4}{\xi}\ln\frac{vt\xi}{2l} + \frac{2}{\xi} - \frac{vt}{l} - \frac{1}{2}\ln\frac{2}{\xi} - \frac{2\alpha^2}{3}\left(1-\frac{vt}{l}+\frac{2}{\xi}\right) - \frac{1}{2};$$
$$A = \beta u + \frac{2}{\alpha\xi}\left(\ln\frac{vt\xi}{2l} - \frac{2\alpha^2}{3}\right) + \frac{2\alpha}{3}\left(\frac{vt}{l}-1\right) - \frac{1}{2\alpha}.$$

For small and intermediate k Eq. (23) is identical with Eq. (22), while when $k \to \infty$ it slowly accumulates a relative error of a few percent but not exceeding

$$\frac{\left(\frac{2\alpha}{3}-\frac{2}{\pi}\right)\frac{vt}{l} + \frac{2}{\alpha\xi}\left(\ln\frac{vt\xi}{2l}+\frac{2\alpha^2}{3}\right)}{\beta u + \frac{2}{\pi}\frac{vt}{l}}$$

when $N_0(u,t) \neq 0$.

Let us now integrate Eq. (18) with the aid of the well-known expression (cf., [8])

$$\int_0^\infty J_p(\beta x)\frac{K_q(\alpha\sqrt{x^2+z^2})}{(\sqrt{x^2+z^2})^q}x^{p+1}\,dx = \frac{\beta^p}{\alpha^q}\left(\frac{\sqrt{\alpha^2+\beta^2}}{z}\right)^{q-p-1}K_{q-p-1}(z\sqrt{\alpha^2+\beta^2}).$$

The final result is

$$N(\mathbf{r}, u, t) = \frac{\alpha^2 e^B K_1(\alpha\sqrt{A^2+r^2})}{2\pi^2 l^2\xi\sqrt{2\pi}\sqrt{A^2+r^2}}. \tag{24}$$

Since $\sqrt{r^2+A^2} \simeq \sqrt{r^2+\beta^2u^2+2\beta u\Delta(t)}$; $\frac{\Delta}{\beta u} \ll 1$ for all t for which N(r, u, t) is practically different from zero, this root can be expanded into a series and second-order terms can be neglected. Next, using the asymptotic expansion for the Bessel function we obtain the space-energy distribution of neutrons from a pulsed source:

$$N(\mathbf{r}, u, t) = \frac{\xi v}{l} N_{st}(\mathbf{r}, u) N_0(u, t)[1 + \varepsilon(r, u, t)], \tag{25}$$

where $N_0(u, t)$ is given by Eq. (16) and

$$N_{st}(r, u) \simeq \frac{\alpha^{3/2}\exp(\alpha\beta u - \alpha\sqrt{r^2l^{-2}+\beta^2u^2})}{\xi 2\pi\sqrt{2\pi}\,l^2 v} \tag{26}$$

is the stationary distribution discussed in detail in [3]. The values of coefficients α and β are also given in [3] for multicomponent media. The function $[1 + \varepsilon(r, u, t)]$ is not very different from unity for times of the order of the effective pulse width $\left(\approx t_{\max} \pm \frac{2l\sqrt{\pi}}{v\sqrt{\xi}} \right)$ and distances $r < \beta u l$ (which roughly corresponds to the applicability of the age approximation):

$$1 + \varepsilon(r, u, t) = F^{1 - \frac{\beta u}{\sqrt{r^2 + \beta^2 u^2}}} \left[1 + \frac{\beta u \ln F}{\alpha (r^2 + \beta^2 u^2)} \right]^{-\frac{3}{2}};$$

$$F = F(t) = \left(\frac{vt\xi}{2l} \right)^{\frac{2}{\xi}} \exp \left[\frac{2\alpha^2}{3} \left(\frac{vt}{l} - 1 - \frac{2}{\xi} \right) - \frac{1}{2} \right]. \tag{27}$$

Integrating Eq. (24) with the weight of r^2, and using the formulas given in [8], we find the following expression for the mean square of the slowing-down length

$$\frac{\overline{r^2}}{6} = \frac{\overline{r_{st}^2}}{6} + \frac{1}{3} \left(\frac{vt}{l} + \frac{3}{\xi\alpha^2} \ln \frac{vt\xi}{2l} - \frac{2}{\xi} - 1 - \frac{3}{4\alpha^2} \right), \tag{28}$$

where $\frac{\overline{r_{st}^2}}{6}$ is the slowing-down length for the stationary distribution and the second term represents a typical diffusion correction. When $u \gg 1$, $\overline{r^2}$ is not very different from $\overline{r_{st}^2}$ for all t for which $N_0(u, t)$ differs from zero; $\overline{r^2}/6$ increases monotonically with increasing t.

The following important conclusions may be drawn from Eqs. (25), (26), and (28):

1. The space-energy distribution of neutrons up to distances of the order of $\beta u l$ is found to take the form of the product of the space (stationary) distribution and the energy-time distribution. In other words, the slowing-down of a neutron to a velocity v over a distance r from the source, and the time necessary for the slowing-down to the velocity v, are independent events and their probabilities can be multiplied.

2. The mean square of the slowing-down length given by Eq. (28) is equal to the sum of the mean square of this quantity in the stationary case plus a diffusion type time-dependent addition which is proportional to t. The latter is small compared with $\overline{r_{st}^2}$ when $v \ll v_0$ for all instants of time for which the time distribution is different from zero. The presence of this additional term gives rise to a monotonic increase in the mean square slowing-down length with increasing t.

3. Thus, the physical interpretation of the slowing-down process is as follows: At the end of a certain time interval (which is characteristic of the given medium) after the emission of fast neutrons, neutrons of a given energy appear simultaneously in all space except for $r \gg \beta u l$.

Their numbers reach a maximum at

$$t_{\max} \simeq \frac{2l}{v\xi} \left(2 - \frac{\beta u}{\sqrt{r^2 + \beta^2 u^2}} \right) \left[1 - \frac{2\alpha}{3} \left(1 - \frac{\beta u}{\sqrt{r^2 + \beta^2 u^2}} \right) \right]^{-1},$$

which is slightly dependent on r and then falls to zero.

The height of the maximum is roughly equal to $\frac{v\sqrt{\xi}}{2l\sqrt{\pi}} N_{st}(r, u)$, and the area under the curve is equal to the stationary neutron density. Thus the effective width of the "pulse" of neutrons with velocity v is

$$\Delta t_{\text{eff}} \simeq \frac{2l\sqrt{\pi}}{v\sqrt{\xi}}.$$

The complete space, energy, angular, and time distribution of neutrons from a source of unit strength, located at an arbitrary point r_1 and emitting neutrons having a logarithmic energy u_1 in the time interval between t_1 and $t_1 + dt_1$, is given by Eqs. (6), (12), (19), and (20). These formulas are required in the development of the perturbation theory.

Solution of a specific problem with a variable mean free path

Equations (16), (25), (26), and (28) are so simple that they do not require a graphical interpretation. Their clear physical interpretation enables one to predict space-energy neutron density for media with variable mean free path.

In fact, if the total density is represented as a product of the stationary space density and a time factor, then in the case of a variable path it is necessary to take the stationary density for the variable l as discussed in [3]. The value of l corresponding to the velocity v, i.e., $l(u)$, should be substituted into the time factor since for $v \ll v_0$ the latter is quite independent of v_0 and therefore completely "forgets" the initial energy and the first collisions. This will also apply to the first approximation.

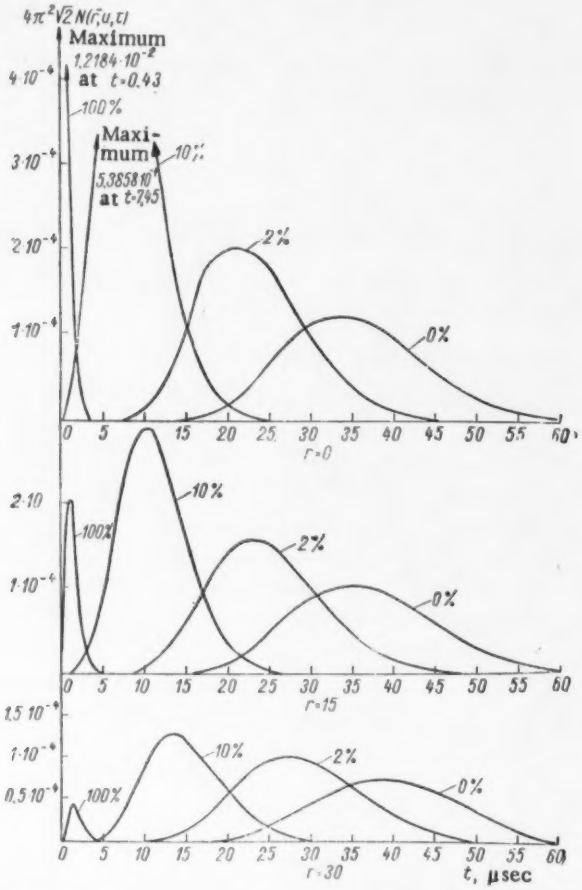

Fig. 1. Distribution of neutrons in space and time for neutron energy of 1.5 ev in sand with various water concentrations.

This approximation can be further improved with the aid of the formalism of integral equations for Green functions.

Nonstationary neutron prospecting is beginning to be widely used in nuclear geophysics both in the USSR and the USA [9]. The stratum under investigation is irradiated with neutrons from a pulsed neutron source for a short interval of time and the neutron density in the stratum is measured after a further short interval of time. The density is very dependent on the amount of hydrogen in the stratum. Figure 1 shows computed curves representing the variation in the neutron density in wet sand (SiO_2 + m%H_2O) at various distances from the pulsed neutron source. It is clear from this figure that for each porosity there is a characteristic time interval during which neutrons of given energy are

present. The dependence of t_{max}, i.e., the time to the appearance of the maximum, on the effective neutron pulse width for the energy corresponding to the indium resonance (1.5 ev, $v_{ind} \simeq 12$ cm/sec) is shown in Fig. 2 for r = 0.

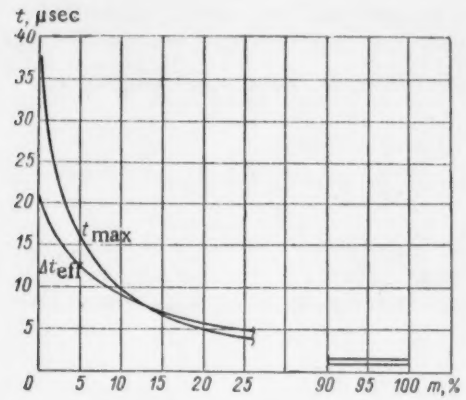

Fig. 2. Dependence of neutron pulse parameters on water concentration in sand.

For neutrons having different energies the values of t_{max} and t_{eff} given in Fig. 2 should be multiplied by v_{ind}/v. The beginning of the pulse (the instant at which the neutron density reaches e^{-4} of the maximum value) corresponds to the point $t \approx t_{max} e^{-2\xi-1}$.

These curves can be used in the design of the corresponding apparatus in the choice of the distance between source and detector, and in the interpretation of experimental results.

LITERATURE CITED

1. I. G. Dyad'kin, Zh. eksperim. i teor. fiz., 34, 1504 (1958).
2. I. G. Dyad'kin, Solution of Vik's problem and the corresponding partial probabilities [in Russian]; Paper in the Collection "Neutron Physics", Gosatomizdat, Moscow, 1961 [at press].
3. I. G. Dyad'kin, Space-energy-angular distribution of Neutrons in Multicomponent Infinite Media [in Russian], loc. cit..
4. V. A. Ditkin and P. I. Kuznetsov, Handbook on Operational Calculations [in Russian], Gostekhteorizdat (Moscow-Leningrad, 1951) p. 137.
5. L. Landau and E. Lifshits, Quantum Mechanics, Part 1, Gostekhteorizdat (Moscow-Leningrad, 1948) p. 560.
6. R. Marshak, Rev. Mod. Phys., 19, 185 (1947).
7. M. V. Kazarnovskii, Atomnaya Energiya 4, No. 6, 539 (1958).
8. I. M. Ryzhik and I. S. Gradshtein, Tables of Integrals, Sums, Series and Products, 3rd Edition, Gostekhteorizdat (Moscow-Leningrad, 1951) p. 262.
9. B. G. Erozolimskii and A. S. Shkol'nikov, Nuclear Geophysics, A Collection of Papers edited by F. A. Alekseev [in Russian], Gostoptekhizeat (1959) p. 337.

FRAGMENT YIELD IN THE FISSION OF U^{233} AND Pu^{239} BY FAST NEUTRONS

E. K. Bonyushkan, Yu. S. Zamyatnin, V. V. Spektor,

V. V. Rachev, V. R. Negina, and V. N. Zamyatnina

Translated from Atomnaya Énergiya Vol. 10, No. 1,
pp. 13-18, January, 1961
Original article submitted April 16, 1960

A radiochemical method has been used to determine the absolute yields for a number of fragments in the fission of U^{233} and Pu^{239} by 14.5 Mev neutrons and fission-spectrum neutrons. Some regularities in changes in the fragment mass distribution are discussed. The dependence of the difference Δm between the average masses of the heavy and light fragments on the mass number A of the dividing nucleus is considered.

The present work is a continuation of [1] which was concerned with the determination of the fragment yield in the fission of heavy nuclei by fast neutrons. It was carried out in order to augment existing data on the fragment yield in the fission of U^{233} and Pu^{239}.

Most of the information on the fragment yield in the fission of U^{233} and Pu^{239} refers to the fission of these isotopes by thermal neutrons [2]. There is practically no information on the fragment yield in the fission of U^{233} by fast neutrons, while data on the yield of some of the fragments in the fission of Pu^{239} are available in a limited number of papers [2-4].

The relatively limited amount of data available for U^{233} and Pu^{239} is due to their high (as compared with U^{235} and U^{238}) specific α-activity and the resulting difficulties in chemical treatment. In view of this, and in distinction to [1], in the present work we have used small specimens of fissile isotopes, and as large fast-neutron fluxes as possible.

Measurements and results

We have measured the yields of a number of fragments (Sr^{89}, Mo^{99}, Ru^{103}, Ru^{106}, Ag^{111}, Cd^{115}, Te^{129m}, Te^{132}, Cs^{136}, Cs^{137}, Ba^{140}, Ce^{141}) in the fission of U^{233} and Pu^{239} by fission-spectrum neutrons and 14.5 Mev neutrons. The experimental part consisted in neutron irradiation of U^{233} and Pu^{239} specimens, separation and radiochemical purification of the required fission fragments, and the measurement of their β-activity.

The U^{233} specimens (in the form of U_3O_8) and the Pu^{239} specimens (in the form of metal foils) had a weight of 120-150 mg and were placed in hermetically sealed brass cassettes ~ 10 mm in diameter.

The fission-spectrum neutrons were obtained from a U^{235} breeding system without a moderator. The cassettes were placed inside the system. The 14.5 Mev neutrons were obtained from the target of an accelerating tube, which was saturated with tritium and bombarded by ~ 150 kev deuterons. The uranium and plutonium specimens were placed in the immediate neighborhood of the target. The irradiation time both in the breeding system and in the accelerating tube was 7-10 hours, and the total number of neutrons entering a specimen during this time was $\sim 5 \cdot 10^{14}$.

The absolute number of U^{233} fissile events occurring in the specimen during its irradiation by fission-spectrum neutrons was determined with the aid of a small ionization fission chamber with a suspended layer of U^{233} placed in the position of the specimen. In this way it was possible to obtain simultaneously the absolute yields of all the fragments under investigation.

In the case of the specimens irradiated with 14.5 Mev neutrons, the absolute fragment yields of U^{233} were obtained by determining the absolute yields of Ba^{140} and Ce^{141} and the relative yields of the remaining fragments (relative to Ba^{140} and Ce^{141}). The specimens used in the absolute measurements were placed at a constant distance from the target (48.5 mm) during the irradiation, and the number of fissile events in the specimens was determined from the known neutron flux, measured with the aid of an α-particle counter.

Fragment Yields in the Fission of U^{233} and Pu^{239}

Fragments	U^{233}		Pu^{239}	
	Fission-spectrum neutrons	14.5 Mev neutrons	Fission-spectrum neutrons	14.5 Mev neutrons
Sr^{89}	6,30±0.60	—	—	—
Mo^{99}	4.75±0.35	3.5±0.3	5.9±0.6	4.16±0.40
Ru^{103}	0.413±0.045	2.31±0.30	6.0±0.7	6.25±0.80
Ru^{106}	0.16±0.02	1.52±0.20	4.8±0.6	4.16±0.5
Ag^{111}	0.0837±0.008	1.22±0.12	0.55±0.06	1.46±0.14
Cd^{115}	0.052±0.006	0.98±0.18	0.09±0.01	1.23±0.10
115 tot	0.056±0.006	1.05±0.20	0.095±0.010	1.30±0.11
Te^{129m}	0.602±0.050	—	0,45±0.09	—
129 tot	1.57	—	1.17	—
Te^{132}	4.36±0.40	3.98±0.35	3.5±1.0	4.58±0.50
Cs^{136}	0.11	0.5	—	—
Cs^{137}	6.28±0.50	4.7±0.5	—	5.1±0.8
Ba^{140}	6.31±0.50	—	5.4±0.5	4.35±0.40
Ce^{141}	6.77±0.60	5.0±0.5	—	—

In the case of the fission of Pu^{239}, the absolute fragment yields were found by equating the total fragment yield as determined from their mass distribution curve to 200%. In the case of U^{233} this procedure served as an additional check on the values obtained for the absolute yields.

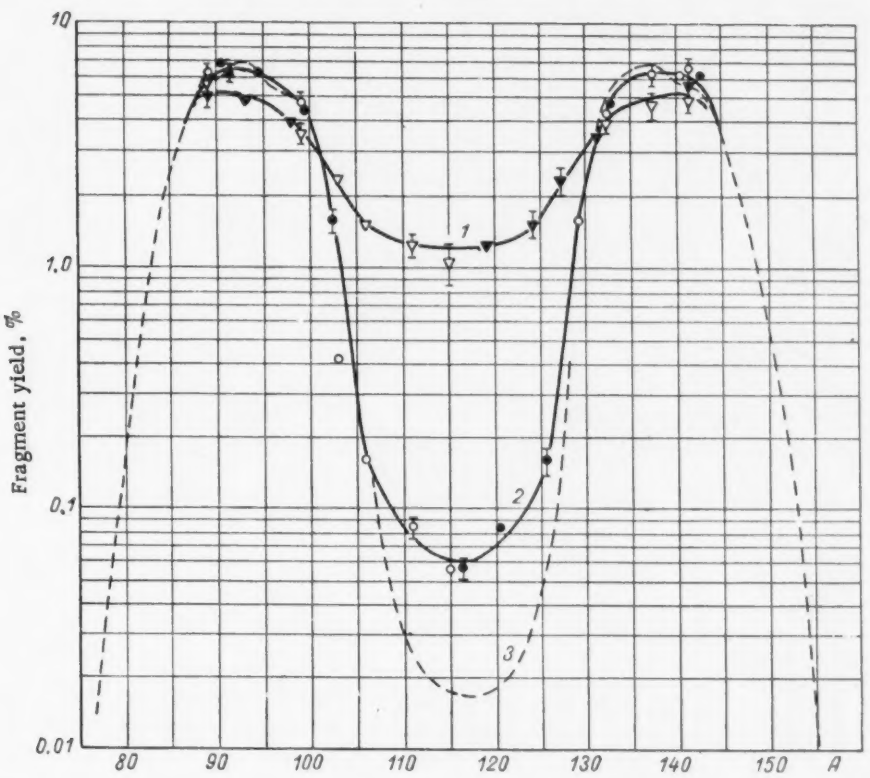

Fig. 1. Fragment-mass distribution in the fission of U^{233}. ▽, ○: experimental, ▼, ●: reflected points.

In order to separate the fragments from the irradiated U^{233} and Pu^{239}, use was made of the isotopic carrier method. All the fission fragments were separated from a single sample because of their relatively low activity. The separation of Pu^{239} from the carrier was carried out by the precipitation of its peroxide from 3N hydrochloric acid with a preliminary removal of silver chloride. The separation of U^{233} from the carriers was carried out by extraction from 6N hydrochloric acid, using a 15% solution of tributyl phosphate in benzene (also with preliminary removal of silver chloride). The separation and the radiochemical purification of the carriers was carried out with the aid of methods described in handbooks on analytical chemistry and radiochemistry [5-7]. For physical measurements, the specimens were taken in the form of $PbMoO_4$, RuO_2, AgCl, $Cd_2P_2O_7$, Te, Cs_2SO_4, $BaCrO_4$, CeO_2, and $SrSO_4$.

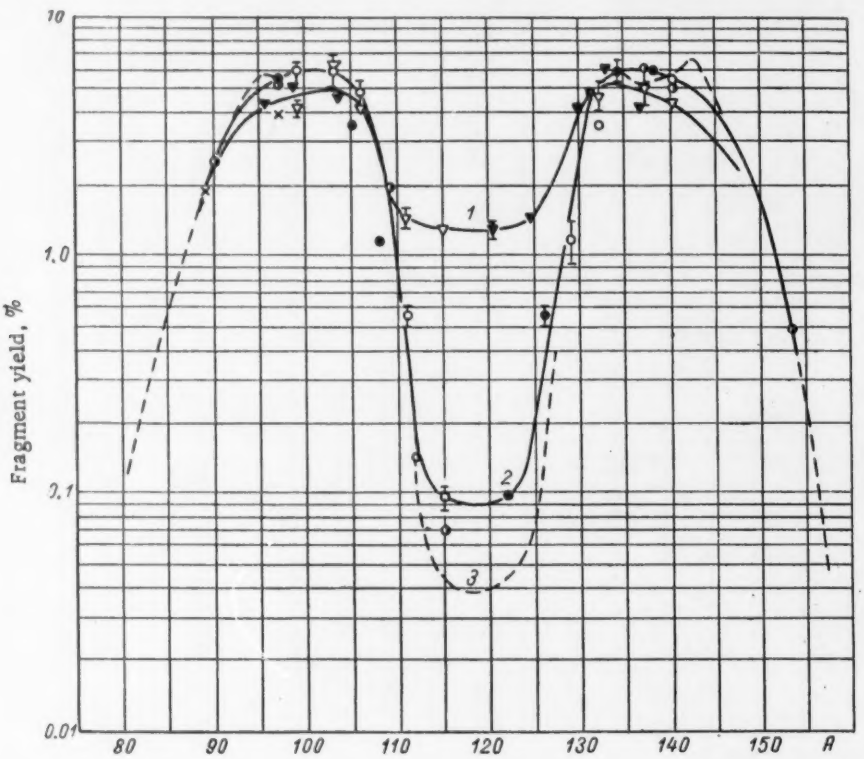

Fig. 2. Fragment-mass distribution in the fission of Pu^{239}. ▽, ○: experimental; ▼, ●: reflected points; ×: data from [3]; ◑: data from [2].

The number of fragments per sample was determined from their β-activity, measured with a counter calibrated against a 4π-counter.

The fragment yields for U^{233} and Pu^{239} are given in the table and represent averages of sixty independent measurements. These values include the yields of all the members of the radioactive chain which precede the given isotope, and are practically total yields of isotopes of the given mass (Te^{129m} and Cs^{136} are the only exceptions).

Figures 1 and 2 show the fragment-yield curves in the case of the fission of U^{233} and Pu^{239} by 14.5 Mev neutrons (curve 1) and fission-spectrum neutrons (curve 2). For comparison curve 3 [2] shows the results obtained for the fission of U^{233} and Pu^{239} by thermal neutrons. The figures also show the yields of additional fragments: the reflected points found for $\bar{\nu}_{U^{233}} = 2.7$ and $\bar{\nu}_{Pu^{239}} = 3.2$ in the case of fission by fission-spectrum neutrons, and $\bar{\nu} = 4.5$ in the case of fission by 14.5 Mev neutrons (the dependence of $\bar{\nu}$ on the fragment mass was neglected).

Discussion of results

The dependence of the relative probability of a symmetric fission of nuclei on the excitation energy for a dividing nucleus and its Z^2/A parameter, has already been discussed in [1]. The latter paper contains data for U^{233}

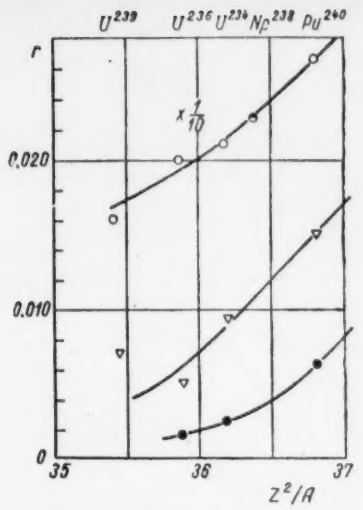

Fig. 3. The relative probability of symmetric fission as a function of Z^2/A; ○: fission by 14.5 Mev neutrons, (◓: points taken from [12]); ▽: fission-spectrum neutrons; ●: thermal neutrons [2].

and Pu^{239} as well as U^{235} and U^{238} (Fig. 3). The dependence of the position of the maxima in the fragment-mass distribution curve on the mass number A of the dividing nucleus in the case of fission by fission-spectrum neutrons was discussed in [1]. Analogous curves for the fission of U^{233}, U^{235}, U^{238} and Pu^{239} by 14.5 Mev neutrons, shown in Fig. 4, indicate that in this case also, the main effect is the change in the average mass of the light fragment.

It is necessary to investigate in somewhat greater detail the dependence of the difference between the average mass of heavy and light fragments Δm (degree of asymmetry) on the mass number A and the excitation energy of the dividing nucleus. An attempt to establish a relation between Δm and Z^2/A was made in [8] and led to the formula

$$\Delta m = 0.090 \left[(40.2 \pm 0.7) - \frac{Z^2}{A} \right]^{1/2} A,$$

which was deduced from the linear dependence between $(\Delta m/A)^2$ and Z^2/A. This relation does not appear to be well founded since it follows from experimental data obtained for different isotopes of a given element (for example, U^{233}, U^{235} and U^{238}) that the average mass of the heavy fragment in these isotopes is approximately constant.

The present results, as well as other published data, show that there is a simple linear relation between Δm and A, which follows directly from the fact that the average mass of the heavy fragment remains constant. In this connection, the effect of the parity of the dividing nucleus on the magnitude of Δm remains somewhat obscure and it is difficult to explain it on the usual versions of the liquid-drop model. It is possible that this may be explained by the effect of the separate nucleon states on the fission process, and in particular, on the mass of the heavy fragment [9].

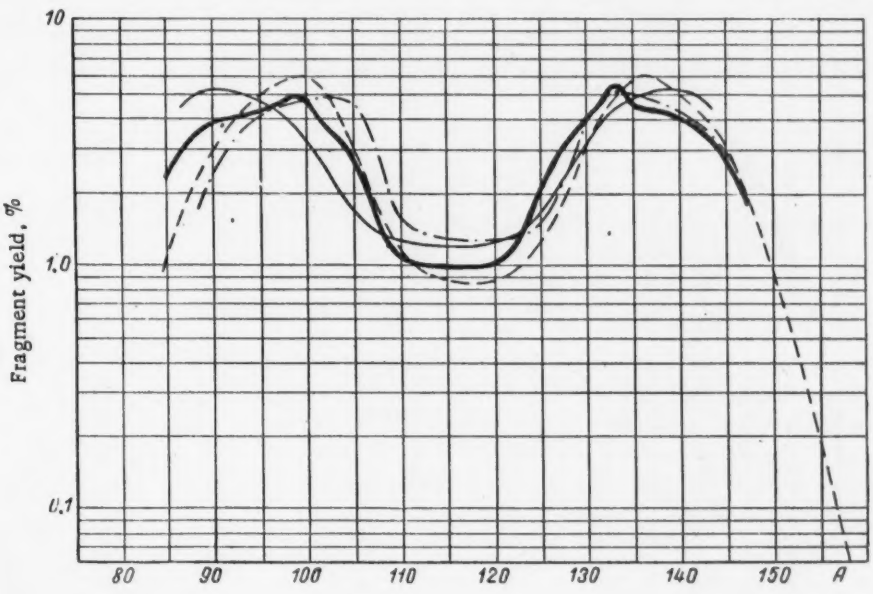

Fig. 4. Fragment-mass distribution in the fission of U^{233} (light curve), U^{235} (heavy curve) U^{239} (dashed curve) and Pu^{239} (dot-dash curve) by 14.5 Mev neutrons.

Figure 5 shows Δm as a function of A for the dividing nucleus in the case of fission by thermal neutrons and fission-spectrum neutrons. Line 1 is drawn through points corresponding to the fission of nuclei with even A. Points corresponding to nuclei with odd A are displaced from line 1 by two or three mass units (line 2) with the average masses of the heavy and light fragments measured to an accuracy of 0.2-0.5 mass units. In the mass range under consideration, the dependence of Δm on A is well represented by the expression

$$\Delta m = 288 - 1.04A + \delta$$

where

$$\delta = \begin{cases} 0 \text{ for even A} \\ \sim 2 \text{ for odd A.} \end{cases}$$

The small difference between the coefficient of A and unity is due to the fact that the average mass of the heavy fragment tends to decrease with increasing A.

As was pointed out in [1], the degree of asymmetry in the fission depends also on the excitation energy of the dividing nucleus. The values of Δm in the case of fission-spectrum neutrons, by reactor neutrons and also thermal neutrons, are equal to within experimental error, owing to the small variation in the energy of the primary neutrons. An increase in the energy of the neutrons to 14.5 Mev leads to a reduction in Δm by 3 or 4 units. On the other hand, in the case of spontaneous fission the values of Δm are greater by approximately 3 units as compared with fission by fission-spectrum neutrons.

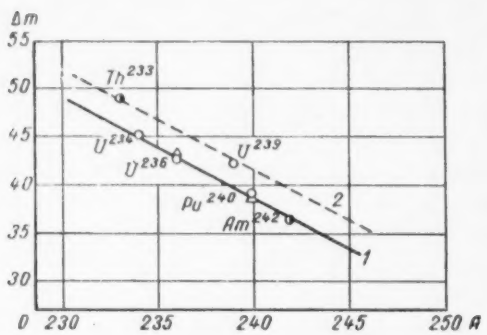

Fig. 5. Dependence of Δm on A: 1) dividing nuclei with even A, 2) odd A; fission by fission-spectrum neutrons (O), pile neutrons (◑) [10, 11], and thermal neutrons (▽).

It should be noted that in the case of fission by 14.5 Mev neutrons, and also in the case of spontaneous fission, it is found that Δm depends on the parity of A.

In conclusion, the authors wish to express their deep gratitude to A. A. Malinkin, Yu. A. Vasil'ev, and V. I. Shamarukhin for the irradiation of the specimens, to P. N. Moskalev, N. V. Shuvanova, A. A. Egorova, and K. N. Borozdina for carrying out some of the chemical work, and also to V. V. Zakatilov and L. N. Sorokina for assistance in the physical measurements.

LITERATURE CITED

1. E. K. Bonyushkin, et al., Neutron Physics, a collection of papers [in Russian] (Gosatomizdat, Moscow, 1961) [at press].
2. S. Kotcoff, Nucleonics, 16, No. 4, 78 (1958).
3. A. N. Protopopov, et al., Atomnaya Énergiya 5, No. 2, 130 (1958).
4. Radiochemical Studies: The Fission Products. National Nuclear Energy, Series IV, Book 3. New York, McGraw-Hill Book Co., (1951) p. 1331.
5. A. Noyes and V. Bray, Qualitative Analysis of Rare Elements [in Russian] (ONTI, Moscow, 1936).
6. V. F. Gillebrand and G. É. Lendel', Practical Handbook on Inorganic Analysis [in Russian] (Goskhimizdat, Moscow, 1957).
7. Radiochemical Studies: The Fission Products. National Nuclear Energy, Series IV, Book 3, New York, McGraw-Hill Book Co., (1951) p. 1419.
8. W. Swiatecki, Phys. Rev., 100, 936 (1955).
9. V. V. Vladimirskii, Zh. éksperim. i teor. fiz., 32, 822 (1957).
10. A. Turkevich and J. Niday, Phys. Rev., 84, 52 (1951).
11. J. Cuninghame, J. Inorg. and Nucl. Chem., 4, No. 1 (1957).
12. R. Coleman, B. Hawker, and J. Perkin, J. Inorg. and Nucl. Chem., 14, 8 (1960).

THE OPTIMUM TEMPERATURE FOR REGENERATIVE WATER-HEATING SYSTEMS AT ATOMIC POWER STATIONS WITH WATER-COOLED AND WATER-MODERATED POWER REACTORS (WWPR)

Yu. D. Arsen'ev

Translated from Atomnaya Énergiya, Vol. 10, No. 1,
pp. 19-25, January, 1961
Original article submitted March 24, 1960

The "base point" method is used to determine the optimum temperature t_r^{opt} for a regenerative water-heating system which corresponds to a minimum calculated cost c_e (kopeks/kwh) for electrical energy. It is shown that for an atomic power station having a water-cooled and water-moderated power reactor (WWPR) the value of t_r^{opt} is near the maximum defined by the steam conditions after the first turbine stage.

The optimum temperature t_r^{opt} of a regenerative water-heating system is determined by engineering-economic calculations and corresponds to the minimum calculated cost for electrical energy, c_e (kopeks/kwh). An increase in t_r and an increase in the number of heating stages reduces the fuel component of c_e, but increases the cost of the regenerative system and the investment component, which may nullify the gain in c_e.

In atomic power stations with a constant reactor thermal power Q the temperature of the regenerative heating system in general influences the construction of the boiler, determining its surface F and the relation between the economizer and evaporator sections. However, the boilers used at atomic power stations with WWPR differ from the usual type in not having a separate economizer section [1-3], and the heating of the water from the temperature t_r to t_s takes place basically as a result of the partial condensation of steam which forms on the lower tube banks and of turbulent mixing. Therefore, in such boilers, in determining the heating surface F, the water temperature in the second loop is taken as constant and equal to the saturation temperature t_s. Consequently, for constant reactor power Q, coolant inlet and outlet temperatures t_{T_1} and t_{T_2} and minimum temperature drive Δt_{min}, the calculated boiler surface F does not depend on the temperature t_r of the regenerative water-heating system. This is the difference, in principle, between a WWPR boiler and a boiler with an economizer section.

The author of [4] started with the incorrect assumption that the boiler in a WWPR atomic power station has a separate economizer section. This is what led to the incorrect conclusion as to the dependence of the temperature t_{T_1} on the temperature of the regenerative heating system.

In a turbine at limiting power with constant steam consumption by the last stage, an increase in t_r causes an increase in power as a result of the larger steam consumption by the first stages and the subsequent discharge of steam into the regenerative system. This is very important, since an increase in the power of a saturated-steam turbine is a problem of great interest at present [5,6].

The influence of the regenerative system temperature t_r on the calculated electrical energy cost c_e was investigated by the base-point method [5]. All parameters referring to the base point with fixed regenerative system temperature t_r' are marked with a single apostrophe, and a double apostrophe is used for other regenerative system temperatures. The choice of a particular base point has no effect on the final results of the investigation.

The Effect of Regenerative Heating System Temperature on Power Station Efficiency and Unit Turbine Power

In saturated-steam cycles the maximum possible regenerative heating system temperature t_r^{max} is determined by the steam conditions after the first turbine stage, while the minimum temperature depends on the deaerator parameters.

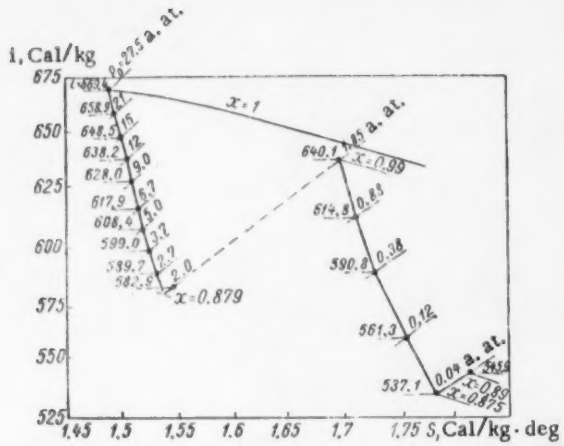

Fig. 1. Steam operation in a type AK-70 turbine (a.at.: absolute atmospheres).

In order to extend the limits of variation of t_r we took a scheme with low-pressure deaerators.

The regenerative heating system temperature was investigated for a turbine with an expansion process similar to that of the AK-70 turbine, the parameters for which are shown in the i-S diagram in Fig.1.

It is known that the heating system temperature t_r^* should be related to the number of regenerative heaters z_r^*. For t_r = constant, we have a definite minimum number of heating stages z_r^{min}, corresponding to the maximum of the efficiency curve $\eta = f(t_r, z_r)$. When $z_r < z_r^{min}$, an increase in t_r leads to a decrease in η, which is inadmissible. Therefore, for an increase in t_r the minimum number of heaters should be increased. In real schemes the number of heating stages z_r is always greater than the minimum z_r^{min}, since increasing z_r to infinity increases the efficiency of the power station. However, the investment cost for the regenerative system limits the increase of z_r. When faced with the practical selection of the number of heating stages, one should keep in mind the fact that when the number of heaters is greater than three or four, the addition of each new stage adds less and less to the efficiency. However, for a fixed feed water consumption and for t_r = constant, the fewer the heating stages z_r the greater must be the surface of each heater. The number of heating stages z_r, therefore, must not be taken smaller than the number for which the heater surface F exceeds the value for heaters manufactured by industry at the present time. For F = constant, an increase in t_r, as well as an increase in feed water consumption, leads to an increase in the number of heating stages. To ensure uniformity of equipment, all high-pressure heaters (HPH) and all low-pressure heaters (LPH) must have equal surfaces.

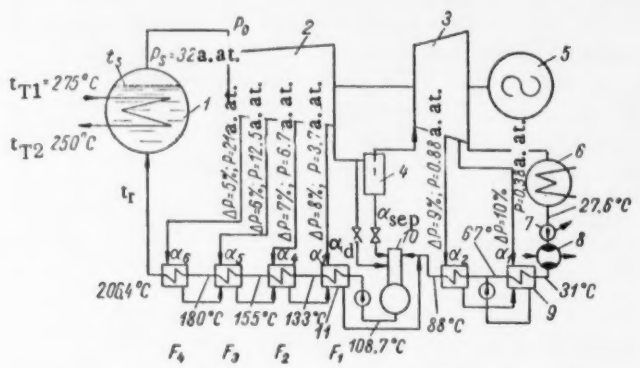

Fig. 2. Heat flow schematic for the second loop: 1) boiler; 2) high-pressure cylinder; 3) low-pressure cylinder 4) steam separator; 5) generator; 6) condenser; 7) pump; 8) condensate heater, using steam from the ejectors and turbine effluent; 9) LPH; 10) deaerator; 11) HPH (a. at.: absolute atmospheres).

Considering the maximum surfaces of the regenerative manufactured by the Khar'kov Turbogenerator Factory (KhTGZ) (F = 200 m^2 for LPH and F = 490 m^2 for HPH) a regenerative water-heating scheme was computed using a constant water subcooling value of 5°C and a condensate supercooling value of 3°C, for the volume of steam to the last AK-70 turbine stage equal to G_k = 285.6 tons per hour (Fig. 2). The temperature t_r' = 108°C, corresponding to the water temperature after the deareator, was taken as the base point.

The heating temperature was analyzed for a change in t_r from 108.7 to 206.4°C; the number of LPH's was kept constant. Such a scheme satisfies the general thermodynamic principle that with an increase in t_r" the optimum number of heating stages is increased.

The volumes of steam alloted to the LPH's $\alpha_1 + \alpha_2$, the deaerator α_d, and the HPH's $\alpha_3 + \alpha_4 + \alpha_5 + \alpha_6$, the separated moisture content α_{sep}, and the surfaces of the heaters are shown in the table. The table also gives the values of unit steam consumption d_e (kg/kwh) calculated for a generator efficiency of 0.98 and a turbine mechanical efficiency of 0.93.

For a constant exhaust area the relative change in turbine unit power N_T'/N_T" may be expressed [6,7] by the formula

$$\frac{N_T'}{N_T''} = \frac{d_e''(1-\Sigma\alpha'')}{d_e'(1-\Sigma\alpha')}, \qquad (1)$$

where $1-\Sigma\alpha$ is the relative volume of steam arriving at the last turbine stage.

Power Station Characteristics for Various Regenerative Water Heating Temperatures t_r

Characteristics	t_r, °C				
	108.7	133	155	180	206.4
No. of HPH's	0	1	2	3	4
α_1	2.22	5.16	4.91	4.63	4.33
α_2	3.36	3.02	2.87	2.22	2.7
α_{sep}	10.7	10.15	9.66	9.15	8.6
α_d	3.61	3.12	2.66	2.22	1.73
α_3	—	5.39	5.14	4.87	4.59
α_4	—	—	5.1	4.78	4.43
α_5	—	—	—	5.72	5.81
α_6	—	—	—	—	6.4
$1-\Sigma\alpha$	77.1	72.1	69.6	65.9	61.9
d_e, kg/kwh	5.44	5.62	5.8	6.07	6.43
N''_T/N'_T	1	1.035	1.04	1.05	1.054
F_1, m²	—	340	352	371	394
F_2, m²	—	—	350	369	392
F_3, m²	—	—	—	380	405
F_4, m²	—	—	—	—	435

Note. The values of α and $1-\Sigma\alpha$ are given in percentages.

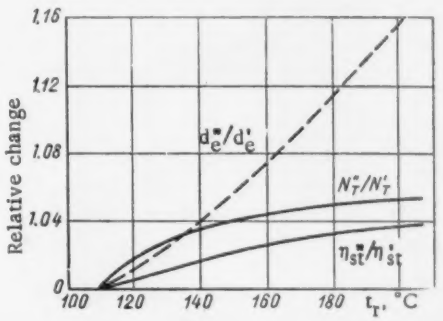

Fig. 3. Relative changes in power station efficiency, η_{st}''/η_{st}', in turbine unit power, N_T''/N_T', and in unit steam consumption, d_e''/d_e', as functions of regenerative water heating temperature t_r.

The relative changes N_T''/N_T' in turbine power and in power station efficiency are shown in Figure 3.

Relative Calculated Cost for Electric Power δc_e and Relative Unit Investment Cost δq_c as Functions of t_r

The basic equation for the analysis of relative calculated cost $c_e = c_f + c_c + c_{op}$ by the base point method for constant reactor thermal power is of the form

$$\delta c_e = \bar{c}_f'\delta\eta + \bar{c}_c'\delta q_c + \bar{c}_{op}'\delta c_{op}, \qquad (2)$$

where $\bar{c}_f'$, c'_{op}, and $\bar{c}'_c = 1 - \bar{c}'_f - \bar{c}'_{op}$ are the relative components of calculated cost at the base point; $\delta\eta = \eta'_{st}/\eta''_{st} - 1$ is the relative change in power station efficiency; $\delta q_c = q''_c/q'_c - 1$ is the relative change in unit investment cost; δc_{op} is the relative change in the operating component. At atomic power stations the operating component is small, and in calculation by the base method any change in it can be neglected. Taking $\delta c_{op} = 0$ and $\bar{c}'_{op} = c'_{op}/c'_e = 0.1$, using Eq. (2) we obtain the following simplified relation:

$$\delta c_e = \bar{c}_f'\delta\eta + (0.9 - \bar{c}_f')\delta q_c. \qquad (3)$$

The relative change in the fuel component $\delta c_f = c_f''/c_f' - 1$ in the case under consideration is equal to the relative change $\delta\eta$ in efficiency (Fig. 4).

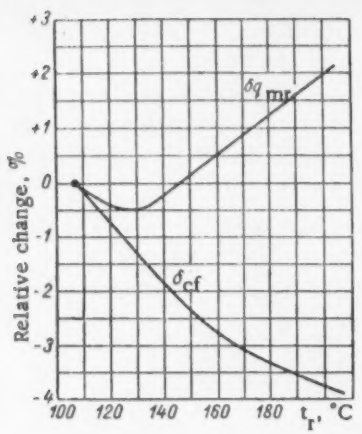

Fig. 4. Relative change in the fuel component δc_f and the unit investment cost δq_{mr} for the power station machine room as functions of t_r.

The relative change in the investment component $\delta c_c = c''_c/c'_c - 1$ is equal to the relative change in unit investment cost, which for constant investment cost for the first loop (C_{rz} = constant) may be represented in the following manner:

$$\delta q_c = [1 - b'_{mr}(1 - n'_{el} - n'_{iws})]\delta\eta + \\ + b'_{mr}(\delta q_{mr} + n'_{iws}\delta q_{iws}), \quad (4)$$

where δq_{mr} and δq_{iws} are the relative changes in unit investment cost for the machine room and for the industrial water supply: $b'_{mr} = q'_{mr}/q'_c$ is a basic constant equal to the ratio of the machine room investment cost to the investment cost for the entire station; $n'_{iws} = q'_{iws}/q'_{mr}$ and $n'_{el} = q'_{el}/q'_{mr}$ are basic components equal to the ratios of the industrial water supply and electrical equipment investment costs to the investment cost for the machine room.

The ratios of industrial water supply and electrical equipment investment costs to the machine room investment cost have average values of $n'_{iws} = 0.25$ and $n'_{el} = 0.15$, and we therefore have from Eq. (4)

$$\delta q_c = (1 - 0.6b'_{mr})\delta\eta + b'_{mr}(\delta q_{mr} + 0.25\,\delta q_{iws}). \quad (5)$$

The unit investment cost for the machine room, calculated for t_r = 108°C, may be subdivided into a number of components (for an upper limit to the cost of the regenerative system):

Component of investment cost	Amount
n'_{tur} (turbine)	0.365
n'_{gen} (generator)	0.315
n'_{eq} (equipment)	0.085
n'_{sp} (structural parts)	0.105
n'_{r} (regenerative system)	0.025
n'_{con} (condenser)	0.105
n'_{i} (total)	1.00

Then the relative change in unit investment cost for the machine room may be expressed by the formula

$$\delta q_{mr} = \frac{q''_{mr}}{q'_{mr}} - 1 = \sum_{1}^{n} n'_i\left(\frac{q''_i}{q'_i} - 1\right). \quad (6)$$

The unit investment cost for the condenser q_{con} is proportional to the unit surface f_{con} required for 1 kw of electric power. From Eq. (1) for the case of a constant vacuum we obtain the relation

$$\frac{q''_{con}}{q'_{con}} = \frac{f''_{con}}{f'_{con}} = \frac{d''_e(1-\Sigma\alpha'')}{d'_e(1-\Sigma\alpha')} = \frac{N'_T}{N''_T}. \quad (7)$$

In calculating the unit investment cost for the turbine the exhaust area is taken as constant. Therefore, if there is a change in t_r, there is a corresponding change in turbine power (Fig. 3).

The saturated-steam turbines manufactured by the KhTGZ have a high-pressure cylinder HPC and a low-pressure cylinder LPC. Since the length of a turbine blade in the last stage is constant and the amount of steam $\alpha_1 + \alpha_2$ separated for regeneration from the LPC changes little (see table), it may be assumed that the costs for the LPC are constant (C_{lp} = const). According to the data supplied by the KhTGZ the cost for the LPC is 1.5 times the cost for the HPC, and the cost for the turbine blades amounts to about 20% of the cost for the whole turbine. Then, assuming that the cost of the HPC blades is directly proportional to the blade length in the first stage, we obtain

$$\frac{q''_{tur}}{q'_{tur}} = \frac{(K'_{lp} + K''_{hp})}{(K'_{lp} + K'_{hp})} \frac{N'_T}{N''_T} = \left(0.08 \frac{1-\Sigma\alpha'}{1-\Sigma\alpha''} + 0.92\right) \frac{N'_T}{N''_T}. \quad (8)$$

As can be seen from Fig. 5, an increase in t_r produces little change in the turbine investment cost.

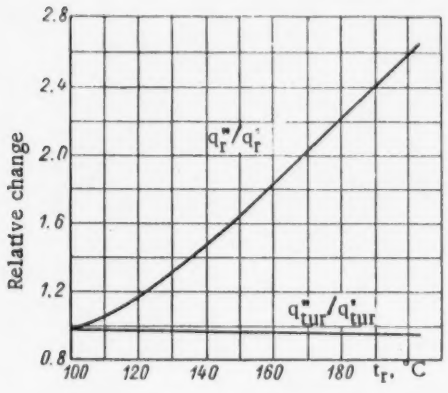

Fig. 5. Relative change in unit investment cost for the regenerative system q''_r/q'_r and the turbine q''_{tur}/q'_{tur} as functions of t_r.

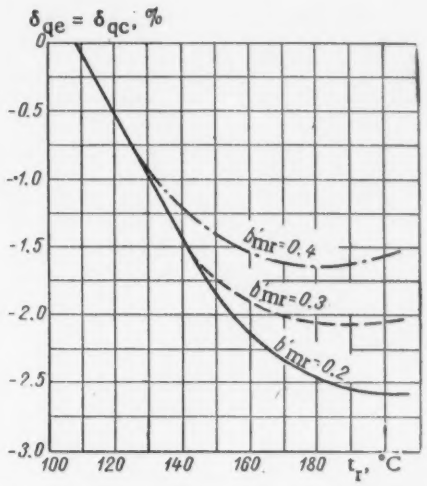

Fig. 6. Relative change of unit investment cost δq_c as a function of t_r and of the fraction of investment cost spent for the machine room b'_{mr}.

The changes in unit investment costs for the generator, structural parts, and auxiliary equipment can be neglected.

The cost of one HPH as a function of its surface area, equal to 300-450 m^2, is defined by the approximate formula

$$C_{HPH} = 32 + 0.245F \text{ thousand rubles.}$$

The data on the effects of changes in t_r on the surface area of the HPH are shown in the table; in the calculation the coefficient of heat transfer k was taken equal to 2100 Cal/m^2 · hour · °C. The unit investment cost for the regenerative system changes with an increase of HPH's from 0 to 4 as follows:

$$\frac{q''_r}{q'_r} = \frac{[K_{LPH} + \sum_0^4 (32+0.245F)]}{K_{LPH}} \frac{N'_T}{N''_T}. \quad (9)$$

The dependence of the unit investment cost for the heaters on the regenerative system temperature for C_{LPH} = 290,000 rubles is shown in Fig. 5, from which it can be seen that an increase of t_r from 108 to 206°C increases q_r more than 2.5 times.

The relative change in the unit investment cost for the entire machine room δq_{mr}, calculated from Eqs. (6-9), has a minimum value for t_r = 130°C, and for higher t_r values the unit investment cost for the machine room increases as a result of the greater expense for the regenerative system (see Fig. 4).

The unit investment cost for the industrial water supply decreases with an increase in t_r:

$$\delta q_{\text{iws}} = \frac{N'_\tau}{N''_\tau} - 1. \qquad (10)$$

The dependence of δq_c and δc_e on the temperature t_r is shown graphically in Figs. 6 and 7.

Evaluation of the Results

From Fig. 7 it can be concluded that δc_e decreases for each version with an increase of t_r up to the maximum possible value. Consequently, for the WWPR atomic power station under discussion the optimum temperature t_r^{opt} for any fuel component corresponds to the maximum temperature of regenerative water heating t_r^{max}, defined by the steam conditions of the first turbine stage. In the present article we consider an upper limit for the investment cost for the regenerative system $n_r = q_r/q_{mr}$; obviously, for a cheaper regenerative system it is even more profitable to increase t_r^{opt}

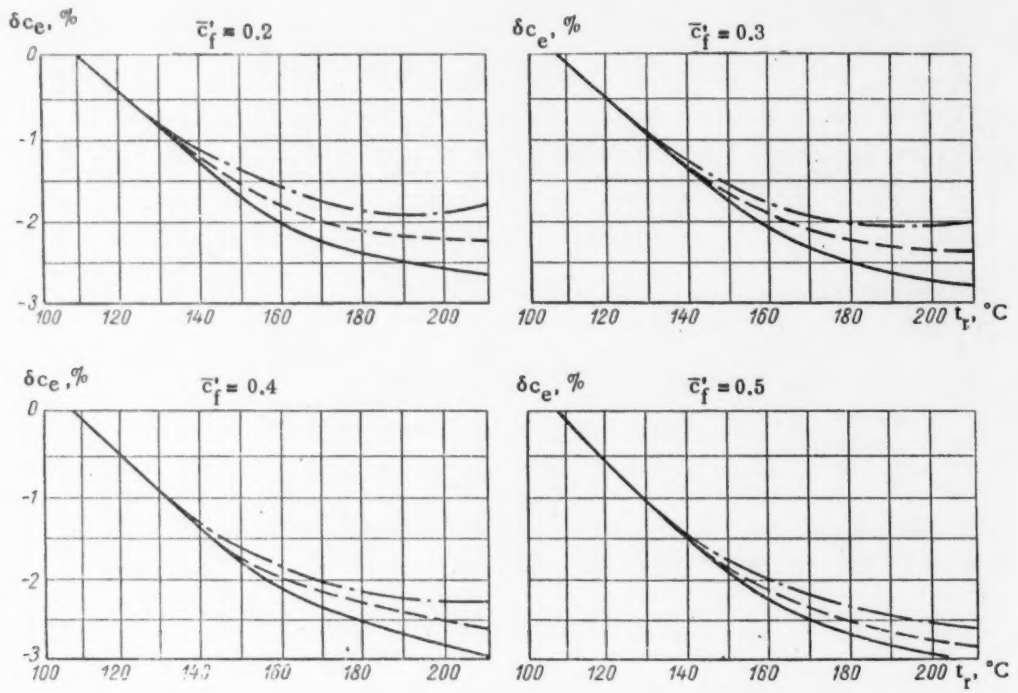

Fig. 7. Relative change in calculated cost for electric power δc_e as a function of t_r, relative fuel component c'_f, and fraction of investment cost spent on the machine room b'_{mr}:

——— $b'_{mr} = 0.2$; — — — $b'_{mr} = 0.3$; —·—·— $b'_{mr} = 0.4$.

The conclusion thus reached is not at all typical, and for this reason we have devoted considerable space to the reasons for such a result. As has already been indicated, the optimum regenerative heating temperature t_r^{opt} corresponds to the minimum electric power cost c_e, that is, to the minimum of the sum $c_f + c_c$. As t_r increases, the fuel component c_f always decreases, and therefore the minimum of c_e depends on the nature of the change in the capital investment component c_c. In the case under consideration, an increase in t_r essentially also produces a decrease in the investment component c_c (see Fig. 6).

The decrease of c_f and c_c with an increase in t_r caused the optimum heating temperature t_r^{opt} to coincide with the maximum t_r^{max}. Therefore, in this case it was profitable to use the maximum possible regenerative water heating temperature, taking into account, of course, the engineering possibilities of the construction of a rational scheme. As a result of the concavity of the $\delta c_e = f(t_r)$ curve, shown in Fig. 7, it is possible to reduce somewhat the calculated value of t_r^{opt} so as to decrease the unit investment cost (see Fig. 6) and the initial cost for the power station $K_c = q_c N_e$.

LITERATURE CITED

1. S. A. Skvortsov, Atomnaya Énergiya, 5, No. 3, 245 (1958).
2. G. V. Ermakov, Teploénergetika, No. 10, 88 (1957).
3. J. Simpson et al., Collection: "Atomic Power Engineering" [Russian translation] Moscow, Gosénergoizdat, 1956, p. 487.
4. I. A. Trub, Atomnaya Énergiya, 4, No. 3, 286 (1958).
5. Yu. D. Arsen'ev, Teploénergetika, No. 10, 27 (1959).
6. Yu. D. Arsen'ev, Physics and Heat Technology of Reactors [in Russian]. Supplement No. 1 to the journal "Atomnaya Énergiya" Moscow, Atomizdat, 1958, p. 176 [English translation, Consultants Bureau, New York, 1960].
7. L. I. Kertselli and V. Ya. Ryzhkin, Heat-powered Electric Power Stations [in Russian] Moscow, Gosénergoizdat, 1956.

BOUNDARY CONDITIONS IN THE METHOD OF SPHERICAL HARMONICS

G. Ya. Rumyantsev

Translated from Atomnaya Énergiya, Vol. 10, No. 1,
pp. 26-34, January, 1961
Original article submitted March 9, 1960

The equations of the method of spherical harmonics are derived for use with the single-velocity transport equation. From an analysis of the equations, conditions are obtained for the boundary between two different scattering media. It is shown that these conditions completely define a solution in any-order approximation (we are concerned here with the so-called P_N approximations) including even-order approximations. The possibility of using even-order approximations is of major practical interest. Thus, for example, the relatively simple P_2 approximation may serve as a method for improving the elementary diffusion theory without introducing excessive complexity.

Even-order approximations, and in particular the P_2 approximation, have not as yet been used in calculations.

Introduction

The transport equation can be successfully solved with the aid of the method of spherical harmonics. This method consists in that the required distribution function $F(\mathbf{r}, \Omega)$ is expanded into a series of spherical functions. The expansion coefficients which depend only on the space coordinates, are related to each other by an infinite set of differential equations. If one limits one's attention to spherical functions up to N-th order only in the expansion of $F(\mathbf{r}, \Omega)$, then the set of equations for the coefficients will be finite, and can often be solved analytically. This is known as the P_N approximation. The uniqueness of the solution is ensured by providing a sufficient number of boundary conditions.

The method of spherical harmonics is frequently used in the solution of one-dimensional problems [1, 2]. The derivation of the equations for the P_N approximation has been given by Davison [3] for the general case. However, the problem of the formulation of the boundary conditions in the method of spherical harmonics cannot be considered as entirely solved. This is true not only for the general case but even for the one-dimensional problems with simple geometry. This is probably the reason why it is generally believed the P_2, P_4, etc. approximations, i.e., the even-order approximations, are inferior and less convenient for the solution of the equations than the odd-order approximations.

Let us state the problem more carefully. In the selection of the boundary conditions on the boundary between two media, one must distinguish between two cases. In the first case, the P_N approximation equations cannot be applied to one of the media (for example, a semi-infinite vacuum), or they can be applied to both media but do not hold on the boundary itself and in its neighborhood, i.e., the P_N approximation serves only for the description of the asymptotic behavior of the solution. In this case, the boundary conditions are known to be artificial and hence not unique. Their choice should be dictated by considerations drawn from some other, more accurate method for the solution of the transport equation, or by the physical interpretation of the problem.

In the second case, the P_N approximation equations are assumed to hold throughout both media, including the separation boundary. This assumption can be admitted if the adjacent media are good scatterers and their physical properties are not too different. Such conditions are relatively frequently encountered in heterogeneous systems. Here, the boundary conditions are required only because it is not possible to express the solution by a single analytical formula which would hold for the entire heterogeneous medium. The solution is written down in the form of separate functions each of which is a solution within a single homogeneous region. The boundary conditions, i.e., the conditions for mating these functions, should satisfy the requirement that the general solution made up of these functions should also hold at the mating points on the separation boundary. Here the conditions at the mating points cannot be arbitrary and are a unique consequence of the form of the equations.

Let us consider this type of boundary condition.

Derivation of the equations of the method of spherical harmonics

Consider a single-velocity transport equation for a medium of arbitrary geometry. Suppose the function $F(\mathbf{r}, \Omega)$ describes the spatial and angular distribution of the neutron current. Let us introduce a vector distribution function defined by

$$\mathbf{F}(\mathbf{r}, \Omega) = \Omega F(\mathbf{r}, \Omega),$$

where Ω is the unit vector in the direction of the velocity.

Clearly, the function $\mathbf{F}(\mathbf{r}, \Omega)$ is the vector neutron current at the point $\mathbf{r}$, Ω while the function $F(\mathbf{r}, \Omega)$ is the absolute magnitude of this current, i.e.

$$F(\mathbf{r}, \Omega) = |\mathbf{F}(\mathbf{r}, \Omega)|.$$

Suppose further that $W(\mu_0)$ is the probability that the neutron will be scattered and undergo a change of direction from Ω' to Ω, and

$$\mu_0 = (\Omega' \Omega).$$

The density of neutron sources in the medium will be noted by $S(\mathbf{r}, \Omega)$.

Using this notation, the transport equation is of the form

$$\operatorname{div} \mathbf{F}(\mathbf{r}, \Omega) + \Sigma F(\mathbf{r}, \Omega) - \Sigma_s \int_{4\pi} F(\mathbf{r}, \Omega') W(\mu_0)\, d\Omega' = S(\mathbf{r}, \Omega). \tag{1}$$

Let us expand the functions $\mathbf{F}(\mathbf{r}, \Omega)$ and $F(\mathbf{r}, \Omega)$ into a series of spherical functions (cf., [4]):

$$\mathbf{F}(\mathbf{r}, \Omega) = \sum_{n=0}^{\infty} \mathbf{F}_n(\mathbf{r}, \Omega); \tag{2}$$

$$F(\mathbf{r}, \Omega) = \sum_{n=0}^{\infty} (2n+1) Y_n(\mathbf{r}, \Omega), \tag{3}$$

where $\mathbf{F}_n(\mathbf{r}, \Omega)$ and $Y_n(\mathbf{r}, \Omega)$ are, respectively, the spherical functions with vector and scalar coefficients depending on $\mathbf{r}$.

Each spherical function consists of $2n + 1$ linear independent components:

$$\mathbf{F}_n(\mathbf{r}, \Omega) = \sum_{m=-n}^{n} \mathbf{f}_{nm}(\mathbf{r})\, Y_{nm}(\Omega); \tag{4}$$

$$Y_n(\mathbf{r}, \Omega) = \sum_{m=-n}^{n} \Psi_{nm}(\mathbf{r})\, Y_{nm}(\Omega). \tag{5}$$

The choice of the form of $Y_{nm}(\Omega)$ is immaterial.

The source density can be represented in a similar way:

$$S(\mathbf{r}, \Omega) = \sum_{n=0}^{\infty} S_n(\mathbf{r}, \Omega), \tag{6}$$

and the probability $W(\mu_0)$ will be expanded into a series of Legendre polynomials:

$$W(\mu_0) = \frac{1}{4\pi} \sum_{n=0}^{\infty} (2n+1) C_n P_n(\mu_0). \tag{7}$$

From the normalization condition $C_0 = 1$.

Bearing in mind that the spherical functions have the following properties [4],

$$\int_{4\pi} Y_k(\Omega') P_n(\mu_0)\, d\Omega' = 0 \quad \text{for} \quad k \neq n,$$

$$\int_{4\pi} Y_n(\Omega') P_n(\mu_0)\, d\Omega' = \frac{4\pi}{2n+1} Y_n(\Omega),$$

we find that

$$\int_{4\pi} F(\mathbf{r}, \Omega') w(\mu_0)\, d\Omega' = \sum_{n=0}^{\infty} (2n+1) C_n Y_n(\mathbf{r}, \Omega).$$

Since the spherical functions of various orders are linearly independent, Eq. (1) can be rewritten in the form

$$\begin{gathered} \operatorname{div} \mathbf{F}_n(\mathbf{r}, \Omega) + \Sigma_n Y_n(\mathbf{r}, \Omega) = S_n(\mathbf{r}, \Omega), \\ 0 \leqslant n < \infty. \end{gathered} \tag{8}$$

In this expression

$$\Sigma_n = (2n+1)(\Sigma - \Sigma_s C_n). \tag{9}$$

It is now necessary to establish the relation between F_n and Y_n. In accordance with the definition of $\mathbf{F}(\mathbf{r}, \Omega)$ we have

$$\mathbf{F}(\mathbf{r}, \Omega) = \sum_{n=0}^{\infty} (2n+1) \Omega Y_n(\mathbf{r}, \Omega). \tag{10}$$

It is known from the theory of spherical functions that•

$$Y_n(\Omega) = U_n(\mu)_{|\mu=1},$$

where $\boldsymbol{\mu}$ is the radius-vector in the three-dimensional space μ_x, μ_y, μ_z, i.e.,

$$\boldsymbol{\mu} = \mu_x \mathbf{i} + \mu_y \mathbf{j} + \mu_z \mathbf{k},$$

where $\mu_x = \mu\Omega_x$, $\mu_y = \mu\Omega_y$, $\mu_z = \mu\Omega_z$ and $U_n(\boldsymbol{\mu})$ is the n-th degree harmonic polynomial in μ_x, μ_y, μ_z.

Using the Hamiltonian operator

$$\dot{\nabla} = \mathbf{i}\frac{\partial}{\partial \mu_x} + \mathbf{j}\frac{\partial}{\partial \mu_y} + \mathbf{k}\frac{\partial}{\partial \mu_z},$$

it follows from the definition of the polynomial U_n that it should satisfy the Laplace equation

$$\dot{\nabla}^2 U_n(\boldsymbol{\mu}) = 0.$$

We can also write

$$\Omega Y_n(\Omega) = \mu U_n(\boldsymbol{\mu})_{|\mu=1}. \tag{11}$$

The product μU_n is a homogeneous polynomial of degree n + 1, although it is not a harmonic polynomial. It follows that when $\mu = 1$ it does not become identical with a spherical function of degree n + 1. Let us represent it by the following identity:

• This mathematical transformation is derived in a chapter of Davis' book [3].

$$\mu U_n = \left[\mu U_n - \frac{\mu^2}{2n+1} \dot{\nabla} U_n \right] + \frac{\mu^2}{2n+1} \dot{\nabla} U_n$$

It can be immediately verified that $\left[\mu U_n - \frac{\mu^2}{2n+1} \dot{\nabla} U_n \right]$ and $\dot{\nabla} U_n$ satisfy the Laplace equation* and at the same time are homogeneous polynomials of degree n + 1 and n−1, respectively. This means when $\mu = 1$, the first expression forms a spherical function of order n + 1 and the second, a spherical function of order n−1.

On rewriting the expansion (10) in the form

$$F_n = \sum_{n=0}^{\infty} \left\{ \left[2n+1) \mu U_n - \mu^2 \dot{\nabla} U_n \right]_{\mu=1} + \left[\dot{\nabla} U_n \right]_{\mu=1} \right\}$$

(the arguments $\mathbf{r}$ and Ω will be omitted from now on), and selecting from the above sum spherical functions of order n, we have

$$F_n = [\dot{\nabla} U_{n+1} + (2n-1) \mu U_{n-1} - \mu^2 \dot{\nabla} U_{n-1}]_{\mu=1}. \tag{12}$$

Next, let us introduce the further Hamiltonian operator

$$\nabla \equiv \mathbf{i} \frac{\partial}{\partial x} + \mathbf{j} \frac{\partial}{\partial y} + \mathbf{k} \frac{\partial}{\partial z} .$$

The equations for the spherical harmonics will then assume the form

$$[(\nabla \dot{\nabla}) U_{n+1} + (2n-1)(\nabla \mu) U_{n-1} - \mu^2 (\nabla \nabla) U_{n-1}]_{\mu=1} + \Sigma_n Y_n = S_n. \tag{13}$$

We note that $(\nabla \dot{\nabla})$ and $(\nabla \mu)$ are scalar operators which, from the formal point of view, are the scalar products of the corresponding vector operators, i.e.,

$$(\nabla \dot{\nabla}) = (\nabla \dot{\nabla}) \equiv \frac{\partial^2}{\partial x \partial \mu_x} + \frac{\partial^2}{\partial y \partial \mu_y} + \frac{\partial^2}{\partial z \partial \mu_z} ;$$

$$(\nabla \mu) = (\mu \nabla) \equiv \mu_x \frac{\partial}{\partial x} + \mu_y \frac{\partial}{\partial y} + \mu_z \frac{\partial}{\partial z} .$$

In order to remove the condition $\mu = 1$ it is sufficient to multiply Eq. (13) by μ^n, since each term of this equation is a homogeneous polynomial in μ_x, μ_y, μ_z. At the same time, let us replace n by n - 1 so that

$$(\nabla \dot{\nabla}) U_n = Q_{n-1} - \Sigma_{n-1} U_{n-1} - (2n-3)(\nabla \mu) U_n + \mu^2 (\nabla \nabla) U_{n-2}, \tag{14}$$

where $Q_n = \mu^n S_n$ are harmonic polynomials of degree n.

Using Eq. (14) for n−2, n−4, n−6, etc., we can eliminate the operator $(\nabla \dot{\nabla})$ from the righthand side of Eq. (14) and rewrite it in the following form:

$$\begin{aligned} (\nabla \dot{\nabla}) U_n = {} & [Q_{n-1} + \mu^2 Q_{n-3} + \mu^4 Q_{n-5} + \ \ldots] - [\Sigma_{n-1} U_{n-1} + \mu^2 \Sigma_{n-3} U_{n-3} + \mu^4 \Sigma_{n-5} U_{n-5} + \ldots] \\ & - (\nabla \mu) [(2n-3) U_{n-2} + \mu^2 (2n-7) U_{n-4} + \mu^4 (2n-11) U_{n-6} + \ldots] \end{aligned} \tag{15}$$

(terms with negative numbers are zero).

*This can be verified with the aid of Euler's identity $(\mu \dot{\nabla}) \mathscr{P}_n = n \mathscr{P}_n$, where $\mathscr{P}_n$ is a homogeneous polynomial of degree n.

In passing on to the P_N approximation we shall assume that $(\nabla\dot{\nabla})U_{N+1} = 0$. In that case, Eq. (15) with the maximum number n = N + 1 assumes the form

$$\begin{aligned}\Sigma_N U_N &= [Q_N + \mu^2 Q_{N-2} + \mu^4 Q_{N-4} + \ldots] \\ (\nabla\mu)\,&[(2N-1)\,U_{N-1} + \mu^2\,(2N-5)\,U_{N-3} + \ldots] \\ &- [\mu^2 \Sigma_{N-2} U_{N-2} + \mu^4 \Sigma_{N-4} U_{N-4} + \ldots].\end{aligned} \tag{16}$$

Let us now consider the method of solution of the set of equations derived above, and determine the number of arbitrary coefficients in the general solution. According to the theory of linear equations, the number of coefficients is equal to the number of proper solutions of the corresponding homogeneous system. For this reason we shall determine the form of the solution on the assumption that the terms Q_n are absent.

Equation (16) gives the function U_n in terms of lower-number functions. All the terms of the equation are homogeneous polynomials of degree N, and we shall therefore refer to it as an N-th order equation. If we apply the operator $(\nabla\dot{\nabla})$ to the whole equation, the order of the equation will be reduced by one. It is easy to verify that the following operator relations will hold:

$$(\nabla\dot{\nabla})\,(\nabla\mu)^l = (\nabla\mu)^l\,(\nabla\dot{\nabla}) + l\,(\nabla\mu)^{l-1}\nabla^2;$$
$$(\nabla\dot{\nabla})\mu^{2k} = \mu^{2k}\,(\nabla\dot{\nabla}) + 2k\mu^{2(k-1)}\,(\nabla\mu),$$

and consequently

$$\begin{aligned}(\nabla\dot{\nabla})\,(\nabla\mu)^l\mu^{2k} &= (\nabla\mu)^l\,\mu^{2k}\,(\nabla\dot{\nabla}) \\ &+ 2k\,(\nabla\mu)^{l+1}\mu^{2(k-1)} + l\,(\nabla\mu)^{-1}\mu^{2k}\nabla^2.\end{aligned}$$

Thus, as a result of the application of the operator $(\nabla\dot{\nabla})$ to Eq. (16), no new scalar operators other than $\nabla^2 \equiv \Delta$ can be obtained, and the operator $(\nabla\dot{\nabla})$ can always be excluded from the final expression with the aid of Eq. (15). We note that Δ commutes with all the other operators in the equations, just as $(\nabla\mu)$ commutes with μ^{2k}.

If we repeat the operation $(\nabla\dot{\nabla})$ on Eq. (16) m times, we obtain a new equation whose structure can easily be deduced. Firstly, it should be of order N−m, and secondly, it will only contain functions of order N−m or lower, since each time the operator $(\nabla\dot{\nabla})$ is eliminated with the aid of Eq. (15), the function with the largest number is also eliminated. In view of this, the form of the equation should be

$$L_{N-m}U_{N-m} = \varphi_{N-m}\,[(\nabla\mu)\,U_{N-m-1};\ \ \mu^2 U_{N-m-2}\ \text{etc.}]. \tag{17}$$

The operator L_{N-m} cannot contain $\nabla\mu$ or μ^2 since this would be in conflict with the order of the equation. At the same time, this operator should include differentiation with respect to r m times if m is even, and m+1 times if m is odd. This is due to the fact that the operator $(\nabla\dot{\nabla})^m$ is equivalent to differentiation with respect to r m times, and the functions N_{M-1}, U_{N-3}, etc., in the original equation (16) are already being operated on by a multiple differentiation operator with respect to r. However, differentiation with respect to r in the operator L_{N-m} can be expressed through the operator Δ, i.e., L_{N-m} should be a polynomial of degree m/2 in Δ if m is even, and of degree $(m + \frac{1}{2})$ if m is odd.

When m = N the equation contains the function U_0 only:

$$L_0\,(\Delta)\,U_0 = 0. \tag{18}$$

It follows that the characteristic equation of the homogeneous system of equations will be of the form

$$L_0\,(p) = 0.$$

It is clear that the number of roots of the characteristic equation, i.e., the eigenvalues $\varkappa^2$, is equal to N/2 if N is even, and (N + 1)/2 if N is odd. To each $\varkappa^2$ there belongs a pair* of eigenfunctions U_0. These eigenvalues and the corresponding solutions will be referred to as principal.

*For each $\varkappa^2$, the special solutions should be formed from $\Delta U = \varkappa^2 U$, which in general has an infinite number of solutions. However, assuming separation of variables, one can reduce it to an ordinary second-order differential equation.

Next, let us proceed in the reverse order and consider the equation for m = N−1:

$$L_1(\Delta)\,U_1 = \varphi_1[(\nabla\mu)\,U_0]. \tag{19}$$

On solving this equation we obtain

$$U_1 = L_1^{-1}(\Delta)\,\varphi_1[(\nabla\mu)\,U_0] + U_1^*, \tag{20}$$

where U_1^* is the solution of the homogeneous equation, i.e., $L_1(\Delta)U_1^* = 0$. Here we come across new eigenvalues which are the roots of the equation $L_1(p) = 0$. We shall call them subsidiary roots. There are two subsidiary proper solutions to each root.

The function U_1 should satisfy Eq. (15), according to which the quantities $(\nabla\dot{\nabla})U_n$ should be expressable in terms of lower-number functions only. It follows that

$$(\nabla\dot{\nabla})\,U_1^* = 0. \tag{21}$$

Similarly, the solution for the functions U_n (for $n < N$) is of the form

$$U_n = L_n^{-1}(\Delta)\,\varphi_n[(\nabla\mu)\,U_{n-1};\ \mu^2 U_{n-2}\ \ldots] + U_n^*, \tag{22}$$

subject to the condition

$$(\nabla\dot{\nabla})\,U_n^* = 0. \tag{23}$$

The functions U_N can be found directly from Eq. (16).

It is clear that it is possible to determine the number of arbitrary coefficients in the general solution. We recall that each function U_n has $2n + 1$ linear independent components, i.e., each equation of order n is in reality a set of $2n + 1$ equations. This means that in the solution for U_n, to each subsidiary root there correspond $2n + 1$ pairs of different subsidiary solutions. The condition given by Eq. (23) represents an equation of order $n - 1$, i.e., equivalent to $2n-1$ equations, and since it should be satisfied by each linearly independent solution of the pair, it follows that to each subsidiary root there correspond $2n-1$ pairs of conditions. Consequently, the number of arbitrary coefficients belonging to a single subsidiary root is equal to

$$2[(2n+1)-(2n-1)] = 4.$$

Solutions corresponding to the principal roots do not have to obey additional conditions, although the number of spherical components in U_0 is equal to unity. It follows that to each principal root there correspond two arbitrary coefficients. It is now quite easy to compute the total number of arbitrary coefficients.

Let us divide Eq. (17) into pairs beginning with the N−1 term. In each pair the degree of the operator-polynomial L_{N-m} with respect to Δ is the same and equal to t (the number of the pair), i.e., the number of subsidiary roots in the pair is 2t. The following two cases will be considered separately.

1. N odd. After subtracting the equation of number N we obtain N equations. The number of pairs is equal to $(N-1)/2$; and the zero-number equation does not form a pair. The number of all the arbitrary coefficients is

$$8\sum_{t=1}^{\frac{N-1}{2}} t + 2\,\frac{N+1}{2} = N(N+1).$$

2. N even. Let us divide the N equations, with the exception of equation of number N, into pairs. The total number of pairs is N/2. Of these, $(N/2)-1$ pairs contain subsidiary roots only. In the last pair one-half of the roots are subsidiary and the rest principal. The number of arbitrary coefficients is

$$8\sum_{t=1}^{\frac{N}{2}-1} t+6\frac{N}{2}=N(N+1).$$

We thus see that the number of arbitrary coefficients in the general solution of the system is independent of the parity of the approximation and is equal to N(N + 1).

In order to obtain the solution of the nonhomogeneous system of equations it is sufficient to add to the general solution of the homogeneous system a special solution associated with the presence of the righthand side, which in our case can be expressed in terms of the polynomials Q_n. Proceeding in accordance with the above scheme, we shall find that the righthand part $q_{N-m}[Q_0; Q_1; Q_2 \cdots Q_N]$, will appear in Eq. (17), and hence the required special solution will be of the form

$$U_n = L_n^{-1}(\Delta)\, q_n[Q_0; Q_1; Q_2 \cdots Q_N]. \tag{24}$$

A more detailed analysis of the solution is not of interest in the present context.

Boundary conditions in the P_N approximation

It is usually assumed as self-evident in the method of spherical harmonics that all the spherical harmonics retained in the P_N approximation should be continuous across the separation boundary between the two scattering media.

In one-dimensional problems, the number of arbitrary coefficients in the solution is equal to the number of spherical harmonics if the order of the approximation is chosen to be odd. In this case the requirement that all the harmonics should be continuous can be satisfied, and it is probably for this reason that one-dimensional problems are always discussed in the literature in terms of the odd (most frequently P_1 and P_3) approximations. However, in the general case, the continuity condition for all the harmonics, right up to N, cannot be satisfied even in the case of the odd approximations, owing to the lack of coefficients. This can be easily verified in the case of the P_1 approximation for the three-dimensional problem. The number of spherical harmonics in this case is equal to four, while the number of coefficients given by the formula derived above is two. It followed that the conditions for the mating of all the harmonics cannot, in general, be mathematically incorrect. The problem of the boundary conditions in the general case is treated in Davison's book [3], but in our opinion a satisfactory solution of this problem is not given. We shall try to derive the boundary conditions which, without loss of generality, should remain applicable for any N.

We note that in the derivation of the initial equations (8) or (13) it is not necessary for the cross-sections to be constant in the medium, and hence the equations are applicable to the heterogeneous ensemble as a whole, provided it is assumed that the cross-sections are piecewise constant functions of the spatial coordinates. It is important that the equations are assumed to hold also at points lying on the boundary itself. This will enable us to formulate the necessary boundary conditions.

In a medium with continuously distributed sources, the terms S_n and $\Sigma_n Y_n$ in Eq. (8) are bounded everywhere, including points on the boundary. It follows that the magnitude of div $\mathbf{F}_n$ should also be bounded at all points. We shall derive a condition for the magnitude of div $\mathbf{F}_n$ to remain bounded on the separation boundary of two media.

Let us construct three mutually perpendicular unit vectors ν, η, ξ at an arbitrary point $\mathbf{r}_0$ on the separation boundary. Suppose that one of them, for example, ν, is in the direction of the normal to the surface. It is clear that the two remaining unit vectors η and ξ will be tangential to the surface. In the neighborhood of the point $\mathbf{r}_0$, he vector $\mathbf{F}_n$ can be represented by

$$\mathbf{F}_n = F_{n\nu}\boldsymbol{\nu} + F_{n\eta}\boldsymbol{\eta} + F_{n\zeta}\boldsymbol{\zeta},$$

in which case

$$\operatorname{div}\mathbf{F}_n = \frac{\partial F_{n\nu}}{\partial \nu} + \frac{\partial F_{n\eta}}{\partial \eta} + \frac{\partial F_{n\zeta}}{\partial \zeta}.$$

The components of the vector $\mathbf{F}_n$ in the two media are finite at all points adjacent to the boundary. This means that on the boundary itself they are either continuous or have a finite discontinuity.

Let us assume that $F_{n\eta}$ and $F_{n\zeta}$ are discontinuous. This means that they are indeterminate on the boundary. The derivatives $\frac{\partial F_{n\eta}}{\partial \eta}$ and $\frac{\partial F_{n\zeta}}{\partial \zeta}$ along the η and ζ directions, which are tangential to the boundary, will in general also have a finite discontinuity and will be indeterminate at $\mathbf{r}_0$. However, since the discontinuity is finite, the indeterminancy does not mean that the function will be infinite, i.e., the discontinuity in the components $F_{n\eta}$ and $F_{n\zeta}$ does not contradict the fact that $\operatorname{div}\mathbf{F}_n(\mathbf{r}_0)$ is bounded. If, on the other hand, the component $F_{n\nu}$ has a discontinuity at $\mathbf{r}_0$, then in accordance with the definition of the derivative,

$$\frac{\partial F_{n\nu}}{\partial \nu}(\mathbf{r}_0) = \lim_{\varepsilon \to 0} \frac{F_{n\nu}\left(\mathbf{r}_0 + \frac{\varepsilon}{2}\nu\right) - F_{n\nu}\left(\mathbf{r}_0 - \frac{\varepsilon}{2}\cdot\nu\right)}{\varepsilon} = \infty,$$

since

$$F_{n\nu}(\mathbf{r}_0 + 0\nu) \neq F_{n\nu}(\mathbf{r}_0 - 0\nu).$$

It follows that $\operatorname{div}\mathbf{F}_n$ can only be bounded at $\mathbf{r}_0$, if $F_{n\nu}$ is continuous at this point. Since the point $\mathbf{r}_0$ is arbitrary, the result is general and holds at all points on the separation boundary. The boundary conditions for the P_N approximation can be expressed in terms of the requirement that the quantities $F_{n\nu}$ should remain continuous for all numbers between 0 and N.

Let us determine the number of equations which have to satisfy this requirement. According to Eq. (12), for the P_N approximation

$$\mathbf{F}_n = [\dot{\nabla} U_{n+1} + (2n-1)\,\mu U_{n-1} - \mu^2 \dot{\nabla} U_{n-1}]_{\mu=1} \quad \text{for } n < N; \tag{25}$$

and

$$\mathbf{F}_N = [(2N-1)\,\mu U_{N-1} - \mu^2 \dot{\nabla} U_{N-1}]_{\mu=1}. \tag{26}$$

The boundary conditions can then be written down in the following form:

$$[(2N-1)(\nu\mu) - \mu^2(\nu\dot{\nabla})]\,U_{N-1}; \tag{27}$$

$$(\nu\dot{\nabla})U_{n+1} + [(2n-1)(\nu\mu) - \mu^2(\nu\dot{\nabla})]\,U_{n-1} \tag{28}$$

are continuous for n < N.

The components of the normal ν_x, ν_y, ν_z are determined by the form of the boundary.

The condition given by (27) is equivalent to 2N + 1 algebraic equations containing only 2N−1 components of the function U_{N-1}. It follows that the condition (27) can only be satisfied if the function U_{N-1} is continuous.

Consider now the conditions (28) for n = N−2, in which case

$$(\nu\dot{\nabla})\,U_{N-1} + [(2N-5)(\nu\mu) - \mu^2(\nu\dot{\nabla})]\,U_{N-3} - \tag{29}$$

is continuous.

Since the continuity of U_{N-1} is a consequence of the continuity of $(\nu\nabla)\,U_{N-1}$, it follows that the second term in Eq. (29) should also be continuous, and this means that the function U_{N-3} should be continuous. Proceeding in this way we find that all the spherical harmonics U_{N-1}, U_{N-3}, U_{N-5}, etc., are necessarily continuous. We shall call these the first group of conditions.

This conclusion does not hold for the harmonics U_N, U_{N-2}, U_{N-4}, etc. For these harmonics the boundary conditions have to be written down in the original form (28), i.e.,

$$\left.\begin{aligned}&(\nu\dot{\nabla})\,U_N+[(2N-3)\,(\nu\mu)-\mu^2\,(\nu\dot{\nabla})]\,U_{N-2};\\&(\nu\dot{\nabla})\,U_{N-2}+[(2N-7)\,(\nu\mu)-\mu^2\,(\nu\dot{\nabla})]\,U_{N-4}\\&\cdots\cdots\cdots\cdots\cdots\cdots\cdots\end{aligned}\right\} \tag{30}$$

are continuous.

It is easy to see that the neglect of the function U_N in this group of conditions would lead to the continuity of the functions U_{N-2}, U_{N-4}, U_{N-6}, etc. It follows that in our approximation the discontinuity in the above functions is of the order of U_N. If with increasing n, the spherical harmonics U_n become attenuated, then in the limit, i.e., for an infinitely increased N, the magnitude of the discontinuity would become arbitrarily small. Let us call these the second group of conditions. We can now calculate the number of equations to which the above conditions can be reduced.

The mating of each harmonic of number $N-2t-1$ (in the first of the above two groups) is equivalent to a set of $2(N-2t-1)+1$ equations. Each mating in the second group is also equivalent to $2(N-2t-1)+1$ equations. In summing up all the equations it is necessary to consider the limits of t in the following two cases:

1) N even. Here, in the first group

$$1\leqslant 2t+1\leqslant N-1$$

and in the second group

$$0\leqslant 2t\leqslant N-2,$$

i.e., in both groups $0 \leq t \leq (N/2)-1$. It follows that the total number of all the matings is

$$2\sum_{t=0}^{\frac{N}{2}-1}[2\,(N-2t-1)+1]=N\,(N+1).$$

2. N odd. In the first group

$$1\leqslant 2t+1\leqslant N,$$

and in the second

$$0\leqslant 2t\leqslant N-1,$$

i.e., in both groups $0 \leq t \leq (N-1)/2$. Hence the number of matings is

$$2\sum_{t=0}^{\frac{N-1}{2}}[2\,(N-2t-1)+1]=N\,(N+1).$$

The coefficients of the two media take part in the mating process, although one-half of the coefficients in each medium are used to satisfy the conditions on the opposite boundary, at infinity, at the origin, etc. Thus, the total number of unknown coefficients and the number of mating equations are equal, whatever the order of the approximation. In special cases when, owing to symmetry conditions, some of the harmonics vanish, the number of matings is correspondingly reduced, but then some of the subsidiary solutions will vanish. In one-dimensional problems all the subsidiary solutions should vanish, since otherwise condition (23) cannot be satisfied. Consequently, the number of coefficients is equal to twice the number of the principal roots, i.e., 2N if N is even and $2(N+1)$ if N is odd. In this case each spherical function contains only one component and hence, the number of mating equations is also equal to N and $N+1$, respectively, as can be easily verified by direct calculations. It is clear that with odd N the number of equations is equal to the number of spherical harmonics, and hence it is necessary to mate all the harmonics separately.

Since the spherical functions are orthogonal it may be shown that the boundary conditions derived above are equivalent to the requirements that the following integrals should be continuous:

$$\int_{4\pi} \Omega_\nu F(\mathbf{r}, \Omega) Y_{nm}(\Omega)\, d\Omega, \qquad (31)$$
$$0 \leqslant m \leqslant n, \quad 0 \leqslant n \leqslant N.$$

In other words, these boundary conditions ensure the continuity of the function $\Omega_\nu F$ with the aid of spherical moments of order up to N inclusive.

It is well-known that the continuity of $\Omega_\nu F$ can be obtained directly from the original transport equation, but in the exact solution the multiplier Ω_ν is unimportant because it is common. As we have seen, Ω_ν plays an important role in the method of spherical harmonics. The requirement that F rather than $\Omega_\nu F$ should be continuous leads in the P_N approximation to incorrect boundary conditions, since it involves the mating of all the spherical harmonics of order 0 to N, which in general is not possible.

Extrapolated Boundary of a Semi-infinite Medium

Order of approximation	Boundary with vacuum*	Boundary with black-body
P_1	0.667	0.577
P_2	0.667	0.776
P_3	0.705	0.694
P_4	0.702	0.730
P_∞	0.710	0.710

*With Marshak conditions

SUMMARY

We have obtained the boundary conditions only for the case where the P_N approximation of the method of spherical harmonics is used in both of the adjacent media. If, on the other hand, the solution of the transport equation is required on one side of the boundary only, then the number of free coefficients available for the conditions on the boundary is reduced by a factor of 2. In that case, the boundary condition should be specified by a distribution function defined within one-half of the total solid angle (if the medium is convex throughout). These quite new considerations prevent a straightforward extension of the above boundary conditions to the present case. However, one can probably maintain that any approximate boundary conditions must be based on the behavior of the function $\Omega_\nu F$ and not F alone. For example, on the boundary with a vacuum, and in the case of the Marshak conditions [3, 5], this consideration enables one to decide in favor of functions which are odd in Ω_ν, since the expansion of F in the interval $-1 \leq \Omega_\nu \leq 0$ in terms of odd harmonics is roughly equivalent to the expansion of $\Omega_\nu F$ in terms of even harmonics, while the expansion of F in terms of even harmonics cannot be reduced to the expansion of $\Omega_\nu F$. The number of odd functions of order between 0 and N is $\frac{1}{2}N(N+1)$, i.e., the number of boundary conditions is the same as the number of free coefficients.

The vacuum is physically equivalent to a perfect black body, and hence, it is occasionally replaced by a medium in which the capture cross-section tends to infinity. This formal device enables one to use boundary conditions of the type discussed in the present paper even though, strictly speaking, the P_N approximations of not too high an order are not applicable in a strongly absorbing body.

The table gives a summary of the computed extrapolated boundary for a semi-infinite non-absorbing medium with a plane surface. It is known that with an isotropically scattering medium the extrapolated boundary lies at a distance of $\gamma\lambda_s$ from the real boundary. The table gives the values of γ in the first four approximations, and also the exact value.

It should be pointed out that in the case of one-dimensional plane geometry, and in the absence of absorption, the contributions due to even approximations are the least significant. The above table can only provide limited information about the errors and the convergence of even approximations as compared with odd approximations.

In multidimensional problems, concerned with the diffusion of neutrons in directions perpendicular and tangential to the boundary, even approximations will have the property that all the components of the diffusion current will be continuous and not only the normal component as in the odd approximations. This is important in the averaging of the diffusion coefficients over various directions in a heterogeneous medium. The P_2 approximation, which has so far remained practically unexplored, is of interest.

The P_2 approximation is in many cases more accurate than the P_1 approximation, and is capable of including certain effects which are omitted in the P_1 approximation, for example, the dependence of γ on absorption in the medium, the curvature of the surface, and other defects. The P_2 approximation gives a more correct description of the diffusion of neutrons in multidimensional problems. It gives good results in media with relatively large absorp-

tion. At the same time, the P_2 approximation involves roughly the same order of complexity as the P_1 approximation, and is of course, much simpler than the P_3 approximation. However, as in the case of the P_1 approximation, it can only provide the asymptotic solution of the transport equation. This must be borne in mind whenever the dimensions of the medium are small.

In conclusion, the author wishes to thank Candidate of Physicomathematical Sciences, V. V. Orlov, for his consideration, interest and frequent discussions of the results. Thanks are also due to É. I. Gladyshev for assistance, and to all other colleagues who took part in discussions.

LITERATURE CITED

1. A. D. Galanin, Theory of Thermal-neutron Reactors [in Russian], Atomizdat, (Moscow, 1959).
2. S. Glasstone and M. C. Edlund, Elements of Nuclear Reactor Theory [Russian translation] Izd. inostr. lit. (1954).
3. B. Davison, Neutron Transport Theory [Russian translation], Atomizdat (1960).
4. V. I. Smirnov, A Course of Higher Mathematics [in Russian], Vol. III, Pt. 2, Gostekhizdat (Moscow, 1950).
5. R. Marshak, Phys. Rev., 71, 443 (1947).

THE RED COLORATION OF MINERALS IN URANIFEROUS VEINS

Yu. M. Dymkov and B. V. Brodin

Translated from Atomnaya Énergiya, Vol. 10, No. 1,
pp. 35-42, January, 1961
Original article submitted June 15, 1960

This paper describes different types of hematitization of ferruginous carbonates (siderite, ankerite and ferruginous manganocalcite) in uraninite-bearing veins.

It has been ascertained that hematitization not spatially associated with uraninite may be pre-ore or post-ore and may differ in origin. It may be related to oxidation of iron carbonates as a result of chemical activity by hydrothermal solutions and may also be due to mechanical transfer of fine particles, by solutions, of previously formed hematite. Hematitization, systematically associated with uraninite and forming, in ferruginous carbonates, aureoles about uraninite lenses, is of radiogenic origin.

In conclusion, note is taken of the practical value of the various types of hematitization as indicators in prospecting for uranium in hydrothermal vein deposits.

Introduction

For a long time miners and geologists have known that a reddish aureole ("red alteration") is commonly found around uraninite in carbonates, barite, and feldspars, the color being due to fine flakes of hematite or finely-dispersed hematite in these minerals. Such hematitization is thought to be the result of radioactive irradiation [1,2] or of oxidation-reduction processes originating in the solutions between Fe^{2+} ions and uranyl ions (UO_2^{2+}) [3,4]. It has been suggested that the hematitization may be associated with the oxidizing action of carbonic acid solutions devoid of sulfur ions [5]. Not long ago, a new view was advanced – that the cause of the red coloration in rocks containing uranium deposits is due to the oxidation of iron associated with "... radiation-chemical reactions originating in hydrothermal uranium-bearing solutions" [6]. It should be noted that the existing views give no consideration to the possibility of different origins for the hematitization found in uraninite-bearing veins. It is well known that hematitization is also observed at nonuraniferous deposits and in barren veins at uranium deposits. On the other hand, some districts containing rich uranium ores show no red alteration [7,8].

The authors of the present paper have studied the red coloration of minerals in uraniferous carbonate veins consisting of the paragenetic sequence of siderite, ankerite and manganocalcite and of calcite of several generations. The uraninite in these veins is closely associated with late nonferruginous calcite and a very small quantity of sulfides, most of which formed after deposition of the great bulk of the uraninite.

In spatial relations the red coloration in the uraniferous carbonate veins may be divided into two types of hematitization, varying in practical importance: hematitization spatially unrelated to the accumulations of uraninite and hematitization forming reddish aureoles about uraninite lenses.

Hematitization Spatially Unrelated to Uraninite

In relation to the time of deposition of the uraninite, hematitization may be divided into an early (pre-ore) and a late (post-ore) phase in the vein carbonates. The best defined is the early phase, being characterized by an intimate association of hematite and goethite. Both minerals arise from oxidation of ferrous iron in siderite, ankerite, and ferruginous calcite. The hematite-goethite association is commonly observed through extensive parts of the veins, measured along the strike or down the dip in tens and hundreds of meters, and occurring in places where there is absolutely no uraninite nor any other minerals of the uraninite stage. In the lower parts of the veins the hematitization locally increases in intensity, whereas the level of mineralization in the same vein is considerably nearer the surface.

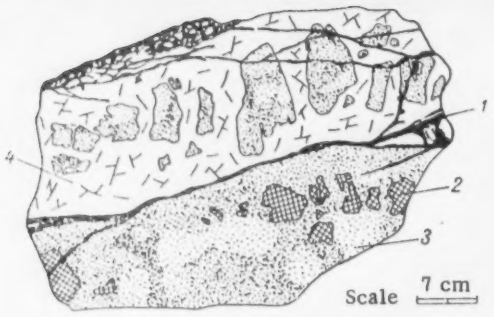

Fig. 1. Intersection of uraninite veinlets (1) with fragments of extensively hematitized ankerite (2) and hematitized ferruginous manganocalcite (3). The hematitization occurred before the deposition of grayish white granular calcite (4). Drawn from a hand specimen.

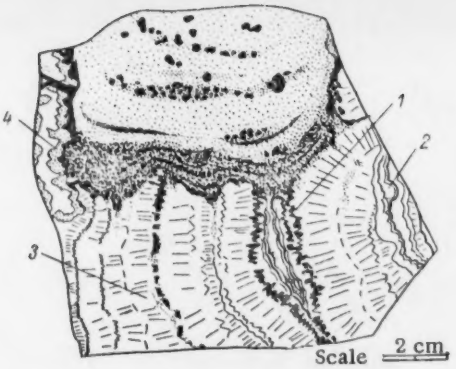

Fig. 2. Mineral level in a solution cavity of a carbonate vein. The level consists of alternating layers of "alluvial" hematite, clay material, and rock fragments cemented with calcite: 1) hematite, partly invading along growth zones in crystals of manganocalcite; 2) colloform manganocalcite; 3) radiating manganocalcite; 4) partly hematitized ankerite. Drawn from a polished hand specimen.

Of the iron oxides, the most widespread is dispersed cherry-red hematite (identification confirmed by x-ray studies); well-crystallized hematite and radiating goethite are less abundant. The latter occurs as metacrysts in already hematitized siderite, partly replacing early hematite. Locally, the goethite forms extensive accumulations of radiating aggregates. It is characteristic that in such zones chalcopyrite, of the early sulfides, proves to be unstable, being replaced by bornite and then by cubic chalcocite.

Thus, the early hematitization in the investigated uraniferous veins does not differ fundamentally from the hematitization observed in a number of nonuraniferous lead-zinc deposits [9-11].

The deposition of the uraninite occurred considerably after the early hematitization, and the formation of goethite was not genetically related to either process. Proof of this is found in widely observed intersections of hematitized siderite and ankerite with fresh manganocalcite (containing about 1% $FeCO_3$), its pale rose or white color unchanged. In individual veins fragments of hematitized ankerite and early manganocalcite are cemented by gray granular calcite and then cut by veinlets of uraninite (Fig. 1). Furthermore, the early hematitization in ore veins apparently had an adverse influence on the localization of uraninite. In zones where siderite has been extensively replaced by goethite and early hematite, uraninite is generally absent or present only in small quantities.

Apart from the described early hematitization, the age of which is clearly established, red coloration of dispersed hematite and later calcite is also observed locally. This hematite probably represents a residuum from the solution of the early hematitization of the carbonates. Dispersed and colloidal particles of hematite invaded crystal aggregates of calcite along the seams between grains, and also attacked calcite in the process of crystallization. On the floor of hypogene solution cavities of early carbonates (ankerite and early manganocalcite), one may find layered aggregates of dispersed hematite* (Fig. 2). The hematite penetrates along the contacts between grains of the ferruginous manganocalcite to some distance from the layered precipitates, although the great bulk of the manganocalcite is not hematitized. These facts represent good examples of "mechanical" redeposition.

It is possible that some of this hematite was formed by oxidation of ferrous iron in the carbonates in the solutions from which the minerals of the uraninite stage were deposited [13]. It is assumed that such solutions, during the transport of the uranium, were essentially oxidizing. The activity of these solutions was also responsible for dolomitization of manganocalcite, producing dark gray borders about the grains of this mineral, and for the precipitation of hematite immediately before the deposition of uraninite.

The late hematitization in the ore veins, occurring much later than the deposition of uraninite and the succeeding sulfides (Fig. 3). is of limited development. Apart from zones of red coloration in post-ore calcite, microscopic

*Such formations have been termed "mineral levels" [12].

inclusions of goethite or hematite spherulites are found in individual crystals of calcite and quartz. The origin of the late hematitization is unclear.

Hematitization Associated with Uraninite (Radiogenic Hematitization)

Hematitization systematically associated with uraninite is found only about uraninite lenses, forming distinct aureoles (Fig. 4). In carbonate veins the hematitization involves only the ferruginous carbonates. Nonferruginous carbonates, even near large accumulations of uraninite, remain unaltered.

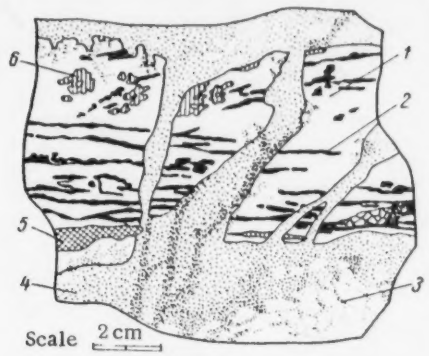

Fig. 3. Intersection of uraninite veinlets with later hematitized calcite: 1) grayish-white calcite; 2) uraninite; 3) rose-colored granular calcite; 4) late hematitized calcite; 5) hematitized ankerite; 6) chalcocite with inclusions of chalcopyrite grains. Drawn from a polished hand specimen.

Near the ore lenses ankerite (9.27% FeO) shows various degrees of hematitization; manganocalcite (1.08% FeO) is very strongly hematitized, and white calcite (up to. 0.28% FeO) only weakly hematitized. The latter mineral commonly remains unchanged.

The extent of the aureoles of hematitization along the strike and down the dip corresponds approximately to the dimensions of the uraninite lens or nest, and the width is generally limited by the thickness of the vein.* Below is shown the relation between dimensions of aureoles of reddened carbonates and the dimensions of uraninite segregations. This relation is most clearly observed in small point-like segregations:

Diameter of uraninite spherulites, mm	Width of hematitization aureole in the carbonates, mm
0.05	2
0.1	3†
0.3	8
0.5	25
0.15-1 (incrustation)	7-8
3.5	more than 180

The morphology of the red-colored aureoles depends on the internal structure, the dimensions, and the position of the ferruginous carbonates in the veins.

Manganocalcite shows the greatest alteration near the uraninite. The primary color of the manganocalcite is rose, pale rose, or white. In individual zones not associated with segregations of uraninite, the manganocalcite is zonally or spottily (near minute fractures) gray or dark gray, apparently because of disseminated manganese oxides.

TABLE 1. Chemical Composition of Manganocalcite (analyzed by B. M. Eloev)

No. of analysis	Color	FeO	MnO	MgO	CaO	Fe_2O_3	CO_2	Insoluble residues	Totals
1	Red-brown, beige	0.75	5.34	0.54	49.55	0.37	43.10	0.20	99.85
2	Dark gray	0.44	4.94	1.21	49.85	Not detected	43.72	0.20	100.36
3	Rose	1.03	5.05	0.68	49.30	0.48	43.30	0.22	100.11
4	Cherry-red	0.61	4.88	0.18	50.02	1.20	42.67	0.20	99.76
5	Cherry-red	0.61	4.67	0.12	49.75	2.63	42.35	0.20	100.33

Hematitization near uraninite rarely extends to the zones of gray coloration. Individual zones of earth manganocalcite are grayish brown or light brown with rose-yellow tints. Admixtures of goethite generally impart such colors to

*In places such aureoles of red coloration were observed superimposed on zones of early hematitization, creating a very complex picture of alteration in the vein carbonates.

† An inner dark-colored ring 0.75 mm wide can be distinguished in this aureole.

the carbonates. Around individual segregations of uraninite, locally in zones, one may see dark red, beige, and dark gray colors. The mangocalcite varies somewhat in composition in the different zones, as chemical analyses show.

Thus, gray zones contain a high quantity of magnesium and are characterized by a rather low content of ferrous oxide (see analysis 2, Table 1)*.

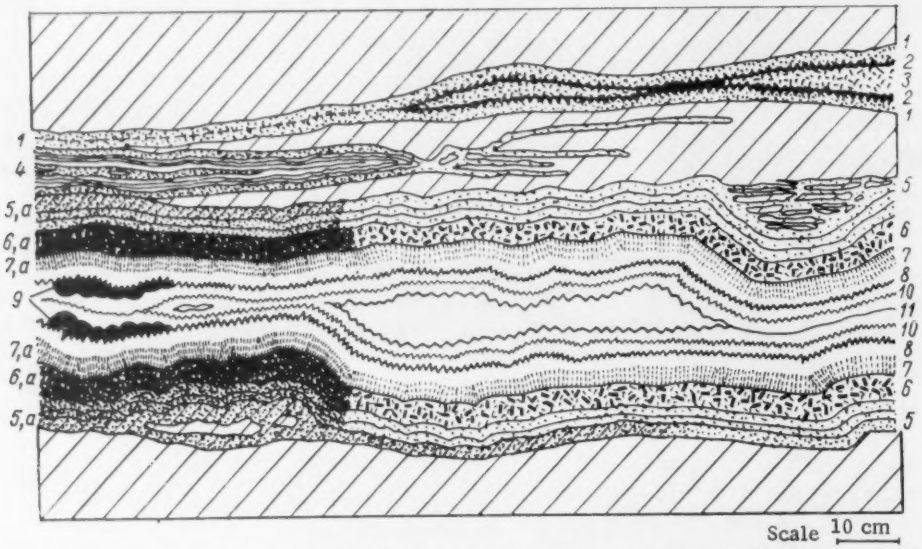

Fig. 4. An aureole of red coloration about a nest of uraninite: 1) hematitized siderite (without goethite); 2) smoky quartz; 3) hematitized ankerite; 4, 5, 6) different generations of manganocalcite; 5a, 6a) intensely hematitized manganocalcite; 7) columnar calcite; 7a) columnar calcite hematitized; 8) scalenohedral white calcite (nonferruginous); 9) uraninite; 10) scalenohedral late calcite; 11) stubby rhombohedral calcite. Center of a drusy cavity. Drawn from a zone in the roof of a mine working.

A comparison of hematitized cherry-red (0.5 m from uraninite) and rose-colored (3 m from uraninite) manganocalcite from the base of an earthy incrustation shows a connection between the hematitization and the oxidation of ferrous iron that was present at the site (see analyses 3 and 4, Table 1).**

A recomputation of the data of analyses 3 and 4 (Table 1) to metals indicates that the quantity of iron increases 0.14% in the hematitized zones (analysis 3, Table 2). In zones where uraninite is segregated in fractures that cut manganocalcite, films of introduced hematite are observed along individual slippage plains, barren of uraninite; these are due to a substantial increase in the Fe_2O_3 content in the manganocalcite (see analysis 5, Table 1).

Partial analyses of unaltered and hematitized carbonates (see analyses 1 and 2, Table 2) show that the amount of iron may increase substantially both in the aureoles of hematitization of manganocalcite and in the zones of early red coloration of ferruginous calcite. The increase in iron in the colored aureoles about uraninite lenses attests not only to the oxidation of ferrous iron of carbonates in place but also to some introduction of iron from the solutions that deposited hematite at the zones of oxidation.

* Spectral and x-ray analyses of the ferruginous manganocalcite have shown that the content of microscopic admixtures did not change noticeably during hematitization.

** No "blackening" of manganocalcites (by oxidation of Mn^{2+}) was observed in the aureoles of hematitization, despite a marked preponderance of Mn^{2+} over Fe^{2+}. This may be due to the relatively high oxidation-reduction potential of the reaction $Mn^{2+} \rightarrow Mn^{4+} + 2e$ (Mn^{3+} gives a rose color) in comparison with $Fe^{2+} \rightarrow Fe^{3+} + e$ [14]. Intense oxidation of Mn^{2+} in manganocalcite is known only in zones of exogene processes.

X-ray studies of the insoluble residue and the elutriation products of comminuted manganocalcite have shown that the great bulk of the staining substance, as also in the zones of early coloration, is hematite.* Brown oxides of iron (goethite) are less commonly present near the uraninite lenses than is hematite. In the aureoles of hematitization they formed mostly after the hematite, being related in time with the late (post-ore) hematitization.

There is no reliable data indicating simultaneous formation of hematite and uraninite. Where nonferruginous pre-ore calcite is associated with uraninite, no aureoles of red coloration are observed about the uraninite. Hematite and goethite are also absent in the white nonferruginous scalenohedral calcite that was deposited simultaneously with uraninite in thin veinlets.

TABLE 2. Change in Content of Iron Oxides during Hematitization of Pre-Ore Carbonates

Number of analysis	Minerals	Content in unaltered mineral, %		Content in hematitized mineral, %		Quantity of FeO changed to Fe_2O_3	Total introduction of iron	Type of hematitization
		FeO	Fe_2O_3	FeO	Fe_2O_3			
1	Early columnar calcite	1.58	0.50	0.86	2.90	0.72	1.12	(*)
2	Colloform manganocalcite	1.00	0.12	0.79	2.34	0.21	1.40	(**)
3	The same	1.08	0.48	0.61	1.20	0.47	0.14	(**)

(*) Early, not associated with the formation of uraninite.
(**) Aureole of alteration about accumulations of uraninite.

These facts indicate that the aureoles of red coloration in the carbonates about uraninite are not associated directly with the deposition of the uraninite, but were formed later. The hematite in these aureoles, as analyses have shown (see Tables 1 and 2) was formed not only by oxidation of ferrous iron in the carbonates but also by oxidation of iron introduced from outside in later stages. Different relative ages for the iron oxides attest that the oxidation of Fe^{2+} about the uraninite continued for a long period of time.

The morphological features of the segregated hematite in the zones of red coloration in the carbonates and, above all, the isolation of hematite along the contacts of crystal grains of manganocalcite (Fig. 5) show that the hematite was deposited from hydrothermal pore solutions (the calcite rock containing the lenses and nests of uraninite has a porosity of 0.7-2%).

The striking restriction of hematite to uraninite segregations, the later formation of the hematite, and the absence of any connection between hematitization and the deposition of uraninite—all these point to a relationship between the formation of hematite and the effect of uraninite on the hydrothermal solutions. An increase in the width of an aureole of hematitization up to a certain limit (on the order of one meter) corresponding to an increase in the mass of uraninite in a lens suggests, in some degree, a dependence of the penetration of gamma radiation in the rocks on the mass of ore. This leads one to explain the phenomenon of the aureoles of hematitization by radiation chemical processes.** It may be assumed that the aureoles of red coloration were formed by oxidation of a ferrous iron by pore and capillary solutions, the oxygen in which came from radiogenic-chemical reactions associated with prolonged radiation of uraninite. The extensive size of the aureoles of red coloration may be explained by the action of penetrating gamma radiation.*** Prolonged action of radon on the pore solutions that produced the expansion of the aureole of red coloration may have been of fundamental importance.

---

* The x-ray analysis was made by N. G. Nazarenko.

**However, if it is considered that the oxidation occurs because of alpha and beta radiation of uranium ions (or colloidal particles) [6], then it is necessary to assume that these ions existed in solution an extremely long time and in very great concentrations. On the other hand, during such a process (even if the intensity of radiation were sufficient for development of hematite) uraninite should not be associated with the hematite, since the uranium would be oxidized by the same oxygen and would be found in the hexavalent state.

***It is assumed that the inner aureole (0.75 mm) may be referred to the aureole of beta radiation. The aureole of alpha radiation may be observed only under the microscope.

As a result of decay of the uraninite, there may have occurred displacement and redeposition of the uranium in a disseminated state in the carbonates and other minerals. This may have led to the development of numerous new centers of red coloration farther removed from the uraninite lenses.

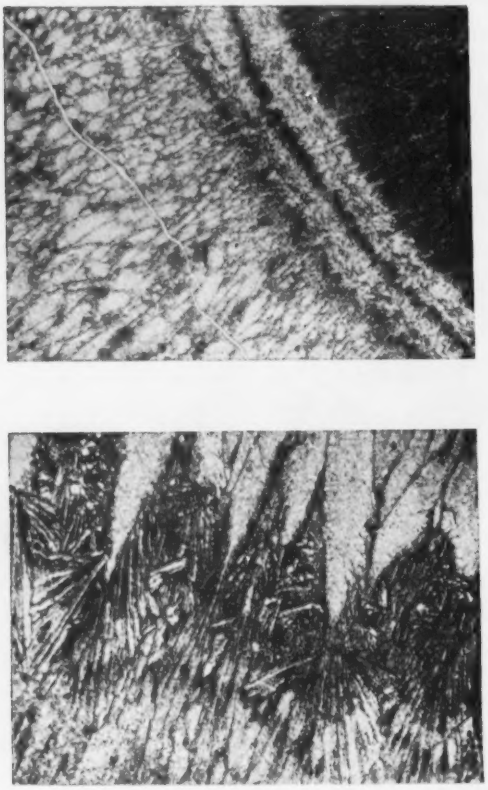

Fig. 5. Distribution of hermatite (black) in hematitized colloform manganocalcite from an aureole of red coloration about uraninite. Photomicrograph of a thin section. Parallel nicols. × 70.

Existing data on the content of uranium in the hematitized and nonhematitized carbonates do not permit us, however, to claim a connection between intensity of hematitization and the presence of disseminated uranium in a mineral.

The clearest increase in uranium content is found in hematitized (of the early coloration) siderite (0.00027%, 0.0045% U), where the quantity of uranium increases a hundredfold in comparison with the unaltered (0.000052%) and tenfold in comparison with the slightly dolomitized siderite (0.00016% U). Inasmuch as the uranium mineralization occurred after the early red coloration, the increase in uranium content in the hematitized carbonates is apparently a consequence of alteration of siderite associated with the hematitization, and is not a cause of the hematitization.

In the hematitized ankerite and manganocalcite such increase in uranium content is not observed. In one of the two analyzed samples of hematitized (early coloration) ankerite, the content of uranium shows a tenfold increase (0.001%U); no change is detected in the other (0.00017% U). The intensely hematitized manganocalcite from the aureoles (0.00014-0.00052% U) shows no substantial increase in uranium content over the slightly altered (0.00001-0.0001% U) varieties (in one sample the increase was on the order of 0.00105% U). The nonferruginous (stained with later iron oxides) yellowish-grayish-white calcite accompanying uraninite generally contains 0.00n% uranium.

Analyses of ten samples of later post-ore nonferruginous calcite show a content of uranium on the order of 0.000n-0.0000n%. A comparison of the intensely hematitized (hydrothermally altered) and nonhematitized rocks also shows no substantial change. Thus, no clear relationship between hematitization and disseminated uranium has been detected.

CONCLUSIONS

1. Several types of hematitization of vein carbonates are discussed; these are distinguished both in time of formation (relative to the deposition of uraninite) and in localization in space:

a) hematitization unrelated in space or time with uraninite segregations (pre-ore and post-ore);

b) hematitization forming aureoles about accumulations of uraninite.

2. Three genetic types of hematitization are found in veins:

a) early hematitization of iron-bearing carbonates, locally accompanied by segregations of goethite. This hematitization is related to oxidizing conditions, normal for the end stages of mineralization in sulfide deposits;

b) "alluvial" hematitization, appearing repeatedly at various stages of development of the carbonate-uraninite veins. It is associated with solution of hematitized carbonates and mechanical transfer of colloidal and dispersed particles of iron oxide. Solutions containing suspended particles of hematite invaded along contacts between grains and through fractures of the carbonates, staining them irregularly;

c) hematitization forming aureoles about lenses of uraninite, resulting from radiation-chemical processes.

3. Extensive hematitization of various types attests to the repeated manifestation of an oxidation environment under hydrothermal conditions, favorable for the transfer of uranium. The formation of uraninite was not accomplished by hematitization of the earlier iron-bearing carbonates.

4. Early (pre-ore) hematitization is not a direct indicator of uranium. The "alluvial" hematitization, appearing at various stages throughout the course of vein development, merely attests to hypogene solution of early hematitized carbonates. "Radiogenic" hematitization may indicate large accumulations of uraninite near it.

The identification of hematitization with one of the indicated three genetic types may be made by analysis of the age relations of the altered or unaltered iron-bearing carbonates at a given part of the vein.

LITERATURE CITED

1. H. Schneiderhöhn, Lehrbuch der Erzlagerstättenkunde, I. Band, Jena, G. Fischer, 1941.
2. G. Berg, Geochemistry of Mineral Deposits [in Russian], Novosibirsk State Scientific and Technical Press for Literature on Mining Geology, Moscow-Leningrad, 1933.
3. V. V. Shcherbina, The Geochemistry of the Rare Elements, Part 1 [in Russian], Moscow, State Scientific and Technical Press on Geology and Preservation of Mineral Resources, 1946.
4. V. G. Melkov and L. N. Pukhal'skii, Prospecting for Uranium Deposits [in Russian],(Moscow, State Scientific and Technical Press on Geology and Preservation of Mineral Resources, 1957).
5. D. Everhart and R. Wright, Econ. Geol. 48, No. 2, 77 (1953).
6. É. N. Baranov, Atomnaya Énergiya, 5, 6 (1958) p. 662.
7. S. Robinson, Can. Mining and Metallurg. Bull., 45, 480 (1952).
8. A. G. Betekhtin, Geologiya Rudnykh Mestorozhdenii, 6 (1959) p. 124.
9. A. G. Betekhtin, Collection: Principal Problems in the Study of Magmatic Ore Deposits [in Russian], Moscow, Acad. Sci. USSR Press, 1953, p. 122.
10. V. Hanus, Sbornik UUG, Sv. XXII, 69, Praha, 1956.
11. B. V. Brodin, Zap. Vsesoyuz. Mineralog. O-va, 2 (1958) p. 496.
12. D. P. Grigor'ev, Priroda, No. 3, p. 47, 1948.
13. V. V. Shcherbina and D. I. Shcherbakov, "Chemistry and geochemical features of uranium," in the book: Geology, Prospecting and Exploration for Uranium Deposits, Part 1 [in Russian], Moscow, State Scientific and Technical Press on Geology and Preservation of Mineral Resources, 1955.
14. B. Mason, Collection: Questions on Physical Chemistry in Mineralogy and Petrography [Russian translation], Moscow, IL Press, 1950, p. 133.

THE CONNECTION BETWEEN THE STRUCTURE AND ANISTROPY OF THE THERMAL EXPANSION OF URANIUM, NEPTUNIUM AND PLUTONIUM

N. T. Chebotarev

Translated from Atomnaya Énergiya, Vol. 10, No. 1,
pp. 43-49, January, 1961
Original article submitted April 11, 1960

A connection has been established between the anisotropy of the thermal expansion and the changes occurring in the structure of a number of modifications of uranium, neptunium and plutonium on heating. It has been shown that in all structures considered the anisotropy of the thermal expansion is due to a weakening of the four covalent bonds with increase in temperature and their nonuniform distribution in the various crystallographic directions of the lattice. The regularities given lead to a better understanding of certain specific properties of uranium, neptunium and plutonium which distinguish them from ordinary metals.

Introduction

It is known that noncubic modifications of uranium, neptunium and plutonium have different values for the coefficient of thermal expansion in different crystallographic directions. The anisotropy of the thermal expansion has an important effect on the properties of these metals. The different values of the coefficient of thermal expansion in the various crystallographic directions indicate that during heating or cooling, the crystalline lattice does not remain unchanged. This in its turn means that the mutual positions of the atoms in the crystalline lattice change. Therefore, for an analysis of this phenomenon it is essential to establish those relationships governing the change in the interatomic distances in the crystalline lattices with change in temperature.

Structure and Thermal Expansion of α-Uranium

The alpha-phase of uranium has a rhombic structure with lattice parameters a = 2.853 A, b = 5.866 A and c = 4.955 A. The four atoms of uranium in the unit cell occupy positions 4(c) of the space group D_{2h}^{17}—*Cmcm*:

$$\left.\begin{matrix} 0\ y\ \frac{1}{4} \\ 0\ \bar{y}\ \frac{3}{4} \end{matrix}\right\} + \left(000;\ \frac{1}{2}\ \frac{1}{2}\ 0\right),$$

where y = 0.105.

On the projection of three unit cells on the (001) plane (Fig. 1) it can be seen that the atoms of zigzag chains threading the lattice in the direction of the c-axis are arranged in the form of layers with a distance between them of c/2. One of these layers is represented by the atoms ABCDEFO, the other by the atoms $A_1B_1C_1D_1E_1F_1O_1$. On considering a tetrahedron with a base in the form of an isosceles triangle OAF and apex O_1, the following character of coordination appears: $2d_1 = OO_1 = 2.77$ A; $2d_2 = OB = 2.85$ A; $4d_3 = OA = 3.26$A; $4d_4 = OC_1 = 3.31$ A. The mean interatomic distance $d_m = 3.13$ A. If the total coordination number is equal to 12 then the four shortest bonds are separated out with interatomic distances 2.77 and 2.85 A.

If the triangle OAF was equilateral and the projection of the atom O_1 was exactly at its center, then the structure of the α-uranium would be an ideal hexagonal packing. Table 1 compares the values of lattice parameters of such an ideal packing (with the condition $r = d_m/2$) with actual values of parameters for the structure of α-uranium. Here we give the coefficients of thermal expansion in the range 20-500°C according to the data of [1].

TABLE 1. A Comparison of the Lattice Parameters of α-Uranium and an Ideal Compact Packing

Lattice parameters	Ideal values of parameters, A	Actual values of parameters, A	Extent of deviation, %	Coefficient of thermal expansion along the axis, 10^6
a	3.13	2.85	−9.0	32.9
b	5.42	5.87	+8.3	-6.3
c	5.11	4.96	-2.9	27.6
y	0.167	0.105	-37	–

It can be seen from these data that under the action of the above four covalent bonds the lattice suffered considerable deformation, being stretched along the b-axis and shortened along the a-and c-axes.

The interatomic distances in the unit cell are determined from the following expressions:

$$\left.\begin{aligned} d_1 &= \frac{1}{2}\sqrt{(4yb)^2 + c^2}\,; \\ d_2 &= a; \\ d_3 &= \frac{1}{2}\sqrt{a^2 + b^2}\,; \\ d_4 &= \frac{1}{2}\sqrt{a^2 + b^2 + c^2 - 8yb^2(1-2y)}\,. \end{aligned}\right\} \qquad (1)$$

Using expressions (1) we can plot the dependence of the interatomic distances on the temperature since the temperature dependence of the lattice parameters a, b and c are now well known [2].

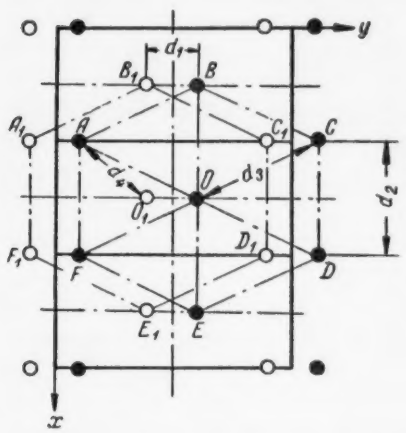

Fig. 1. The projection of three unit cells of α-uranium on the (001) plane. Height in fractions of a parameter c: ●) 1/4; ○)3/4

The results of the calculations are shown in Fig. 2. This figure also gives values of the parameter y which (taking into account the absence of noticeable changes with temperature in the difference in interatomic distances d_4-d_3) can be determined from the following expression:

$$y = 0.250 - \sqrt{0.0656 - \left(\frac{c}{4b}\right)^2}\,. \qquad (2)$$

With increase in temperature the short bonds (see Fig. 2,a) increase considerably, whereas the long bonds (see Fig. 2, b) do not change noticeably. The value of y also increases from 0.105 at room temperature to 0.112 at 640°C, which is in good agreement with the experimental data given in [1].

From equations (1) it follows that $a = d_2$; $b = \sqrt{4d_3^2 - d_2^2}$;

$$c = 2\sqrt{d_1^2 - \frac{d_1^2 + d_3^2 - d_4^2}{4d_3^2 - d_2^2}}\,,$$

i.e., that an increase in the short bonds d_1 and d_2 with temperature in the absence of noticeable changes in d_3 and d_4 leads to an increase in the parameters a and c and a decrease in the parameter b.

The effect of short bonds on the anisotropy of thermal expansion can be seen from a consideration of their orientation with respect to the axes of the lattice. The values of the direction cosines for these types of bonds are as follows:

Type of bond	$\cos\alpha_a$	$\cos\alpha_b$	$\cos\alpha_c$
$2d_1$=2.77 A	0	0.44	0.90
$2d_2$=2.85A	1	0	0

It can be seen from these data that short bonds act mainly in the direction of the a-and c-axes, causing an increase in the coefficient of thermal expansion in these directions with respect to its mean value. On the other hand, in the diection of the b-axis, the coefficient of thermal expansion is much less than its mean value.

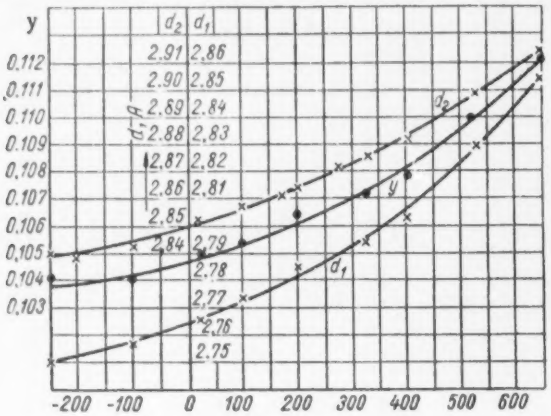

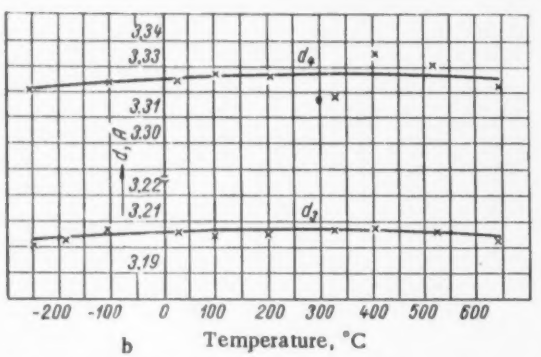

Fig. 2. Temperature dependence of interatomic distances in the structure of α-uranium and the parameter y: a) short bond and parameter y; b) long bonds.

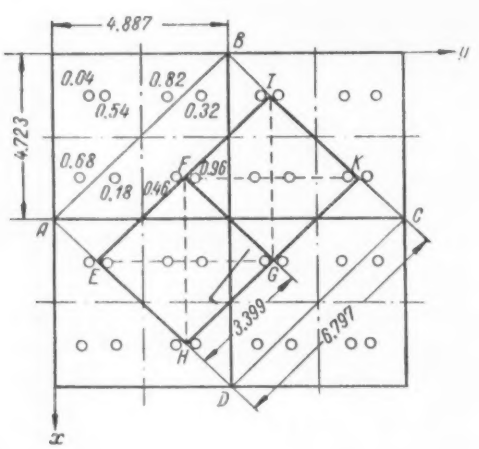

Fig. 3. Projection of four unit cells of α-neptunium on the (001) plane

This analysis shows that the strong anisotropy of the thermal expansion of α-uranium is caused by the considerable weakening of the four covalent bonds with increase in temperature and their uneven distribution along the axes of the crystalline lattice.

Structure and Thermal Expansion of α-Neptunium

According to the data of [3], α-neptunium has a rhombic lattice, the temperature dependence of whose dimensions is given in Table 2. The structure corresponds to the space group D_{2h}^{16} - Pmcn. In each unit cell there are eight atoms occupying the following positions:

$$4\mathrm{Np_I} - 4(c): \pm\left(\frac{1}{4}\, y_1 z_1; \frac{1}{4}, \frac{1}{2} - y_1, \frac{1}{2} + z_1\right),$$

where $y_1 = 0.208 \pm 0.006$; $z_1 = 0.036 \pm 0.006$:

$$4\mathrm{Np_{II}} - 4(c): \pm\left(\frac{1}{4}\, y_2 z_2; \frac{1}{4}, \frac{1}{2} - y_2, \frac{1}{2} + z_2\right),$$

where $y_2 = 0.842 \pm 0.006$; $z_2 = 0.319 \pm 0.006$.

Figure 3 shows the projections of four unit cells of α-neptunium on the (001) plane. From a consideration of the diagonal cells ABCD, which consist of eight cells of the type EFGH and FIKG with dimensions a' = 3.399 A, c' = 3.332A (c'/a' = 0.98) and an apex angle equal to 88° (the cells are on two levels) it can be seen that the structure of α-neptunium is the result of deformations of a body-centered cubic lattice.

Like the previously considered structure, in the α-neptunium structure four covalent bonds appear clearly with distances from 2.60 to 2.63 A. The mean interatomic distance is d_m = 3.10 A.

In accordance with the data given in Table 2, the values of the coefficients of thermal expansion for α-neptunium in the range 20-275°C are equal to:

$$\left.\begin{aligned} \alpha_a &= 24 \cdot 10^{-6}\ 1/°\mathrm{C} \\ \alpha_b &= 25 \cdot 10^{-6}\ 1/°\mathrm{C} \\ \alpha_c &= 34 \cdot 10^{-6}\ 1/°\mathrm{C} \end{aligned}\right\}, \quad \alpha_m = 28{,}6 \cdot 10^{-6}\ 1/°\mathrm{C}.$$

It can be seen from these data that the anistropy of thermal expansion for α-neptunium is expressed rather weakly. Since the anistropy is connected with nonuniform distribution of short bonds along the axes of the lattice, as was observed for the structure of α-uranium, we will consider the projections of these bonds for the α-neptunium structure (Table 3).

It can be seen from these data that the covalent bonds are relatively uniformly distributed along all three axes of the lattice, which is in good agreement with the

absence of clearly expressed anisotropy of the thermal expansion.

At a temperature of 278 ±5°C, a tetragonal structure of β-neptunium forms [3], the result of deformation of the body-centered cubic lattice, but with a degree of distortion much less than for α-neptunium. Of the eight bonds in this structure, four correspond to a minimum interatomic distance $4d_{min}$ =2.79 A and the other four to $4d_{max}$ = + 3.26 A. Hence it can be seen that in the β-neptunium structure, four covalent bonds appear, although in correspondence with the increase in temperature the difference $d_m - d_{min}$ here becomes much less than in the α-neptunium structure (0.23 and 0.48 A respectively). At temperatures of 550-570°C a body-centered cubic lattic of γ-neptunium forms with eight identical bonds at a distance 2.97 A.

Structure and Thermal Expansion of γ-Plutonium

According to the data of [4] γ-plutonium has a rhombic lattice, the temperature dependence of whose dimensions is given in Table 4.

TABLE 2. The Temperature Dependence of the Lattice Parameters of α-Neptunium

Temp., °C	Lattice parameters, A		
	a	b	c
20	4.723±0.001	4.887±0.002	6.663±0.003
212	4.746±0.002	4.909±0.003	6.704±0.004
275	4.752±0.002	4.920±0.003	6.722±0.004

TABLE 3. Projections of Short Bonds on the Axes of the α-Neptunium Lattice

Type of bond	Projections on the axes of the lattice, A		
	d_a	d_b	d_c
$1d_1$=2.598 A	0	1.79	1.87
$1d_2$=2.632 A	0	2.20	1.55
$2d_3$=2.634 A	4.72	1.30	1.94
Σ	4.72	5.29	5.36

TABLE 4. The Temperature Dependence of Lattice Parameters of γ-Plutonium

Temp., °C	Lattice parameters, A		
	a	b	c
213	3.16052	5.76275	10.1442
233	3.15909	5.76769	10.1615
258	3.15622	5.77371	10.1834
312	3.15397	5.78574	10.2290

TABLE 5. The Temperature Dependence of the Interatomic Distances in the Structure of γ-Plutonium

Temp., °C	Interatomic distances, A		
	$4d_1$	$2d_2$	$4d_3$
213	3.022	3.160	3.286
233	3.026	3.159	3.288
258	3.031	3.156	3.290
312	3.052	3.154	3.295

The structure corresponds to the space group D_{2h}^{24} –Fddd. In the unit cell there are eight atoms occupying the position 8(a):

$$\left.\begin{matrix}000\\ \frac{1}{4}\frac{1}{4}\frac{1}{4}\end{matrix}\right\}+\left(000;\ 0\frac{1}{2}\frac{1}{2};\ \frac{1}{2}0\frac{1}{2};\ \frac{1}{2}\frac{1}{2}0\right).$$

The structure of γ-plutonium is an alternation of several distorted pseudohexagonal layers placed perpendicular to the c-axis. Figure 4 shows the projection of three unit cells on the (001) plane and one unit cell on the (100) plane.

The interatomic distances in the γ-plutonium structure and their temperature are given in Table 5. The mean interatomic distance at 213°C is d_m = 3.16 A.

From these data it can be seen that, similar to the previously considered structures, four covalent bonds appear clearly in the γ-plutonium structure, the interatomic distances in the direction of which increase considerably (from 3.022 to 3.052 A) with increase in temperature. The interatomic distances in the direction of the long bond change much less, the distance d_2 even being reduced somewhat with increase in temperature.

The values of the direction cosines for all three types of bond are as follows:

Type of bond	$\cos \alpha_a$	$\cos \alpha_b$	$\cos \alpha_c$
$4d_1=3.022$ A	0.26	0.48	0.84
$2d_2=3.160$ A	1	0	0
$4d_3=3.268$ A	0.48	0.88	0

In accordance with the data given in Table 4 the coefficients of thermal expansion of γ-plutonium in the range 213-312°C are equal to:

$$\left.\begin{aligned} \alpha_a &= -19.7 \cdot 10^{-6}\ 1/°C \\ \alpha_b &= 39.5 \cdot 10^{-6}\ 1/°C \\ \alpha_c &= 84.3 \cdot 10^{-6}\ 1/°C \end{aligned}\right\}, \alpha_m = 34.5 \cdot 10^{-6}\ 1/°C.$$

On comparing these values with the direction cosines given above, it can be seen that the strong anisotropy of the thermal expansion is due to the short bond $4d_1$, mainly acting in the direction of the c-axis. In accordance with this, the coefficient of thermal expansion in the direction of the c-axis has a maximum value, in the direction of the b-axis it is much less, and in the direction of the a-axis it has a negative value.

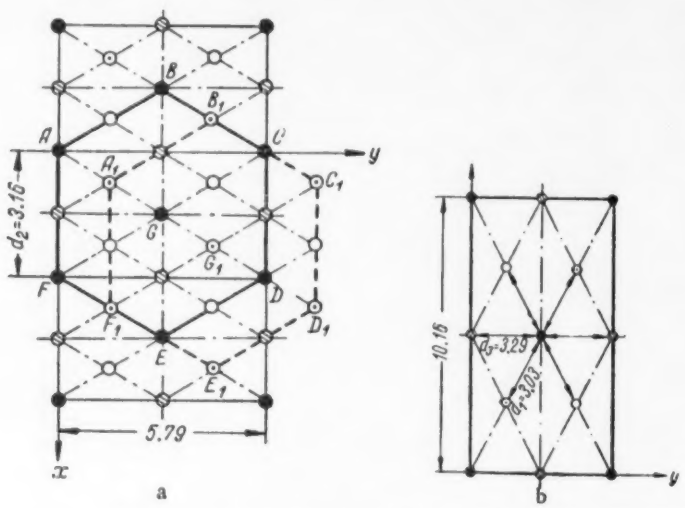

Fig. 4. Projections of three unit cells of γ-plutonium on the (001) plane (a) and one unit cell on the (100) plane (b).
Height in fractions of a parameter c: ●) 0; ⊙) 1/4; ◉) 1/2; ○) 3/4.

Structure and Thermal Expansion of α-Plutonium

According to the data of [5], α-plutonium has a monoclinic lattice, whose parameters at 21°C are:

$$a = 6.1835 \pm 0.0005\ \text{A};\quad b = 4.8244 \pm 0.0005\ \text{A};$$
$$c = 10.973 \pm 0.001\ \text{A};\quad \beta = 101.81 \pm 0.02°.$$

The structure corresponds to the space group $C_{2h}^2 - P2_1/m$. In the unit cell there are 16 atoms, occupying eight double positions:

$$2(e)\colon \pm\left(x\,\frac{1}{4}\,z\right).$$

The approximate values of the x and z parameters are as follows:

Parameters	Pu_I	Pu_{II}	Pu_{III}	Pu_{IV}
x	0.332	0.767	0.138	0.651
z	0.152	0.169	0.337	0.456
Parameters	Pu_V	Pu_{VI}	Pu_{VII}	Pu_{VIII}
x	0.013	0.459	0.335	0.885
z	0.617	0.642	0.924	0.897

Figure 5 shows the projection of four unit cells of α-plutonium on the (010) plane. The numbers near the atoms indicate the number of the position, the atoms with a minus sign are placed at a height equal to half of the parameter with respect to the remaining atoms lying in the plane of the diagram. The structure of the α-phase can be represented as an alternation of very strongly distorted pseudohexagonal layers placed perpendicular to the b-axis at a distance equal to a half of the parameter.

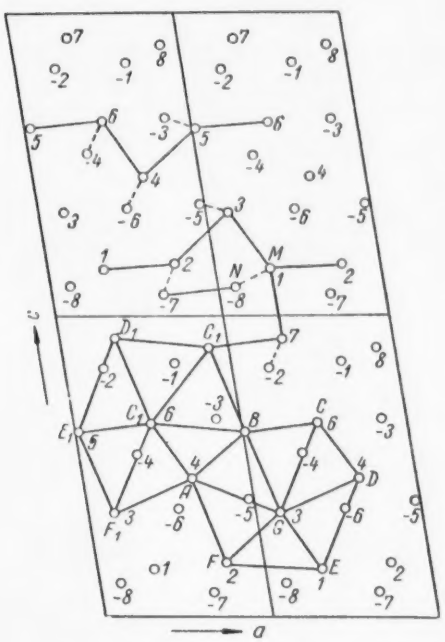

Fig. 5. Projection of four unit cells of plutonium on the (010) plane.

TABLE 6. Interatomic Distances in the α-Plutonium Structure

Position of atoms	Short bonds		Long bonds		Coordination number
	number of bonds	interatomic distances	number of bonds	interatomic distances	
I	5	2.52—2.69	7	3.40—3.51	12
II	4	2.62—2.69	10	3.33—3.62	14
III	4	2.54—2.67	10	3.20—3.67	14
IV	4	2.54—2.70	10	3.20—3.51	14
V	4	2.54—2.73	10	3.30—3.56	14
VI	4	2.58—2.73	10	3.33—3.62	14
VII	4	2.52—2.70	10	3.34—3.56	14
VIII	3	2.68—2.70	13	3.30—3.67	16

TABLE 7. Projections of $d\text{-}d_m$ on the Main Crystallographic Directions of the α-Plutonium Lattice

Direction	Projections of $d\text{-}d_m$, A	
	for short bonds	for long bonds
$\perp c$	—8.8	8.8
$\parallel b$	—7.3	7.3
$\parallel c$	—7.4	9.4

The interatomic distances in the α-plutonium structure for atoms at different positions are given in Table 6.

The top part of Figure 5 shows the short bonds for atoms in all positions, the continuous lines representing bonds lying in one layer and the dotted lines representing bonds between the atoms of neighboring layers (each dotted line corresponds to two bonds).

Atoms at the positions I and VIII (for example, atoms M and N) are joined by a short bond. Considering these atoms as a single whole, we find, as at the other positions, a mean number of bonds per atom of 4, and a coordination number of 14. Therefore, in the α-plutonium structure, as in all the structures considered above, four covalent bonds clearly appear.

TABLE 8. Dependence of the Coefficient of Thermal Expansion on the Main Crystallographic Directions of α-Plutonium and the Temperature

Coefficient of thermal expansion	Temperature range, °C		
	21—104	—196—20	20—100
$\alpha_1 \perp c$	66	49	68
$\alpha_2 \parallel b$	73	53	77
$\alpha_3 \parallel c$	29	14	35

Since the short bonds in the α-plutonium structure nevertheless vary over certain limits (from 2.52 to 2.73 A) in order to characterize their distribution in three mutually perpendicular directions in the lattice, calculations were made for the projections of the difference $d-d_m$ in these directions. The results of the calculations are given in Table 7.

Table 8 gives values of the coefficient of thermal expansion along the directions shown in Table 7 in the temperature range 21—104°C [6], -196—20, 20 to 100°C [7].

It can be seen from the data of this table that the projection of $d-d_m$ both for short and for long bonds has a considerable value along all three directions of the lattice. Therefore, for α-plutonium there is not such a clearly expressed anisotropy of the thermal expansion as for γ-plutonium.

As in the transition from β- to α-neptunium, the difference in the distances d_m-d_{min} increases from 0.23 to 0.48 A, on transition from γ- to α-plutonium this difference increases from 0.12 to 0.56 A. In agreement with this, the covalent character of the bond on transition from high temperature modifications of plutonium to the lower temperature modifications increases considerably and the crystalline structure deviates to a greater extent from the structure of ideal metallic lattices assembled on the principle of compact packing of the atoms.

The saturation of covalent bonds in the low temperature region and their relatively uniform distribution along the various crystallographic directions means the the anisotropy of the thermal expansion for α-plutonium is expressed comparatively weakly.

With increase in temperature, the weakening of the covalent bonds is accelerated and their distribution in the various crystallographic directions becomes more uneven, which finds expression in the strengthening of the anisotropy of the thermal expansion. In fact, the anisotropy of the thermal expansion for β-plutonium, as follows from [6], is expressed more strongly than for α-plutonium, and the anisotropy for γ-plutonium is expressed more strongly than for β-plutonium. The problem of the thermal expansion of δ- and η-plutonium is more complex and requires a special study.

The author is very grateful to S. T. Konobeevskii for discussing the results of this work and for his valuable comments.

LITERATURE CITED

1. S. T. Konobeevskii et al, Proceedings of the Second International Conference on the Peaceful Use of Atomic Energy (Geneva, 1958). Report of Soviet Scientists, Vol. 3, Nuclear Fuel and Reactor Metals [in Russian] (Moscow), Atomic Energy Press, 1959, p. 396.
2. J. Bridge, C. Schwarz and D. Vaughan, J. Metals, 8, No. 10, 1282 (1956).
3. W. Zachariasen, Acta crystallogr., 5, No. 5, 660 (1952).
4. W. Zachariasen and F. Ellinger, Acta crystallogr., 8, No. 7, 431 (1955).
5. Ibid., 10, No. 12, 776 (1957).
6. A. Coffinberry et al, Proceedings of the Second International Conference on the Peaceful Use of Atomic Energy (Geneva, 1958). Selected Reports of non-Soviet Scientists, Vol. 6, Nuclear Fuel and Reactor Materials [in Russian] (Moscow), Atomic Energy Press, 1959, p. 157.
7. N. T. Chebotarev and A. V. Beznosikova, Atomnaya Énergiya, 7, 6, 68 (1959).

THE STRUCTURE AND THERMAL EXPANSION OF δ- AND η-PLUTONIUM

S. T. Konobeevskii and N. T. Chebotarev

Translated from Atomnaya Énergiya, Vol. 10, No. 1,
pp. 50-57, January, 1961
Original article submitted April 11, 1960

Based on the increase in the covalent component of a bond with reduction in temperature in crystalline modifications of uranium, neptunium and plutonium, a new idea is put forward for the structure of δ- and η-plutonium. The crystalline structure of these modifications is considered as the result of a comparatively small deviation from the ideal face-centered lattice under the action of four covalent bonds. This idea makes it possible to explain a number of anomalous properties of δ- and η-plutonium, in particular the negative values of the volume coefficient of thermal expansion and the high values of the atomic volume.

Introduction

The modifications of δ- and η-plutonium have certain specific properties not found in ordinary metals. Of these properties, the first which should be mentioned is the negative value of the volume coefficient of thermal expansion and the anomalously high atomic volume of these phases.

According to the existing data the δ-phase has a face-centered cubic lattice with parameter a = 4.637 A (at 320°C), and an η-phase – a face-centered tetragonal lattice with parameters a = 4.701 A and c = 4.489 A (at 490°C). The density of these phases is 15.9 and 16.0 g/cm^3, respectively, which is much less than the density of the high-temperature body-centered ε-phase (16.5 g/cm^3).

In accordance with the data of [1] the mean value of the coefficient of thermal expansion of the δ-phase in the temperature range 320-440°C is equal to $-8.6 \cdot 10^{-6}$, and the coefficient of thermal expansion of the η-phase in the various axes has the following values:

$$\left.\begin{aligned} \alpha_a &= (305 \pm 35) \cdot 10^{-6} \\ \alpha_c &= (-659 \pm 67) \cdot 10^{-6} \end{aligned}\right\} \text{ according to the data of [1];}$$

$$\left.\begin{aligned} \alpha_a &= (444.8 \pm 12) \cdot 10^{-6} \\ \alpha_c &= (-1063.5 \pm 18.2) \cdot 10^{-6} \end{aligned}\right\} \text{ according to the data of [2].}$$

In a number of papers, attempts have been made to explain the unusual properties of these phases. In particular, in [3] it was suggested that due to the small difference in energy levels of the 5f- and 6d- electrons in plutonium, two forms of the atoms could exist simultaneously with a different electron structure and with different dimensions respectively.

With increase in temperature, the number of atoms with a smaller diameter increases due to a reduction in the number of atoms of larger diameter, which leads to a negative value of the coefficient of thermal expansion. The tetragonal nature of the η-plutonium lattice, according to this concept, is due to the formation of an ordered structure of these two forms of atoms.

An attempt was made in [4] to explain the negative coefficient of thermal expansion of δ-plutonium by the possibility of sharp increase in density of the states in the region at the top of the filled part of the Brillouin zone. However, most authors consider that a satisfactory explanation of the mechanism of the anomalous thermal expansion of δ- and η-plutonium is yet to be found.

In a paper by one of the present authors [5] it was shown that the anisotropy of the thermal expansion of a number of modifications of uranium, neptunium and plutonium is due to a weakening of the four covalent bonds with increase in temperature and their uneven distribution in the various crystallographic directions. The weakening of the covalent bonds means that the minimum interatomic distance d_{min} on transition to higher temperature modifications increases abruptly and the difference $d_m - d_{min}$ decreases accordingly until it is equal to zero in the higher temperature modification (in the body-centered cubic lattice). The values of d_{min} for a number of neptunium and plutonium phases are given in the table.

The Value of d_{min} for Some Phases of Neptunium and Plutonium

Element	Phase	d_{min}, A	Element	Phase	d_{min}, A
Np	α	2.62	Pu	α	2.52–2.73
	β	2.79		β	~2.7*
	γ	3.03		γ	3.05
				ε	3.15

*An approximate value from [6].

For the phases of δ- and η-plutonium, the value of d_{min} is 3.28 and 3.25 A respectively. A comparison with the data of the table shows that these values of d_{min} are much higher than those for the highest temperature modification – ε-plutonium. This lack of correspondence in the value of d_{min} for δ- and η-plutonium contradicts the above considered regularity. Hence it follows that the structure of these phases is actually more complex. If we assume that the four covalent bonds appearing in plutonium in the α- and γ-modifications also occur in the δ- and η-modifications, where d_{min} corresponding to these bonds lie within the limits between these values of d_{min} for γ- and ε-phases (between 3.05 and 3.15A) then it is possible to explain not only qualitatively but in the first approximation quantitatively the anomalous character of the thermal expansion of δ- and η-plutonium. The anomalously high value of the atomic volume and a number of other properties of these phases can also be explained.

Since the structures of the δ- and η-plutonium are considered as the result of distortion of an ideal tightly packed structure under the action of the covalent bond forces, the analysis should start with the higher temperature modifications – the η-phase, in which these bonds should appear more weakly.

Structure and Thermal Expansion of η-Plutonium

It is well known that a body-centered cubic lattice with a parameter a_{bc} can be considered as a tetragonal face-centered lattice with parameters a_{ft} and c_{ft} and a ratio of the axes $c_{ft}/a_{ft} = 0.707$. The deformation of this face-centered cell, accompanied by approach of the ratio of axes c_{ft}/a_{ft} to unity, will be a transition from a body-centered to a face-centered cubic lattice. On transition to the latter the initial body-centered cubic lattice changes to a body-centered tetragonal lattice with ratio of axis $c_{bt}/a_{bt} = 1.41$.

The volumes of the initial and final cells will be respectively

$$V_{bc} = a_{bc}^3; \quad V_{bt} = a_{bt}^2 c_{bt} = \sqrt{2}\, a_{bt}^3.$$

If we assume in the first approximation that the volume of the unit cell does not change during transformation, i.e. we neglect the change in degree of compactness of the packing, then $a_{bc}^3 = \sqrt{2} a_{bt}^3$. Hence it follows that

$$a_{bt} = \frac{a_{bc}}{\sqrt[6]{2}} = 0.89\, a_{bc}; \quad c_{bt} = \sqrt{2}\ a_{bt} = 1.26 a_{bc}.$$

Therefore, for complete conversion of the body-centered cubic cell to a face-centered cell it is essential to have expansion of the initial cell along the z-axis by 26% and compression along the x-and y-axes by 11%. In accordance with this ratio the increases in axes $\frac{\Delta c}{\Delta a} = -\frac{0.26}{0.11} = -2.4$. If the transformation stopped at some intermediate stage, then the values of Δc and Δa respectively decrease.

This transformation of the lattice can be accomplished by displacement of the atoms under the action of four covalent bonds. A crystallographic analysis shows that the tetragonal deformation of a body-centered cubic lattice can be accomplished in two ways, schematically shown in Fig. 1. In the first case (see Fig. 1, a) of four atoms at the centers of the unit cells, two atoms are displaced upwards (the + sign) and two others downwards (the - sign). As a result of these displacements, the atoms under consideration approach the four atoms of the upper or lower bases of the cell and open the hole which is formed by them. A tetragonal structure of the β-neptunium type then forms with a ratio of axes $\frac{c}{a} < 1$.

In the second case (see Fig. 1, b) the atoms at the centers of the unit cells are displaced in the horizontal plane in diagonal directions (the directions of displacements are represented by continuous arrows). In order to preserve the symmetry, the cell should be doubled not only along its base but also along its height. The centering atoms of the second stage of this cell should then be displaced in directions opposite to the displacements of the atoms of the first stage (the directions of the displacement are shown by dotted arrows). The considered displacements of the atoms cause an expansion of the unit cell in the direction of the z-axis with corresponding compression in the direction of the x- and y-axes. The result is a tetragonal cell with a ratio of axes c/a > 1.

This process of transformation of a body-centered cubic cell of the ϵ-phase to a tetragonal cell of the η-phase n only occur according to the second method of deformation.

If we take a doubled cell of the η-phase in a body-centered aspect, then its dimensions will be (at 450°C)

$$\left.\begin{aligned} a_\eta &= 2 \cdot 3.326 = 6.652 \text{ A} \\ c_\eta &= 2 \cdot 4.463 = 8.926 \text{ A} \end{aligned}\right\} \frac{c}{a} = 1.34.$$

It was mentioned above that in deriving the relationship $\frac{\Delta c}{\Delta a} = -2.4$ no account was taken of the change in atomic volume during the transformation of the lattice. A decrease in the degree of compactness of the packing due to the considered transition $\epsilon \rightarrow \eta$ should lead to an increase in the atomic volume. It is known that the transition $\epsilon \rightarrow \eta$ is accompanied by a 3% increase in atomic volume, which corresponds to a 1% increase in linear dimensions. In this case, the effective changes in the parameters c and a should be 27 and -10% respectively (instead of 26 and -11%), i.e.,

$$\frac{\Delta c_{\text{eff}}}{\Delta a_{\text{eff}}} = -\frac{0.27}{0.10} = -2.7.$$

In fact, if the value of the ϵ-plutonium lattice parameter is reduced to its value at 450°C, then, using a value of the coefficient of thermal expansion equal to $36.5 \cdot 10^{-6}$ we obtain $a_\epsilon = 2a' = 7.261$ A, and

$$\frac{\Delta c}{\Delta a} = \frac{c_\eta - a_\varepsilon}{a_\eta - a_\varepsilon} = \frac{8.926 - 7.261}{6.652 - 7.261} = -2.7.$$

The projection of the η-plutonium unit cell on the (001) plane, in accordance with the ideas put forward, is given in Fig. 2. The structure belongs to the space group $I4mmm - D_{4h}^{17}$. The number of atoms in one unit cell is 16. The coordinates of the atoms are as follows:

$$\left.\begin{aligned} &4\text{Pu}_\text{I} - 4(d): 0\,\tfrac{1}{2}\,\tfrac{1}{4};\ \tfrac{1}{2}\,0\,\tfrac{1}{4} \\ &4\text{Pu}_\text{II} - 4(e): 00z;\ 00\bar{z} \\ &8\text{Pu}_\text{III} - 8(h): xx0;\ \bar{x}\bar{x}0 \\ &\qquad\qquad x\bar{x}0;\ \bar{x}x0 \end{aligned}\right\} + \left(000;\ \tfrac{1}{2}\,\tfrac{1}{2}\,\tfrac{1}{2}\right).$$

It was mentioned above that d_{min} for the η-and δ-phases should be between 3.05 and 3.15 A. For the η-phase the value d_{min} should be closer to the upper limit since there is also a δ-phase between the η- and γ-phases. It can be assumed that this distance is equal to about 3.12 A. Then x = 0.265; z = 0.255. The deviation of these values from 0.250 characterizes the displacement of atoms from the positions of an ideal face-centered lattice. It should be mentioned that the change in parameters very sensitively affects the value of d_{min}. For example, with decrease in the parameter x by 0.002, d_{min} = 3.15 A, which corresponds to d_{min} of the ϵ-phase.

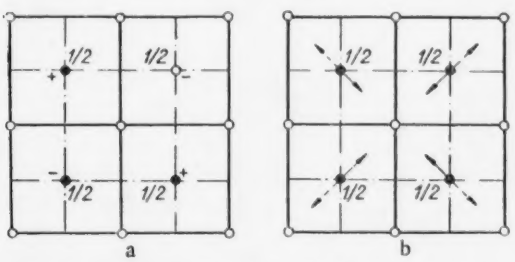

Fig. 1. Two ways of tetragonal deformation of a body-centered cubic lattice under the action of four covalent bonds.

In accordance with the mean value of the minimum interatomic distance d_{min} = 3.12 A, we obtain the following interatomic distances in the structure of the η-phase (in A):

Pu_I	$-8\text{Pu} = 3.25$;	$\text{Pu}_\text{III} - 2\text{Pu} = 3.11$;
	$-4\text{Pu} = 3.33$;	$-2\text{Pu} = 3.13$;
		$-4\text{Pu} = 3.25$;
Pu_II	$-4\text{Pu} = 3.11$;	$-2\text{Pu} = 3.37$;
	$-4\text{Pu} = 3.33$;	$-2\text{Pu} = 3.52$.
	$-4\text{Pu} = 3.37$;	

Here d_m = 3.27 A.

The above considered displacement of atoms from ideal positions of the face-centered lattice should lead to the appearance of additional superlattice lines. The structural factor will be determined by the expression

$$F = 4f\left[\cos\frac{\pi}{2}(2k+l) + \cos 2\pi lz + 2\cos 2\pi hx \cos 2\pi kx\right].$$

The intensity of the superlattice lines should increase with the order of reflection. For example, we will calculate the relationships between the intensities of two back lines 820 and 822 of the x-ray pattern placed side by side, taken in copper radiation. The first of these lines is superlattice, the second is structural:

$$F_{820} = 4f(1+1-2\cdot 0.73\cdot 0.98) = 4f\cdot 0.57; F_{822} = 4f(-1-1-2\cdot 0.73\cdot 0.98) = -4f\cdot 3.43;$$

$$\frac{I_{820}}{I_{822}} \simeq \frac{(pF^2)_{820}}{(pF^2)_{822}} = \frac{8(4f\cdot 0.57)^2}{16(-4f\cdot 3.43)^2} = 0.014.$$

Therefore, the maximum intensity of the superlattice lines is ~1% of the intensity of the main lines. The observation of such weak reflections on the high-temperature powder diagrams of plutonium is very difficult. This also applies to the structure of the δ-phase considered below.

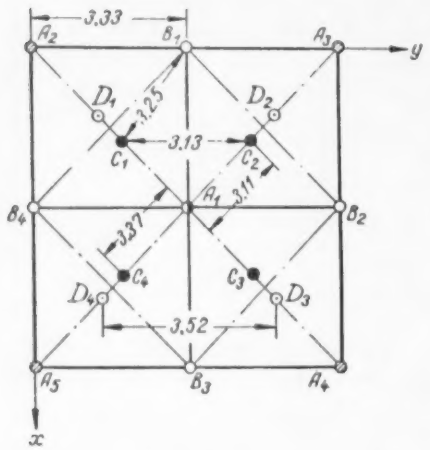

Fig. 2. Projection of the η-plutonium unit cell on the (001) plane. Height in fractions of a parameter c:
○–0 and ½◑–0.005 and 0.495;
●–0.505 and -0.005; ●–¼; ⊙–¾.

We will now explain the behavior of the η-phase with change in temperature.

When the η-phase is heated in the region of its existence, the above considered structure transformation (in the reverse order) will occur only partially, however the ratio between the changes in the parameters c and a, appearing formally as a process of thermal expansion should remain about the same, i.e., - 2.7. Since

$$\Delta c = c\alpha_c \Delta T; \Delta a = a\alpha_a \Delta T$$

(α_a and α_c are the coefficients of thermal expansion in the direction of the a-and c-axes, ΔT is the difference in temperature),

$$\frac{\Delta c}{\Delta a} = \frac{\alpha_c}{\alpha_a}\frac{c}{a}.$$

In accordance with the data given above [1,2] for α_a and α_c the ratio $\Delta c/\Delta a$ is obtained equal to -2.9 and -3.5, which agrees fairly well with the theoretical ratio of -2.7.

If, in the determination of coefficients of thermal expansion of the η-phase we use the latest data [2], then in the range of existence of this phase (451-480°C)

$$\Delta c = -8.926\cdot 1063.5\cdot 10^{-6}(480-451) = -0.275\ \text{A};$$

$$\Delta a = 6.652\cdot 444.8\cdot 10^{-6}(480-451) = 0.086\ \text{A}.$$

Since for the case of total transformation ($\eta \rightarrow \varepsilon$)

$$\Delta c_{\text{total}} = a_{\varepsilon(480)} - c_{\eta(451)} = 7.269 - 8.926 = -1.657\ \text{A};$$

$$\Delta a_{\text{total}} = a_{\varepsilon(480)} - a_{\eta(451)} = 7.269 - 6.652 = 0.617\ \text{A},$$

the values given above comprise from Δc_{total} and Δa_{total}, 16.6 and 14.0% respectively. Hence, it follows that heating the η-phase in the range 451-480°C is accompanied by its structure approaching that of the ε-phase by about 15%. The remaining part of the lattice transformation occurs in the process of the phase transition $\eta \rightarrow \epsilon$.

Structure and Thermal Expansion of δ-Plutonium

We will consider a unit cell of the η-phase in a face-centered aspect. For this purpose on the projection of the unit cell of the η-phase doubled along the x-and y-axes on the (001) plane, we will divide the diagonal cell with a base ABCD (Fig. 3). The dimensions of the cell are a = 9.408 A and c = 8.926 A. The cell consists of eight symmetrically equivalent cells of the type BEFG with dimensions a' = 4.704 A and c' = 4.463 A. Each of the atoms of the type I-IV has four short bonds at a distance 3.11-3.13 A. With reduction in temperature these distances continue

to decrease under the action of the covalent bond forces. It can be assumed that during the transition to the region of the δ-phase d_{min} = 3.09 – 3.10 A.

A decrease in the distance of the type I-II from 3.13 to 3.09 A, i.e., by about 1.3%, should lead to a decrease in the parameter a' by the same value, i.e., from 4.70 to 4.64 A. If in the first approximation we neglect the change in volume during the transformation, then the parameter c' should increase by 3.1% (based on the relationship $\frac{\Delta c}{\Delta a} = -2.4$), i.e., from 4.46 to 4.60 A. If we bear in mind that further displacements of atoms of the type I-IV should also lead to further reduction in the degree of compactness of the lattice, then the value of c' should be obtained somewhat higher. As a result the considered transformations lead to the condition c' = a', i.e. to the development of a cubic lattice.

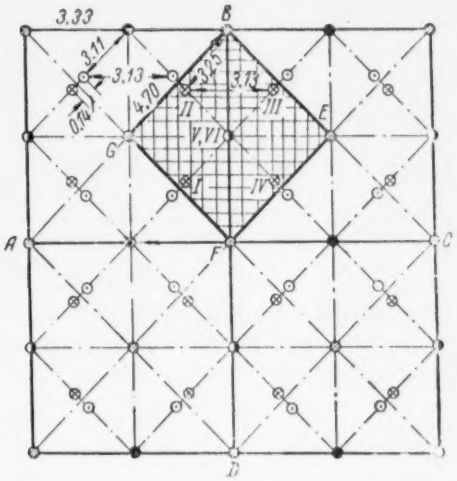

Fig. 3. Projection of four unit cells of η-plutonium on the (001) plane. Height in fractions of a parameter c: ● – 0 and ½; ◑ – 0.005 and 0.495; ◐ – 0.505 and 0.005; ⊗ – ¼; ⊙ – ¾.

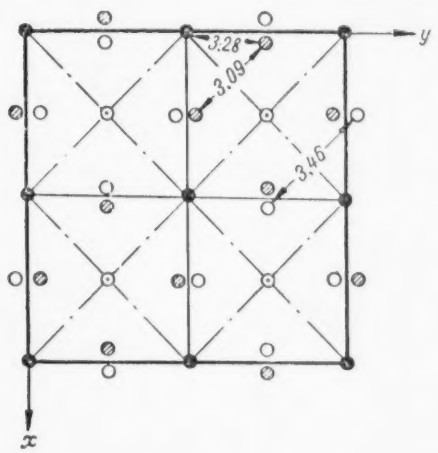

Fig. 4. Projection of unit cell of δ-plutonium on the (001) plane. Height in fractions of a parameter c: ● – 0 and ½; ○ – ¼; ◍ – ¾; ⊙ – 0.014 and 0.486

The unavoidability of satisfying the condition c' = a' also proceeds from the following. The atoms V and VI, like the atoms I-IV, center the upper and lower bases of the unit cells BEFG. However, while the unit cells remain tetragonal, atoms of the type I-IV and the type V-VI are not structurally equivalent. The displacement of these atoms considered above leads to the elimination of their structural nonequivalence, as a result of which the distances of the type II-III should become equal to the distances of the type III-V and the distances of the type II-B equal to distances of the type V-B. The satisfying of these conditions means the presence of a cubic cell.

As a result of this transformation, we arrived at a structure of the cubic cell of the δ-phase of plutonium with parameter a' = 4.632 A (at 450°C). As mentioned above, a certain decrease in the compactness of the packing should lead to a small decrease in density during the η → δ transition. It is known from experimental data [7] that this reduction is 0.4%.

The projection of the unit cell of δ-plutonium on the (001) plane in agreement with the considered ideas is given in Fig. 4. The structure corresponds to the space group F23 $-T^2$. The lattice parameter a = 2a' = 9.274 A; the number of atoms in the unit cell is 32. The positions of the atoms are as follows:

$$\left.\begin{array}{l} 4\mathrm{Pu_I} - 4(a): 000 \\ 4\mathrm{Pu_{II}} - 4(b): \frac{1}{2}\,\frac{1}{2}\,\frac{1}{2} \\ 24\mathrm{Pu_{III}} - 24(g): x\,\frac{1}{4}\,\frac{1}{4};\ \frac{1}{4}\,x\,\frac{1}{4};\ \frac{1}{4}\,\frac{1}{4}\,x \\ \qquad\qquad \bar{x}\,\frac{1}{4}\,\frac{3}{4};\ \frac{3}{4}\,\bar{x}\,\frac{1}{4};\ \frac{1}{4}\,\frac{3}{4}\,x \end{array}\right\} + \left(000;\ 0\,\frac{1}{2}\,\frac{1}{2};\ \frac{1}{2}\,0\,\frac{1}{2};\ \frac{1}{2}\,\frac{1}{2}\,0\right).$$

The value shown above d_{min} = 3.09 A corresponds to the value of the parameter x = 0.014, which means the displacement of atoms from the centers of the faces of an ideal face-centered unit cell by 0.13 A, i.e. by about 4% from d_m. With this value of x the interatomic distances are as follows (in A):

$$\mathrm{Pu_I} - 12\mathrm{Pu} = 3.28;\ \mathrm{Pu_{II}} - 12\mathrm{Pu} = 3.28;$$

$$Pu_{III} - 4Pu = 3.09;$$
$$-4Pu = 3.28; \quad -4Pu = 3.46.$$

The value d_m = 3.28 A, i.e., is equal to that value which was assumed constant for all atoms.

We will now consider the behavior of the δ-phase with change in temperature.

The values d_{min} and d_{max} can be expressed by coordinates of atoms in the following way:

$$d_{min} = \sqrt{2}\left(\frac{1}{4} - x\right)a; \quad d_{max} = \sqrt{2}\left(\frac{1}{4} + x\right)a. \tag{1}$$

In order to establish the character of the temperature dependence of the lattice parameter we will consider the relationship

$$a = \frac{d_{min}}{\sqrt{2}\left(\frac{1}{4} - x\right)}. \tag{2}$$

The derivative from this expression with respect to temperature will be the coefficient of thermal expansion

$$\alpha = \frac{\partial a}{\partial T} = \frac{\partial d_{min}}{\sqrt{2}\left(\frac{1}{4} - x\right)\partial T} + \frac{d_{min}\partial x}{\sqrt{2}\left(\frac{1}{4} - x\right)^2 \partial T}. \tag{3}$$

With reduction in temperature accompanied by an increase in the covalent bond forces there will be a reduction in d_{min} and an increase in the parameter x. The first term of the right side of equality (3) will be a positive component and the second term will be a negative component of the coefficient of thermal expansion. We will designate

$$\frac{\partial d_{min}}{\sqrt{2}\left(\frac{1}{4} - x\right)\partial T} = \beta; \quad \frac{d_{min}\partial x}{\sqrt{2}\left(\frac{1}{4} - x\right)^2 \partial T} = -\gamma,$$

in accordance with which

$$\alpha = \beta - \gamma, \tag{4}$$

where β is a positive component and γ is a negative component of the thermal expansion coefficient. The ratio of these components is

$$\frac{\gamma}{\beta} = \frac{\partial x}{\partial d_{min}} \frac{d_{min}}{\frac{1}{4} - x}.$$

In connection with the fact that the value $\frac{1}{4}$ -x differs little from $\frac{1}{4}$ we can assume

$$\frac{\gamma}{\beta} = 4\frac{\frac{\partial x}{\partial d_{min}}}{d_{min}}.$$

If the parameter x is expressed in absolute units, then the expression assumes the form

$$\frac{\gamma}{\beta} = 4\frac{\frac{dx}{a}}{\frac{\partial d_{min}}{d_{min}}} = 4\frac{\partial x}{\partial d_{min}}\frac{d_{min}}{a}.$$

Since a = 9.274 A, and d_{min} = 3.09 A, then $\frac{d_{min}}{a} \approx \frac{1}{3}$.

Hence $\frac{\gamma}{\beta} = \frac{4}{3}\frac{\partial x}{\partial d_{min}}$, for $\gamma = \frac{4}{3}\beta\frac{\partial x}{\partial d_{min}}$. Substituting the value of γ in expression (4) we obtain

$$\alpha = \beta\left[1 - \frac{4}{3}\frac{\partial x}{\partial d_{min}}\right],$$

and for finite increases

$$\alpha = \beta \left[1 - \frac{4}{3} \frac{\Delta x}{\Delta d_{min}} \right]. \qquad (5)$$

From a comparison of the η- and δ-phases it follows that the value of the displacement Δx in the $\eta \rightarrow \delta$ transition for eight atoms is approximately equal to 0.03 A, and for four atoms to 0.09 A. In the temperature range of existence of this phase, as follows from an analysis of a number of uranium, neptunium and plutonium phases, the value of the displacement should be less. It can be assumed that for the regions of the δ-phase $\Delta x = 0.02$-0.03 A. The change in d_{min} is also equal to a value of this order. Hence it can be assumed that in the temperature region of the δ-phase $\frac{\Delta x}{\Delta d_{min}} \approx 1$. In this case

$$\alpha \simeq -\frac{1}{3}\beta.$$

The positive components of the thermal expansion coefficient can be taken equal to the mean value between the coefficient of thermal expansion of the ϵ-phase ($36.5 \cdot 10^{-6}$) and the coefficient of thermal expansion of the γ-phase ($34.5 \cdot 10^{-6}$), i.e., 35.5×10^{-6}. Then

$$\alpha = -\frac{1}{3} 35.5 \cdot 10^{-6} \simeq -12 \cdot 10^{-6}.$$

The obtained value agrees well with the experimental value of the thermal expansion coefficient of the δ-phase, equal to $-8.6 \cdot 10^{-6}$.

We will now consider in what way the thermal expansion coefficient of the δ-phase should change at a temperature less than 320°C, i.e., in the case of supercooling of the phase. With further reduction in the temperature, the value of x cannot increase to any great extent since then, in accordance with the second equation of expression (1), the value of d_{max} would increase strongly. In [5] it was shown that the value of d_{max} for a number of structures changes very little with temperature. On the other hand, the value of d_{min} during transition in the region of low temperature modifications, as can be seen from the table, changes to a considerable extent. As a result, with supercooling the value of $\Delta x/\Delta d_{min}$ should tend to zero and the value of α should tend to the value of β. Hence, it follows that with supercooling of the δ-phase, its thermal expansion coefficient should become at first equal to zero and then to a positive value. This conclusion agrees well with the data of [8] on the determination of the thermal expansion coefficient of the δ-phase of alloys of plutonium with aluminum.

The addition of an alloying element, weakening the covalent component of the plutonium bond, should lead to a reduction in the values of Δx. As a result, according to equation (5) the thermal expansion coefficient of the δ-phase during addition of the alloying element should change from negative values to positive values in the high temperature region also. The reduction in the difference between d_{min} and d_{max} caused by the decrease in the value of x will also weaken the covalent character of the bond in the structure and facilitate fixations of the alloyed δ-phase at room temperature.

SUMMARY

1. In accordance with the concept of increase in the covalent component of a bond with reduction in temperature, we have considered the most probable character of change in structure during the aleotropic transformations $\epsilon \rightarrow \eta$ and $\eta \rightarrow \delta$ of plutonium. It has been suggested that the ideal face-centered lattices for η-and δ-plutonium are only the first approximation of their structure. Actually the structure of these phases is more complex and is characterized by a displacement of atoms from positions of the ideal face-centered lattice by a value of about 3-4% from d_m. This displacement leads to a reduction in the compactness of the packing in these structures and to an increase in their atomic volume.

2. It has been shown that the strong increase in the parameter a and the still greater reduction in the parameter c of the η-phase which occur with increase in temperature, formally taken as the result of thermal expansion, in actual fact should be considered as a process of continuous transformation of the structure, bringing it nearer to the structure of the ϵ-phase in accordance with weakening of the covalent component of the bond. The difference in the lattice dimensions of η- and ϵ-plutonium in the range of the η-phase region (451-480°C) is reduced by about 15%.

3. It has been shown that the change in the lattice parameter of the δ-phase with reduction in temperature can be considered as the result of simultaneous superposition of two opposite processes. The first of them is the reduction in d_{min} under the action of increase in the covalent component of the bond and a reduction in the vibrational

amplitude of the atoms and leads to a reduction in the lattice parameter (the positive component of the thermal expansion coefficient). The second process is the increase in displacement of atoms from the ideal position and leads to a reduction in the degree of compactness of the structure and to an increase in the lattice parameter (the negative component of the thermal expansion coefficient). It was shown that in the region of high temperatures the predominating role is played by the second process and the overall value for the coefficient of thermal expansion is negative. During supercooling of the δ-phase the first process begins to play a more important role and the thermal expansion coefficient becomes at first equal to zero and then to a positive value.

As a result of alloying of the δ-phase, accompanied by a weakening of the covalent component of the bond, the role of the second process should decrease and the coefficient of thermal expansion of the δ-phase during addition of the alloying element becomes a positive value not only in the region of low temperatures, but also in the region of high temperatures.

LITERATURE CITED

1. F. Ellinger, J. Metals, 8, No. 10, 1256 (1956).
2. A. Coffinberry et al, Proceedings of the Second International Conference on the Peaceful Use of Atomic Energy (Geneva, 1958). Selected Reports of Foreign Scientists. Vol. 6. Nuclear Fuel and Reactor Materials [in Russian]. Moscow, Atomic Energy Press, 1959, p. 157.
3. M. Waldron, Atomics, October, 383, (1957).
4. J. Varley, Proc. Roy. Soc., A237, 413 (1956).
5. N. T. Chebotarev, Atomnaya Energiya, 10, 1, 40 (1961).
6. W. Zachariasen, Acta crystallogr., 12, No. 3, 175 (1959).
7. E. Jette, J. Chem. Phys., 23, No. 2, 365 (1955).
8. M. Waldron et al, Proceedings of the Second International Conference on the Peaceful Use of Atomic Energy (Geneva, 1958). Selected Reports of non-Soviet Scientists. Vol. 6. Nuclear Fuel and Reactor Materials [in Russian] (Moscow, Atomic Energy Press, 1959) p. 142.

SOME PROBLEMS IN THE LOCALIZATION OF RADIOACTIVE ISOTOPES IN CONNECTION WITH THEIR SAFE BURIAL

P. V. Zimakov and V. V. Kulichenko

Translated from Atomnaya Énergiya, Vol. 10, No. 1,
pp. 58-63, January, 1961
Original article submitted April 8, 1960

It is shown that radioactive fission fragments can be safely buried by converting the liquid wastes into solid materials. From the point of view of providing maximum localization of the fragments in a minimum volume of materials such as glass there are undoubted advantages. An analysis is given of the physicochemical principles for preparing these materials and certain features are considered in the behavior and state of radioactive fission fragments included in them. By using methods of fractional chemical and x-ray structural analyses we have shown the heterogeneity of the structure of the fused materials and the related features of behavior of fission fragments during leaching. It has also been shown that the ionizing radiation helps to increase the crystalline fraction in the materials.

A deciding factor in the safe burial of radioactive wastes is their reliable localization at a suitable place for a long period, regardless of the place chosen or the means of burial. The main danger in any "cemetery" is the threat of possible delocalization – the buried radioactive isotopes being scattered from it into the surrounding medium.

The most important problem at the present time is to bury radioactive fission fragments which form in large quantities in many countries in various nuclear power units.

Considering in the wastes of nuclear installations the presence of isotopes such as Sr^{90}, Cs^{137}, Pu^{239}, it has been calculated [1-3] that the time of strict localization needed is several hundreds of years, while the danger of radioactive contamination of the surrounding medium hardly ever disappears.

Most workers have now recognized that the burial of liquid radioactive wastes in containers of any material, regardless of the place and means of burial, is dangerous. Nor is it safe to pour liquid radioactive wastes into the seas, rivers or lakes [4].

A container of any material containing radioactive solution cannot withstand corrosion and hence cannot prevent radioactivity passing through the surrounding medium. Gaseous products of radiolysis, unavoidable in liquid mediums, can increase the pressure and accumulation of explosive gaseous products. In some radioactive solutions the gas evolution per day can reach 10 cm^3 per 1 curie. Furthermore, liquid radioactive wastes, especially highly active wastes, can dry up during self-heating; this leads to steam or pyrochemical ejections and explosions [5]. Putting liquid wastes into deep wells is no guarantee that the radioactive isotopes will not come into contact with the outside layers of the soil and the soil waters. It has been shown that the safest burial of radioactive fission fragments is to convert the liquid wastes into solid materials which can firmly retain the radioactive fragments included in them [1,3,6-12].

A comparison of the characteristics of various solid preparations containing fission fragments (Table 1) shows that the glass type preparations are the most suitable for safe burial since this material can reliably localize the radioactive isotopes within itself. This material is radiation- and thermally stable and gives the greatest reduction in volume of the radioactive material which has to be buried. The direct preparation of this material is preceded by the concentration of radioactive fragments of liquid wastes by sorbing them on difficultly soluble precipitates (hydroxides, salts of phosphoric, oxalic or other acids) or by concentrating to obtain a mother liquor usually containing a large quantity of salt (for example, nitrates). The obtained concentrates (in the form of salts or hydrated oxides) in which the active fragments are distributed contain an excess of water – free, crystallization and constitutional water. The complete removal of water is the first and main condition for giving a radiation-stable prepa-

ration. The second condition is the thermal decomposition of the radiolyzed salts (for example, nitrates) and the almost complete conversion of inert and radioactive elements to the oxides.

Table 1. The Characteristics of Some Solid Preparations Containing Radioactive Fission Fragments

Characteristics	Oxides of metals dried at 200-250°C [1,8,9]	Oxides of metals roasted at 500-700°C [1]	Roasted clays [1, 7, 9, 13]	Cemented blocks [3, 12]	Molten salts [1, 13]	Materials such as glass [1, 9, 14]
Difficulties in preparation	strong dust formation	dust formation	limited exchange capacity of clays	necessity for mixing	corrosion of apparatus	high temperatures (>1000°C)
Change in volume compared with initial volume	100-fold reduction	100-fold reduction	50-fold reduction*	30-50% increase	50-70-fold reduction	350-fold reduction
Liberation of gaseous products due to radiolysis on storage	Yes	No	No	Yes	Yes	No
Thermal stability, °C	>1000	>1000	up to 900	up to 100	up to 300	>1200
Thermal conductivity, kcal/m·hr·°C	0.05	0.03	0.05	no data	~1	to 2
Washing out of fragments in soil waters	considerable	noticeable	small	small	soluble	very small

* Depends on the exchange capacity of the clay, degree of salt saturation and acidity of the solutions.

Figure 1 shows a thermogram for the dehydration of a hydroxide precipitate (pulp) obtained in the treatment of solutions containing fission fragments. Free and adsorbed moisture is removed at low temperatures (up to 150°C) and is accompanied by a noticeable endothermic effect. At higher temperatures (up to 300°C) this effect is caused by the removal of capillary adsorbed water and the dehydration of some less thermally stable hydroxides (for example chromium hydroxide). The exothermic effects observed in the temperature range 300-600°C should be explained by recrystallization of some hydroxides. The dehydration of hydroxides continues to temperatures of 700-800°C; on the thermogram this is represented by several endothermic inflexions. The iron and manganese oxides in the preparation dissociate thermally at higher temperatures, which is shown up on the thermogram by the endothermic effects [14].

Whereas the thermal treatment of the precipitated hydroxides of the metals at temperatures up to 800°C gives radiation-stable preparations, the same treatment of, for example, nitrate mother liquors does not give complete decomposition of the nitrates. In this case, displacement reagents should be used. Thus, if the appropriate amount of silicic acid is added to the mother liquor, there is almost complete decomposition of the nitrates with the liberation of oxides of nitrogen.

This treatment still does not provide sufficiently stable localization of the fragments, especially those such as Sr^{90} and Cs^{137}, the free oxides of which are very soluble in water.

As can be seen from Table 1, the chemical stability of the preparation can be increased by including the fragments in a solidified mass such as glass. For this purpose, the obtained oxides are mixed with various inert additions which can form comparatively readily fusible chemically stable compounds (for example, silicates, on the addition of SiO_2) or can help the solution of high melting components in the liquid phase of readily fusible additions (for example B_2O_3). Inert additions are chosen so as to give the preparation maximum localization of the fragments; easily fusible compounds such as B_2O_3, Na_2CO_3, etc., are therefore added in small amounts. The main components giving minimum solubility of the fused preparations are aluminum oxide, silicon dioxide and some others.

It should be borne in mind that the high-temperature treatment of radioactive materials converts a part of the radioactive fragments into the steam-gas phase and aerosols [10-12]. As shown by our investigations, the main reason for the formation of radioactive aerosols is the sublimation of readily volatile compounds, mainly isotopes such as Ru^{106}, Cs^{137}, Zr^{95}, and Nb^{95}.

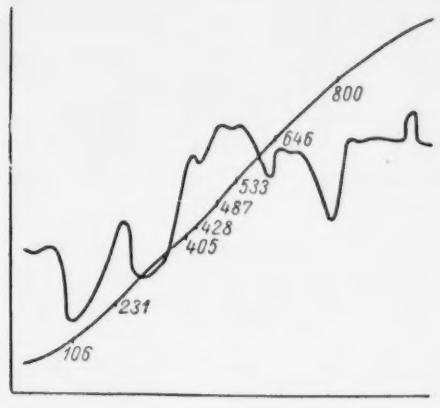

Fig. 1. Thermogram of the dehydration of hydroxide pulp.

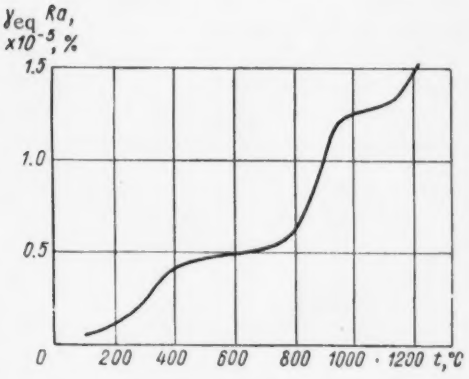

Fig. 2. The formation of aerosols during the thermal treatment of radioactive pulps.

The liberation of radioactive aerosols increases sharply (Fig. 2) at temperatures above 1200°C. Care should therefore be taken when preparing high-melting preparations, especially in the treatment of highly active wastes. Suppressing the formation of aerosols is the object of later investigations. Success can be achieved by firmly locking the fragments in a solid melt, by selecting the fusion conditions and composition of inert additions [11,12].

Figure 3 shows the behavior during fusion of one of the mixtures based on a radioactive hydroxide precipitate. As can be seen by comparing the thermogram, the curves for the change in weight of the mixture and solubility of the obtained material, at the fusion temperature the decomposition of thermally unstable compounds continues and the obtained preparations do not have the maximum chemical stability for the given composition. The working temperature therefore usually exceeds the melting point and is determined separately for each actual mixture [14].

The preparations obtained by high temperature fusion are silicate structures with inclusions of various compounds (such as ferrochromates and other simple and complex oxides).

The washing out of radioactive fragments from these structures can vary between the limits $10^{-4} - 10^{-8}$% (depending on the composition of the flux additions) from 1 cm^2 to a depth of 2 mm per day. The reduction in washing out of radioactive fragments compared with the washing out of roasted oxides is due to the fact that as a result of the high temperature treatment in the presence of silicic acid in the mixture various silicate compounds of separate fission fragments form, the chemical stability of which is much higher than the oxides.

The oxides of other radioactive isotopes, not subjected to serious chemical changes at the selected temperatures due to the presence of a silicate medium surrounding them, become less accessible for the solvents. For example, at 1100°C and a "boiling time" of 2 hours, the formation of strontium silicate could hardly be expected. For this formation, higher temperatures and much longer boiling time for the melts would be needed. If the washing out of Sr^{89} or Sr^{90} from the preparation obtained at 1100°C is $6 \cdot 10^{-4}$%, then for this preparation "boiled" at 1350°C for two hours, the washing out is reduced to $3 \cdot 10^{-4}$% and when boiled for four hours, it is reduced to $5 \cdot 10^{-5}$%. Boiling at 1350°C for six hours reduces the washing out of Sr^{89} and Sr^{90} by one order. In addition, the washing out of Sr^{89} and Sr^{90} from molten preparations obtained even at 1100°C is several times less than the washing out of these isotopes from a simple roasted powder of the oxide. However, increasing the temperature above 1200°C causes a sharp increase in the change of radioactive isotopes to aerosols and to the gaseous phase; therefore operation at 1350°C and excessive increase in the time of boiling of the melts are undesirable. It would be better to strengthen the structure of the silicate medium containing the fragments.

Figure 4 shows the time dependence of the washing out of β-activity from one of the fused fragment concentrates by acid and alkali salt waters. The sharp reduction in the transfer of fission fragments to acid water with time is explained by the formation on the surface of the preparation of a film of silicic acid, protecting the specimen from further destruction. Alkali waters distrub the silicon framework, causing an increase with time in the washing out of the fragments from vitreous concentrates.

It should be mentioned that for vitreous fused preparations containing active fragments, the value of the chemical stability of the preparation cannot be identified with the value of washing out of radioactive fragments from it. As shown by the results of successive treatment of a powdered preparation by various reagents at the temperature of a boiling water bath (Table 2), compounds containing fission fragments behave somewhat differently from the inert components which make up the main mass of the preparation. The heterogeneity of the structure of fused fragment preparations is confirmed by the results of an x-ray diffraction study (Fig. 5).

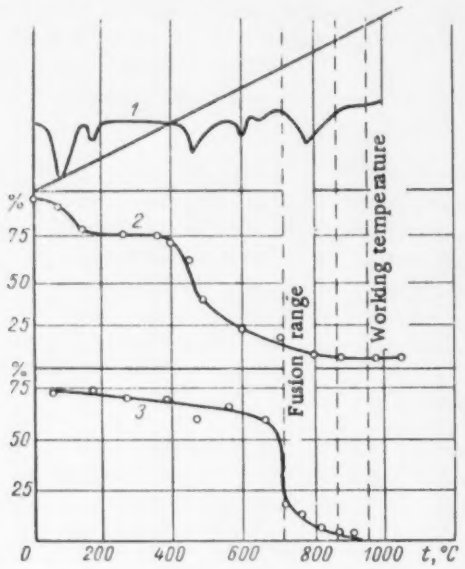

Fig. 3. The behavior during fusion of one of the mixtures based on a radioactive hydroxide precipitate: 1) thermogram; 2) curve showing change in weight during thermal treatment; 3) solubility in water of a preparation obtained at corresponding temperatures [14].

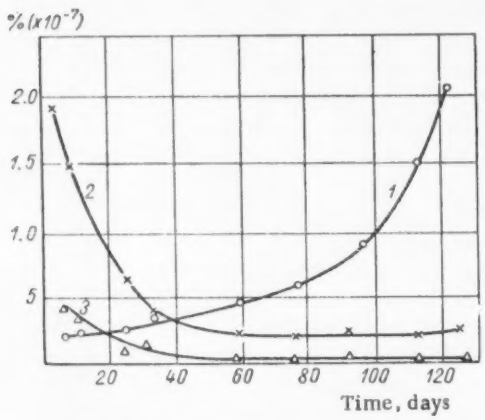

Fig. 4. Time dependence of the washing out of β-activity from a fused fragment concentrate by acid and alkali soil waters: 1,2) washing out at pH of 8 and 4 respectively, from a preparation obtained without additional annealing; 3) washing out after 2 hr annealing in water at pH = 4.

With rapid cooling of the melt, a brittle vitreous preparation is obtained which contains no crystalline inclusions (see Fig. 5: 1). Its strength can be increased considerably by additional "annealing" at 400-600°C. Together with the reduction in the structural stress, there is crystallization of some compounds (mainly iron oxides) contained in the fused preparations (see Fig. 5: 2).

The following conclusions can therefore be drawn. The fused preparations obtained in the treatment of highly active wastes cannot exist in the purely amorphous state; they will always contain crystalline inclusions, mainly compounds of iron, which are basic fragment carriers. In the specimens investigated, most of the silicon compounds remain in the amorphous state.

An inevitable property of radioactive isotopes is their generation of heat due to radioactive decay. Figure 6 shows the extent of the contributions of the separate fission fragments to the total heat liberation of the mixture [6]. The temperatures developed in the preparation, including such isotopes, also depend on the thermal conductivity λ and the specific heat of the preparation C. The dependence of the self-heating temperature of cylindrical fused fragment concentrates on their specific activity, diameter of

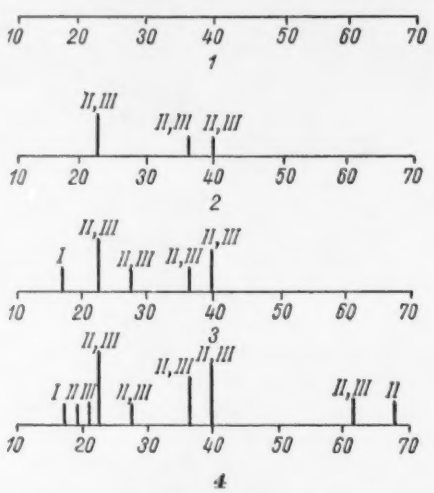

Fig. 5. Results of an x-ray study of fused preparations obtained in the rapid cooling of the melt: 1) before annealing and radiation (lines are not noticeable, amorphous structure); 2) after annealing at 400°C; 3) after Co^{60} radiation; 4) after radiation with simultaneous annealing. I) SiO_2 (quartz); II) γ(Fe_2O_3); III) Fe_3O_4.

TABLE 2. The Fractional Solubility of Vitreous Radioactive Preparation in Powder in Various Mediums

Reagent	Time of treatment at 100°C, hr	Loss in weight, %	Transfer of fragments into solution, %	
			with regard to β-radiation	with regard to γ-radiation
Water	78	13.4	0.03	0.04
NaOH (20%)	42	11.3	2.5	1.4
CH_3COOH (1:1)	72	49.2	93.7	39.8
HCl (1:1)	78	5.8	3.3	41.0
Insoluble residue	–	20.3	0.5	17.8

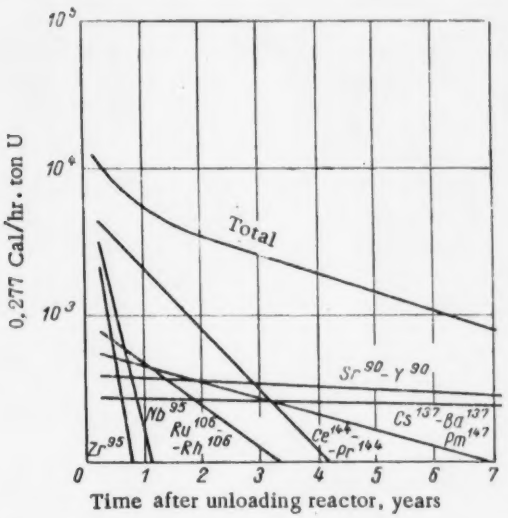

Fig. 6. Change in heat liberation of separate fission fragments with time (enrichment 1.2%; power of reactor 5.5 Mv/ton; radiation level 2750 Mw/ton).

TABLE 3. Self-Heating of Fused Fragment Preparations (λ = 1.1 kcal/m · hr · °C, C = 0.2 kcal/kg · °C)

Specific activity, curie/liter	Diameter, cm	Self-heating temp., °C with age of fragments			
		75 days	180 days	1 year	3 years
30 000	100	15 910	6670	2580	490
	8	490	206	78	15
	4	229	96	38	9
1200	100	640	270	103	20
	10	9	4	1	—
10	100	5	2	—	—
	30	1	1	—	—

the cylinder and age of the fragments is shown in Table 3. The data of Table 3 were obtained by calculation, the thermophysical characteristics C and λ being determined experimentally.

The calculation was checked by an experimental determination of the self-heating temperature of the natural fused concentrates of the fragments.

It can be seen from Table 3 that by selecting the appropriate dimensions of the preparations, the danger of excessive self-heating can be avoided even with the presence of high levels of activity. The self-heating decreases strongly with time.

LITERATURE CITED

1. C. Amphlett, Progr. Nucl Energy, III, Process Chemistry, 2, Pergamon Press, 1958.
2. W. Rodger. Chem. Engng Progr., 50, 263 (1954).
3. W. Rodger, P. Eineman. Progr. Nucl. Energy, III, Process Chemistry, 2, Pergamon Press, 1958.
4. K. Saddington, Progr. Nucl. Energy, III, Process Chemistry, 2, Pergamon Press, 1958.
5. E. Coppinger, R. Tomlinson, Chem Engng. Progr., 52, No. 10, 417 (1957).
6. E. Gluckauf, Material of the International Conference on the Peaceful Use of Atomic Energy (Geneva, 1955) Vol. 9 [in Russian] (Leningrad, State Chemistry Press, 1958), p. 11.

7. A. Walman and A. Gorman, Material of the International Conference on the Peaceful Use of Atomic Energy (Geneva, 1955), Vol. 9 [in Russian] (Leningrad, State Chemistry Press, 1958), p. 19.
8. E. Gluckauf and T. Hill, Material of the International Conference on the Peaceful Use of Atomic Energy (Geneva, 1955), Vol. 9 [in Russian] (Leningrad, State Chemistry Press, 1958), p. 783.
9. L. Hatch, V. Rigen and V. Manowitz, Material of the International Conference on the Peaceful Use of Atomic Energy (Geneva, 1955), Vol. 9 [in Russian] (Leningrad, State Chemistry Press, 1958), p. 801.
10. Watson et al, Proceedings of the Second International Conference on the Peaceful Use of Atomic Energy (Geneva, 1958). Selected Reports of non-Soviet Scientists. Vol. 9. Radiobiology and Radiation Medicine [in Russian] (Moscow, Atomic Energy Press, 1959), p. 187.
11. Landing et al, Proceedings of the Second International Conference on the Peaceful Use of Atomic Energy (Geneva, 1958), Selected Reports of non-Soviet Scientists. Vol. 5. The Chemistry of the Radioelements and Radiation Transformations [in Russian] (Moscow, Atomic Energy Press, 1959), p. 463.
12. M. Geldman, J. Servizi and R. Daniels, Report No. 2004 presented by the USA to the Second International Conference on the Peaceful Use of Atomic Energy (Geneva, 1958).
13. L. Hatch, W. Regan. Nucleonics, 13, No. 12, 27 (1955).
14. P. V. Zimakov et al, Proceedings of the Second International Conference on the Peaceful Use of Atomic Energy (Geneva, 1958). Reports of Soviet Scientists. Vol. 4. The Chemistry of Radioelements and Radiation Transformations [in Russian] (Moscow, Atomic Energy Press, 1959), p. 247.

A METHOD FOR DETERMINING DOSES IN THE INHALATION OF RADON DECAY PRODUCTS

I. I. Gusarov and V. K. Lyapidevskii

Translated from Atomnaya Énergiya, Vol. 10, No. 1,
pp. 64-67, January, 1961
Original article submitted January 12, 1960

This article gives a new method for determining the absorbed energy in the inhalation of radon decay products from the number of α-particles emitted during the total decay of daughter products of radon separated from 1 liter of air. A method is proposed for determining the concentration of radon from the number of α-particles emitted due to total decay of the daughter products collected on a filter from a continuously purified volume.

The determination of doses in the inhalation of radioactive material is a very complex problem. In fact, its solution requires information not only on the quantity of each separate radioactive substance introduced into the organism but also its distribution within the organism. The latter depends on many widely fluctuating factors and it can therefore hardly be studied in a general form.

In addition, it is obvious that since the amount of material taken by the organism during inhalation depends on the quantity of these materials in the air, the study of the whole complex of problems should rest on accurate data as to the content of radioactive substances in the air.

Calculation show that during the inhalation of radon decay products the dose is mainly determined by the α-radiation, since the energy and biological activity of the β-radiation compared with the α-radiation is negligibly small. The main attention is therefore paid to the study of α-active products [1].

The methods now used for the determination of radon decay product concentrations in the air are based on the determination of RaA, RaB and RaC. The latter is achieved either by analyzing curves for the decay of radioactive substances collected on a filter from a given volume of air [2] or by analyzing the amplitudes of impulses given by the α-particles leaving the surface of the filter [3]. These methods are complex, which prevents their widespread use. Furthermore, with low contents of radioactive substances in the air, close to the natural background, the analyses of the decay curves and the impulse amplitudes are hindered due to the high statistical scatter of the experimental points. The method considered in this article is largely free from these faults.

We will determine the energy formed during the total decay of α-active atoms separated from 1 liter of air:

$$E_1 = a\,(E\,\mathrm{RaA} + E\,\mathrm{RaC'}) + (b + c)\,E\,\mathrm{RaC'}, \qquad (1)$$

where E_1 is the total energy; a, b, c are the number of atoms of RaA, RaB, RaC (in 1 liter of air) respectively; ERaA and ERaC are the energies liberated during one act of decay of the appropriate element.

Formula (1) can be written in a different way if we average the energy of α-radiation of RaA and RaC'. We will represent this value by E_α. Then

$$E_2 = E_\alpha\,(2a + b + c) = E_\alpha n, \qquad (2)$$

where n is the number of α-particles emitted during total decay of radon products separated from 1 liter of air.

Calculation shows that if we assume E_α = 7.35 Mev, then the deviation of E_1 from E_2 with a change in the ratio $a\lambda_1 : b\lambda_2 : c\lambda_3$ (λ_1, λ_2, and λ_3 are the decay constants of RaA, RaB and RaC, respectively) from 1 : 1 : 1 to 1 : 0.1 : 0.01 varies within the limits ± 3.5% from E_1. In view of the fact that in the important practical cases the deviation from the equilibrium concentrations varies by not more than the limits shown above, the replacement of E_2 by E_1 can be considered valid.

We will assume, as is usual, that in the inhalation of decay products there is no selective absorption of radioactive materials, i.e., the coefficient of capture η is the same for each of the radon decay products. Then the total energy of radioactive decay liberated within the organism on the inhalation of 1 liter of air is

$$E = \eta n E_\alpha. \tag{3}$$

These discussions show that the initial value for the termination of doses in the inhalation of daughter products of radon can be n, i.e., the number of α-particles emitted during complete decay of radon daughter products, separated from 1 liter of air.

We will deal with different methods for determining the value n.

1. A fixed amount of air is drawn through a filter with a known filtration efficiency φ_1. The α-particles leaving the surface of the filter are recorded by an apparatus. Depending on the geometry of the count and the self-absorption in the filter, the efficiency of recording φ_2 can be different. Then, establishing a continuous count of particles from the start of filtration and up to complete decay of the radioactive materials collected on the filter, it is possible to determine n:

$$n = \frac{N_p}{vt\varphi_1\varphi_2},$$

where N_p is the total number of α-particles recorded by the apparatus; v is the rate of evacuation (liter/min); t is the time during which filtration takes place (min).

2. The second method is based on the assumption that if, with a fixed rate of evacuation v, the number of α-particles n_p recorded in unit time does not change over a large interval of time, then during time Δt within this interval, the number of radioactive atoms remains constant. In other words, during the time Δt the number of radioactive atoms settling on the filter is the same as those which decay during this time.

We will assume that during time Δt one liter of air passes through the filter and that it collects φ_1 (a+b+c) atoms of RaA, RaB, RaC. According to the condition, the same number of atoms should decompose during this time. The corresponding total number of decays $\varphi_1(2a+b+c) = \varphi_1 n$. Hence, it can be seen that if the count rate is equal to n_p impulses per minute and the rate of evacuation v liters per minute, then the total number of decays is

$$n = \frac{n_p}{v\varphi_1\varphi_2}.$$

To use the above method for determining doses, in collaboration with A. M. Konstantinov, we developed an apparatus which could continually record α-particles leaving the filter. One form of the apparatus is a somewhat modified scintillation attachment to the B type apparatus.

A fixed volume of air recorded by a gas counter was drawn through the filter, the α-particles being recorded directly from the moment of start of filtration. The rate of evacuation was measured with a rheometer. The number of impulses was counted every minute. The total number of impulses was recorded simultaneously.

In the first series of experiments, the filtration was carried out during time t and the number of decays from the start of filtration and up to complete decay of the radioactive material was recorded directly by a mechanical counter. In the second series of experiments, air was drawn for a long time through the filter with a constant rate so that the count rate n_p was constant.

The first case corresponds to a short stay of the organism in the contaminated atmosphere, the second corresponds to a long period when a more or less constant concentration of radioactive materials is established in the organism, different from their concentration in the inhaled air.

The amount of suspensions in the atmospheric air varies with time; the measurements were therefore made with two identical instruments, operating simultaneously. The air samples were taken from the same volume.

It was established that the number of α-particles emitted during the total decay of daughter products of radon, separated from 1 liter of air is almost independent of the method of determining the radon daughter products. Thus, despite the fact that the relationship RaA :RaB :RaC on the filter depends on the rate and time of filtration, the total number of decays (on the same filter) is the same in all cases, if the same amount of air is drawn simultaneously through both filters.

As already mentioned, when determining doses from the radon decay products, the initial value is usually the total activity of RaA, RaB and RaC in the air (curie/liter). With the same activity, the total number of α-particles and hence the dose obtained by the organism can vary 2-3 fold depending on the relationship RaA :RaB :RaC. This relationship depends to a large extent on the conditions of the air exchange, the amount of dust in the air and other factors; therefore, the total activity of the decay products does not accurately determine the dose. The determination of the relationship RaA :RaB :RaC in the chain of decay products from the decay curves or by spectrometry is complex.

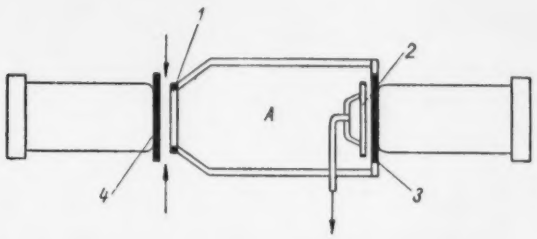

Fig. 1. Apparatus for determining concentration of radioactive materials in the air (the arrows show the direction of movement of the air).

In view of this, in the determination of the dose from radon decay products the initial value should not be taken as the total activity of these substances in the air, but the total number of α-decays n, which is given by the decay products separated from 1 liter.

A similar method can also be used to determine the dose from daughter products of radon forming in the organism itself. For this purpose the air which has first been purified by filter 1 (Fig. 1) from decay products is continuously drawn through the container A. The radon daughter products which are formed in the container A are trapped by the filter 2. By means of scintillation counters 3 and 4, there is continuous recording of the α-particles leaving the surface of the filters 1 and 2.

With regard to the total number of α-particles leaving the filter 1 and 2 it is possible to decide on the ratio of the does obtained by the lungs in the inhalation of radon daughter products contained in unpurified air to the dose obtained by the lungs due to daughter products formed from radon in the lungs themselves. It is assumed that the efficiency of the filters 1 and 2, the volume of air drawn through the filters and the volume of the vessel A are known. The coefficient of capture of the daughter products by the walls of the vessel A is also known.

Figure 2, a and b, gives curves for the collection and decay of radon daughter products collected on filters 1 and 2. It can be seen that the total number of decays on the filter 1 is much greater than on filter 2 (at a rate of evacuation of 15 liters/ min and with the volume of the vessel A equal to 1 liter). These data correspond to the statement that the main danger in inhaling radon and its decay products is connected with the action of radon daughter products in the inhaled air.

The radon concentration (curie/liter) can be determined from the number of α-particles emitted due to total decay of the daughter products collected on the filter 2 during time t. In fact, each atom of radon which decays in the volume A will give two α-particles on the condition of complete collection of daughter products on the filter. If under these conditions the number of impulses in the total decay of daughter products is equal to N_p and the efficiency of recording φ_2, then the number of radon atoms $N = \frac{N_p}{2\varphi_2}$. The activity (curie/liter) can then be expressed by the formula

$$C = \frac{N_p \cdot 10^{-12}}{4.4\,\varphi_2 t V}, \qquad (4)$$

where t is the time of collection on the filter 2 of daughter products formed in the vessels A(min); V is the volume of the vessel A (liter).

The given formula holds when the number of decays of RaA in the volume A and the amount of daughter products settling on the walls of the vessel during the evacuation are negligibly small. In the opposite case for the same radon activity, the total number of decays will depend on the rate at which air is drawn through the vessel A. An experimental study showed that at a rate of evacuation greater than 15 liter/min, there was no dependence on the rate, i.e. under these conditions the decay of RaA in the volume A and settling of the decay products on the walls of the vessel can be neglected.

The described method for determining the activity of radon by measuring the total number of α-decays of daughter products settled on the filter from a measured volume can also be used to measure short lived radioactive gases, for example rhoton or actinon.

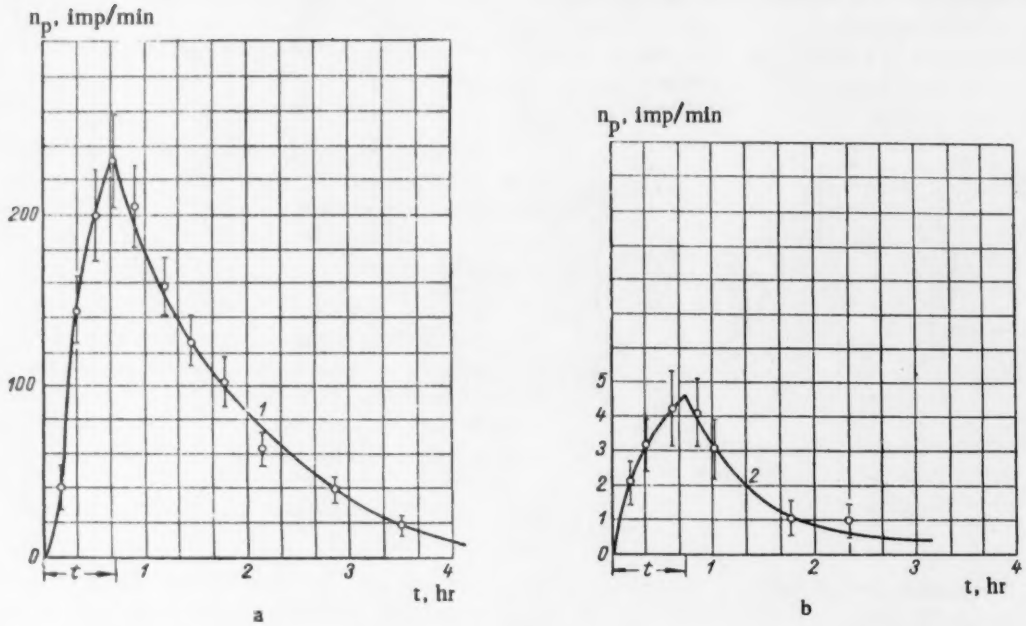

Fig. 2. Curves for collection and decay of radon daughter products: n_p is the count rate; t is the time of evacuation.

The authors would like to thank A. V. Bykhovskii, M. S. Kozodaev and E. V. Shchepot'eva for discussing the work and also A. A. Titov for taking part in the measurements.

LITERATURE CITED

1. B. Hultquist, The Ionizing Radiation of Natural Sources [Russian translation] (Moscow, Foreign Literature Press), 1959.
2. E. Tsivoglou, H. Ayer, D. Holaday, Nucleonics, II, No. 9, 40 (1953).
3. Tsivoglou, Reports of the International Conference on the Peaseful Use of Atomic Energy (Geneva, 1955), Vol. 13 [Russian translation] (Moscow, Foreign Literature Press), 1958, p. 288.

LETTERS TO THE EDITOR

AVERAGE NUMBERS ν AND η OF NEUTRONS IN THE FISSION OF U^{233} AND Pu^{239} BY 14 Mev NEUTRONS

N. N. Flerov and V. M. Talyzin

Translated from Atomnaya Énergiya, Vol. 10, No. 1,
pp. 68-69, January, 1960
Original article submitted May 17, 1960

The fast neutron detector (graphite prism) described in [1] has been used to measure the absolute intensity of neutron sources, the average numbers $\bar{\nu}$ and η of neutrons produced in the fission by, and in elastic interactions of, 14 Mev neutrons on U^{235} and U^{238} nuclei [2], and also to measure the cross-section for the (n, 2n) reaction in beryllium, lead and bismuth [3].

In 1954, this detector was used to measure $\bar{\nu}$ and η for 14 Mev neutrons interacting with U^{233} and Pu^{239} nuclei. These quantities were determined from the increase in the neutron current when 14 Mev neutrons are passed through a specimen of the fissionable element.

Denoting the detector counting rate with and without the specimen by N_1 and N_0, respectively, and assuming that

$$\frac{N_1}{N_0}=1+\gamma,$$

we have the following formula for a spherical specimen with $\underline{n}$ nuclei per cm^3:

$$1+\gamma=e^{-n\sigma_{in}l}+\frac{k_1}{k_0}(1-e^{-n\sigma_{in}l})\,\eta\,(1+\beta), \tag{1}$$

where σ_{in} is the inelastic cross-section, k_0 and k_1 is the sensitivity of the detector to 14 Mev neutrons and neutrons produced in the inelastic process, respectively, and $1+\beta$ is a coefficient allowing for the increase in the number of neutrons as a result of fission by secondary neutrons. The first term on the righthand side represents the fraction of primary neutrons which have passed through the specimen without interacting, and the second term represents the fraction of neutrons produced as a result of the interaction between primary neutrons and the target nuclei. From Eq. (1) we have

$$\eta=\alpha\left(1+\frac{\gamma}{1-e^{-n\sigma_{in}l}}\right), \tag{2}$$

where $\alpha=\frac{k_0}{k_1}\frac{1}{1+\beta}$.

Assuming that the basic processes were fission and the (n, 2n) reaction, we have

$$\eta=\frac{\bar{\nu}\sigma_f+2\sigma_{n,\,2n}}{\sigma_{in}},$$

where $\sigma_f, \sigma_{n,\,2n}$ are the fission and (n, 2n) reaction cross sections, respectively. Hence

$$\bar{\nu}=(\eta-2)\frac{\sigma_{in}}{\sigma_f}+2. \tag{3}$$

Spherical specimens made of metallic uranium and plutonium (outer diameter 4 cm, inner diameter 3.4 cm, diameter of aperture 2.1 cm) were placed in 0.9 mm thick cadmium jackets. These were then inserted into a thin-walled brass container which was located at the center of the graphite-prism cavity so that the center of the specimen coincided with the center of the target forming the source of neutrons. The neutron current was determined from the number of α-particles from the $T(d, n)He^4$ reaction.

Results of measurements

Isotopes	$1+\gamma$	$1+\beta$	η	ν
U^{233}	1.155± ±0.003	1.116± ±0.008	4.07± ±0.22	4.23± ±0.24
Pu^{239}	1.147± ±0.003	1.116± ±0.010	4.53± ±0.25	4.62± ±0.28

The quantity $(1 + \gamma)$ was determined in a series of measurements with and without the specimens. In experiments without the specimens, the empty brass container with the cadmium cover was retained in the working position. The table gives the average results of a large number of measurements of $(1 + \gamma)$.

In the determination of the coefficient γ we used $k_0/k_1 = 0.874 \pm 0.030$, as reported in [1], and an experimentally determined value of $(1 + \beta)$. The latter was obtained with a source which imitated the spectrum of fission neutrons. A correction was introduced for fission by slow neutrons. It was assumed that the correction coefficient for U^{233} and Pu^{239} is the same as that for U^{235} (1.002 ± 0.003, [2]). Assuming that σ_{in} is equal to the value of σ_{in} extrapolated from the data given in [4] for U^{233} and Pu^{239} ($\sigma_{in} = 2.85 \pm 0.10$ barn), we obtain the values of η given in the table.

The fission cross section of U^{233} and Pu^{239} is not very different from σ_{in}.

Assuming that $\sigma_{in} - \sigma_f = 0.2 \pm 0.1$ barn for U^{233} and 0.1 ± 0.1 barn for Pu^{239}, and replacing σ_{in}/σ_f in Eq. (3) by $[1 - (\sigma_{in} - \sigma_f)/\sigma_{in}]^{-1}$, we obtain the values of $\bar{\nu}$ given in the table.

Owing to the large excitation energy of the nuclei, the values of $\bar{\nu}$ for U^{233}, Pu^{239}, U^{235} and U^{238} [2, 5] in fission by 14 Mev neutrons are roughly equal, and according to our measurements approach the value 4.4 ± 0.2.

Our values of $\bar{\nu}$ are in good agreement with the results reported in [6-9].

LITERATURE CITED

1. N. N. Flerov and V. M. Talyzin, Atomnaya énergiya, III, No. 10, 291 (1957).
2. N. N. Flerov and V. M. Talyzin, Atomnaya énergiya, 5, No. 6, 653 (1958).
3. N. N. Flerov and V. M. Talyzin, Atomnaya énergiya, 5, No. 6, 657 (1958).
4. N. N. Flerov and V. M. Talyzin, Atomnaya énergiya, No. 4, 155 (1956).
5. N. N. Flerov and E. A. Tamanov, Atomnaya énergiya, 5, No. 6, 654 (1958).
6. G. Vandreyes, et al., International Conference on the Neutron Interactions with the Nucleus. Held at Columbia University, New York, (September 9-13, 1957).
7. G. N. Smirenkin, et al., Atomnaya énergiya, 4, No. 2, 188 (1958).
8. A. N. Protopopov and M. V. Blinov, Atomnaya énergiya, 4, No. 4, 374 (1958); 5, No. 1, 71 (1958).
9. R. Lichman, Proceedings of the Second International Conference on the Peaceful Uses of Atomic Energy (Geneva, 1958). Selected Reports of Foreign Scientists, Vol. 2, Neutron Physics. Moscow, Atomizdat, 1959, p. 282.

EFFICIENCY OF WAVEGUIDES USED AS ACCELERATING SYSTEMS IN ELECTRON SYNCHROTRONS

A. N. Didenko and E. S. Kovalenko

Translated from Atomnaya Énergiya, Vol. 10, No. 1,
pp. 69-71, January, 1961
Original article submitted August 31, 1960

Paper [1] is concerned with the possibility of using waveguides as the accelerating systems of electron synchrotrons. However, no estimate of the proposed system efficiency has been given. The following is an attempt to correct this omission.

Let the wave LE_{11} propagate at the azimuth angle φ in a closed waveguide with diaphragms. We are interested in its phase and group velocity, attenuation α, and the coupling impedance R_{cou}. Together with the Q-factor, these parameters will determine the branch resistance R_{br}, which represents the measure of the high-frequency system efficiency.

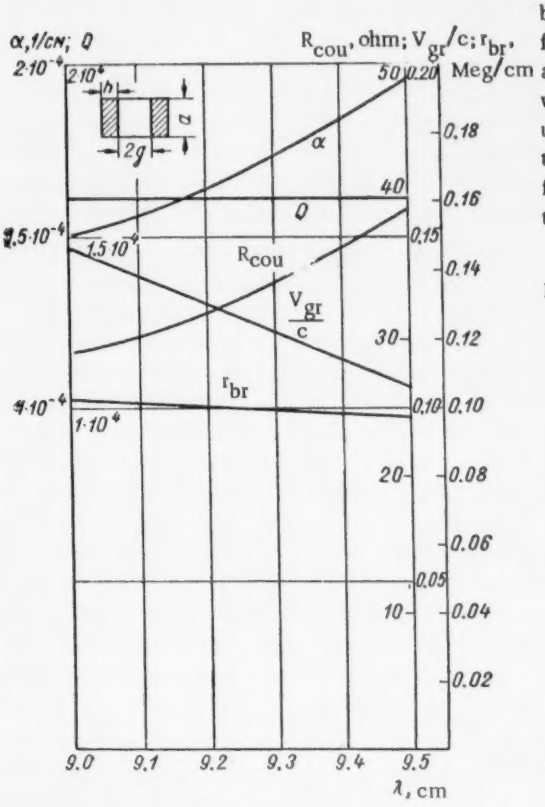

Fig. 1. Dependence of α, Q, R_{cou}, v_{gr} and r_{br} on the wavelength.

The exact calculation of the above quantities would be cumbersome. These calculations can be greatly simplified if we neglect the wave three-dimensional harmonics and the effect of the curvature on the field structure in the waveguide cross section. The first of these assumptions is usually made in such calculations [2], while the validity of the second assumption follows from [1]; it is obvious that, for large synchrotrons, its effect is negligible. By calculating the magnitude of attenuation α, we obtain

$$\alpha = \alpha_1 + \alpha_2. \qquad (1)$$

Here,

$$\alpha_1 = \frac{2W\beta_0\pi^2}{kk_0^3a^3}\left(1+\frac{k_y^2}{\beta_0^2}\,\frac{\operatorname{sh} 2k_yg + 2k_yg}{\operatorname{sh} 2k_yg + 2k_yg}\right);$$

$$\alpha_2 = \frac{2Wk_y^3}{k\beta_0}\,\frac{\dfrac{\operatorname{ch}^2 k_yg}{\sin^2 k_0h}}{\operatorname{sh} 2k_yg - 2k_yg}\left[1+\frac{h}{D}+\frac{2\pi^3h}{k_0^2a^3}+\right.$$

$$\left.+\frac{\pi^2h}{k_0^2a^2D}-\sin 2k_0h\left(1-\frac{k_0^2-\dfrac{\pi^2}{a^2}}{2k_0^2D}\right)\right],$$

where

$$W=\frac{1}{2}\sqrt{\frac{c}{\sigma\lambda}};$$

$$k=\frac{\omega}{c};\ \beta_0=\frac{\omega}{v_{ph}};\ k_0=\sqrt{k^2-\frac{\pi^2}{a^2}};$$

$$k_y=\sqrt{\beta_0^2+\frac{\pi^2}{a^2}-k^2};$$

σ is the conductivity of the walls; ω is the angular frequency; λ is the wavelength; v_{ph} is the wavelength velocity and D is the period of the system (the remaining data are given in Fig. 1).

In a similar manner, we shall find the following expressions for the group velocity v_{gr} and the coupling impedance R_{cou}:

$$v_{gr} = \frac{2k_0^2 k\beta_0 c}{\left(k_0^4 + \frac{\beta_0^2\pi^2}{a^2} + k^2\beta_0^2\right) + \left(k^2 + \frac{\pi^2}{a^2}\right) k_y^2 \frac{\operatorname{sh} 2k_y g + 2k_y g}{\operatorname{sh} 2k_y g - 2k_y g} + A \frac{\operatorname{ch} 2k_y g}{\operatorname{sh} 2k_y g - 2k_y g}}, \tag{2}$$

where

$$A = \frac{2k_y^3 k^2}{k_0 \sin^2 k_0 h}\left(2k_0 h - \frac{\lambda^2}{4a^2}\sin 2k_0 h\right),$$

and

$$R_{cou} = 480 \frac{k_y^3}{\beta_0^3} \frac{k\pi}{k_0^2 a} \frac{1}{\operatorname{sh} 2k_y g - 2k_y g}. \tag{3}$$

By using expressions (1) and (3), we readily find Q and r_{br} – the branch resistance per accelerator unit length:

$$Q = \frac{\omega}{2\alpha v_{gr}}; \quad r_{br} = \frac{4\pi}{\lambda} R_{cou} Q \frac{v_{gr}}{c}. \tag{4}$$

Figure 1 shows the dependence of α, Q, R_{cou}, v_{gr}, and r_{br} on the wavelength λ for $v_{ph} = c$, $2g = 6$ cm, $a = 5.85$ cm and $D = \lambda/4$. In Fig. 2, R_{cou}, v_{gr}/c, and r_{br} are given as functions of 2g for $\lambda = 9.3$ cm. It follows from these diagrams that r_{br}, which characterizes the high-frequency system efficiency, slightly changes with changes in λ, and that it varies considerably with changes in g: if 2g varies from 2 to 6 cm, r_{br} decreases from 0.5 to 0.1 meg/cm. It is of interest to compare these theoretical r_{br} values with the branch resistances of actual linear accelerators. It is known that, for the Stanford 600-Mev accelerator, the interaction space of which is equal to 2 cm, $r_{br} = 0.47$ meg/cm. This confirms the fact that the theoretical r_{br} values which we obtained are within the limits of technical possibilities and that high branch resistance values are characteristic of high-frequency systems based on waveguides.

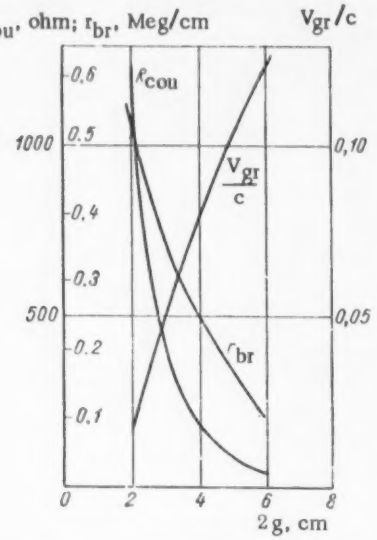

Fig. 2. Dependence of R_{cou}, v_{gr} and r_{br} on 2g.

From Eq. (4), it follows that the expression for R_{br} is given by

$$R_{br} = 4\pi m R_{cou} Q_{eff} \frac{v_{gr}}{c}, \tag{5}$$

where Q_{eff} is the effective waveguide quality factor, which takes into account all the possible losses in it.

Let us compare the efficiency characteristics of a high-frequency system consisting of a closed waveguidewith diaphragms with the efficiency characteristics of the better and the most modern accelerating systems of large synchrotons. With a sufficiently good manufacturing technology, it is possible to obtain a waveguide with the following approximate parameters: $R_{cou} = 50$ ohms, $Q_{eff} = 10^4$, and $v_{gr} = 0.1\,c$. Under these conditions, a waveguide that was used in such an accelerator as the German 6-Bev DESY would have the value $R_{br} = 2000$ meg for $\lambda = 10$ cm. In order to obtain such a branch resistance by means of a resonator system, it is necessary that each of the 80 resonators in DESY has the value $R_{br} = 25$ meg. This greatly exceeds the limits of technical possibilities (the DESY resonators have $R_{br} = 2$ meg). Thus, from the point of view of attainable branch resistances, a waveguide accelerating system offers greater possibilities than a resonator system.

It follows from Eq. (5) that, all other conditions being equal, an increase in multiplicity m leads to an increase in the high-frequency system efficiency, and therefore, from the point of view of high-frequency power, greater m values are advantageous. However, in comparison with ordinary resonator systems, the application of waveguide accelerating systems is unavoidably connected with a q-fold increase in multiplicity. In this case, due to radiation quantum fluctuations, the value of the root-mean-square spread with respect to phase will be $\sqrt{q}$ times as large. In order to avoid this, if we wish that the particle losses remain unchanged, it is necessary to increase the high-frequency voltage amplitude by suitable means. By using the equation proposed by Christie and Robinson [3], it can be demonstrated that the particle losses for two accelerators are equal if

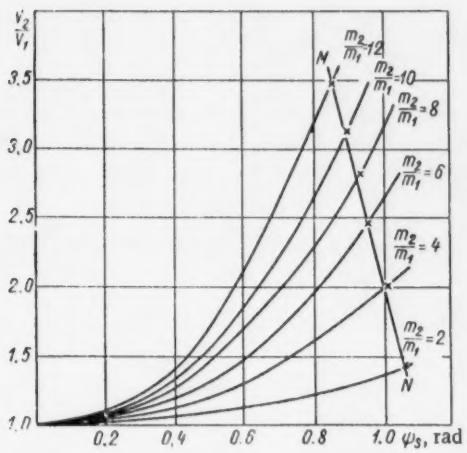

Fig. 3. Results of the numerical solution of Eq. (6).

$$\frac{1}{m_1}(\operatorname{tg}\psi_{s1}-\psi_{s1})=\frac{1}{m_2}(\operatorname{tg}\psi_{s2}-\psi_{s2}). \qquad (6)$$

It follows from Eq. (6) that, with an increase in multiplicity, the phase ψ_s must increase to such an extent that Eq. (6) remains valid. Since the radiation losses are equal in both cases, this will result in a voltage increase given by

$$\frac{V_2}{V_1}=\frac{\cos\psi_{s1}}{\cos\psi_{s2}}. \qquad (7)$$

However, with an increase in multiplicity, the value of R_{br} for system (4) will also increase, and therefore, if we take into account the radiation fluctuations, there is no evidence indicating that an increase in multiplicity would be undesirable. Figure 3 shows the results obtained by solving Eq. (6) numerically for different multiplicity ratios m_2/m_1. The region to the left of the straight line MN corresponds to phase values for which the transition to higher harmonics leads to an energy gain. It is obvious that this region contains all the values of large accelerator equilibrium phases which are most interesting from the practical point of view.

In conclusion, we hereby express our deep gratitude to Prof. A. A. Vorob'ev for his continued interest in the work and the discussion of the results.

LITERATURE CITED

1. A. A. Vorob'ev, A. N. Didenko and E. S. Kovalenko, Atomnaya Énergiya, 8, 4, 459 (1960).
2. L. Levin, Modern Waveguide Theory [Russian translation] (IL, Moscow, 1954).
3. K. Robinson, International Conference on High Energy Accelerators and Instrumentation, CERN Geneva, 1959, p. 293.

TRANSFORMATION OF THE ENERGY OF SHORT-LIVED RADIOACTIVE ISOTOPES

M. G. Mitel'man, R. S. Erofeev and N. D. Rozenblyum

Translated from Atomnaya Energiya, Vol. 10, No. 1,
pp. 72-73, January, 1961
Original article submitted April 22, 1960

The α- and β-active isotopes that are formed as a result of the interaction between neutrons and the atoms of the material can serve as emitters of charged particles, which, as they accumulate on a collector, create a potential difference. On the basis of this principle, it is possible to design a converter consisting of an emitter and a collector which are separated by a solid dielectric or vacuum.

The number of charged particles that are produced by the emitter in unit time is proportional to the current obtainable in the converter:

$$A = \frac{N_a \sigma n G}{M}\left(1 - e^{\frac{-0.693t}{T}}\right),$$

where N_a is Avogadro's number, σ is the neutron capture cross section, n is the neutron flux, G is the emitter mass, M is the emitter material atomic weight, T is the evolving isotope half-life, and t is the emitter irradiation time.*

For small half-life periods ($t \gg T$), the number of charged particles is independent of time. For large half-life periods ($t \ll T$), the number of charged particles is proportional to the irradiation time.

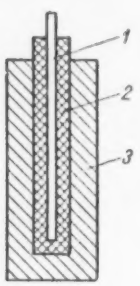

Diagram of the energy converter: 1) emitter; 2) dielectric; 3) collector.

In order to secure stable and time-independent operation of the converter, an emitter material with the shortest possible half-life should be used. For a more efficient utilization of neutrons, this material must have a large neutron capture cross section.

We performed experiments where a rhodium isotope (Rh^{103}) with a capture cross section of 150 barn was used as the emitter. As a result of interaction between the neutrons and rhodium, isotope Rh^{104} was formed, which emitted β-particles with an energy of 2.5 Mev and a half-life of 41.8 sec.

The diagram of the energy converter is shown in the figure. A rhodium wire with a diameter of 0.8 mm and a weight of 0.42 g, which was covered with insulating lacquer and a 1.5 mm thick polyethylene layer, was placed in an aluminum shell which served as the electron collector. In assembling the converter, special attention was paid to the quality of insulation.

The thus prepared converter was placed in a channel of the research reactor at the I. V. Kurchatov Atomic Energy Institute, Academy of Sciences, USSR. An RK-1 television cable was used for the lead-out wires. The current and the voltage were measured by means of an electrostatic voltmeter and a string electrometer.

By placing the converter in a neutron flux of 10^{12} neutrons/cm^2·sec, a current of $4.2 \cdot 10^{-8}$ amp was obtained for an external resistance of 10^{10} ohms and a voltage of 420 v.

The amount of β-particles that are produced by the emitter for the above neutron flux can provide a current of $6 \cdot 10^{-8}$ amp. The observed lower current intensity in comparison with the maximum possible intensity can be explained by the absorption of β-particles in the emitter and the dielectric materials.

After the converter was moved to a reactor zone where the neutron flux was 10^{10}–10^{11} neutrons/cm^2·sec, its current was reduced to $1.6 \cdot 10^{-9}$ amp in 2 min. This result does not contradict the theoretical assumptions.

*R. Murray, Introduction to Nuclear Techniques [Russian translation] (IL, Moscow, 1955).

Converters of this type can be used for constructing high-voltage dc voltage sources. Moreover, the converter can be used for determining the neutron flux and consequently, the reactor power level with respect to the intensity of the current supplied by the converter.

The possibility of securing a steady-state current for a given neutron flux depends on the half-life of the isotope that is formed as a result of the emitter irradiation.

In switching over from a lower neutron flux value to a higher one, accumulation of the radioactive isotope takes place. In practice, equilibrium is attained for $t/T = 6.65$ (deviation 1%), which for rhodium, corresponds to 280 sec. A certain time is required for the transition from a higher neutron flux value to a lower one while the accumulated radioactive isotope disintegrates. If the neutron flux value changes by a factor of 10, equilibrium is established almost for $t/T = 10$ (deviation 1%), which corresponds to 418 sec if rhodium is used. A device with such inertness can be used only in the case where the neutron flux changes slowly.

In the case of fast-changing processes, we must determine the current derivative with respect to time, which is also proportional to the neutron flux:

$$\frac{dA}{dt} = \frac{N_a \sigma n G}{M} \frac{0.693}{T} e^{-\frac{0.693t}{T}}.$$

For small t/T values (≤ 0.0145), we can consider that

$$\frac{dA}{dt} = \frac{N_a \sigma G 0.693}{MT} n = \text{const } n,$$

i.e., the derivative is independent of time. Then $t \leq 0.6$ sec if rhodium is used.

Thus, a converter with a rhodium emitter can be used for measurements that last either less than 0.6 sec or more than 418 sec. For a suitable emitter material, we can vary the inertness of the device and use it for processes that differ from each other with respect to their development rate and duration. For instance, for the Co^{59} (n, p) Fe^{59} reaction, the β-active Fe^{59} isotope with the half-life T = 46 days is obtained; it can be used for measurements over periods $t \leq 11$ hr.

In all the cases considered, the measuring circuit inertness was not taken into account.

DATA ON THE SEPARATION OF BORON ISOTOPES IN THE FORM OF VOLATILE COMPOUNDS*

I. Kiss, I. Opauszky and L. Matush

Translated from Atomnaya Énergiya, Vol. 10, No. 1,
pp. 73-75, January, 1961
Original article submitted June 21, 1960

Various methods developed for the separation of stable boron isotopes suffer from certain drawbacks from the practical point of view [1-7]. An investigation of the change in the isotopic composition of various boron compounds is therefore of theoretical and practical interest. Experiments with different boron compounds showed that isotopic effects arising in phase equilibria were contrary to classical ideas on these processes in many cases. Among the volatile compounds studied, the boron compound containing the heavy boron isotope was found to be more volatile than the corresponding compound with the light isotope. This phenomenon has been observed with other elements besides boron [8,9].

No general theory explaining this phenomenon has been developed up to now. However, it may be surmised that it is explained by both intramolecular and intermolecular interactions, depends on the association or dissociation of molecules in one or both phases, etc. [10]. Due to the lack of a quantum mechanical theory for the liquid phase, certain difficulties arise in the theoretical solution of the problem and therefore it is necessary to supplement experimental data available at the present time by systematic investigations of various types of molecules.

The purpose of the present work was a comparison of the practical efficiency of various oxygen-containing organic compounds with BF_3 when used for enrichment of isotopes, and a study of the differences in nature and degree of the volatility of isotopic compounds of boron.

Investigation of Complex Compounds of BF_3

Boron isotopes are separated most frequently by distillation of organic complexes of BF_3 and also by chemical exchange between a liquid complex and gaseous BF_3.

We investigated the systems anisole – BF_3, ethyl ether – BF_3, acetic acid – BF_3, ethyl acetate – BF_3, etc. The boron isotope separation factor for the first two systems is known from [4, 5, 7, 8]. The separation factor determined by a static method is not the only criterion of the applicability of a given isotope effect for enrichment in a certain system, and therefore experiments for comparing these compounds were carried out on the same enrichment column, 1800 mm high and 12 mm in diameter. The column was packed with three-turn spirals of silver wire 0.2 mm in diameter. The length of the spirals was 1.3 mm.

The complex of anisole with BF_3 decomposes to anisole and BF_3 when heated. Experiments were carried out at 20°C with counter-current flow of the liquid complex and gaseous BF_3 liberated from it. Experiments with the other systems were carried out by the method in [4]. The absorption of neutrons was used to determine the isotopic composition of the fractions obtained. The experimental apparatus and working procedure and also the neutron absorption method were described previosuly [6]. The experimental results are given in Table 1.

The enrichment was calculated from the formula:

$$A=\frac{\left(\frac{B^{11}}{B^{10}}\right)\text{ at column head}}{\left(\frac{B^{11}}{B^{10}}\right)_{\text{in column still}}}.$$

Table 1 shows that the complex of BF_3 with ethyl ether was enriched most. This compound is most stable. Though the separation factor in the system anisole–BF_3 is greater than in the system ethyl ether–BF_3, the enrichment

* Article received from the Hungarian Peoples Republic.

in the first case was less than in the second under the given conditions. In addition, the complex of BF_3 with anisole decomposed considerably. The method of continuous purification of the anisole by distillation [11] complicates the technological process, in which the economy of the method must be considered. Though there was a considerable change in the isotopic composition of the other compounds during distillation, they were unsuitable for the enrichment of isotopes in practice because of irreversible decomposition of the complex.

Table 1. Separation of Boron Isotopes in Various Complex Compounds

Compound	Temperature, °C	Enrichment	Comments
$C_6H_5OCH_3 \cdot BF_3$	20	2.0	The complex formed tar after prolonged heating
$(C_2H_5)_2O \cdot BF_3$	60	2.4	——
$2H_2O \cdot BF_3$	80	1.9	The complex decomposed irreversibly during distillation
$CH_3OH \cdot BF_3$	92	1.7	The complex decomposed irreversibly during distillation
$CH_3COOH \cdot BF_3$	96	1.9	Considerable decomposition of the complex was observed
$CH_3COOC_2H_5 \cdot BF_3$	75	–	The complex decomposed on heating and the degree of enrichment was not determined

Investigation of Trialkyl Borates

Boron halides and their volatile complexes have been used for the separation of boron isotopes up to now. Among the other volatile compounds of boron, it is profitable to investigate the alkyl esters of boric acid first of all. These compounds are stable and their boiling points are suitable for simple distillation.

The distillation of methyl borate was proposed for the separation of boron isotopes in the USA in 1942 [12], but the separation factor found was considered low for the practical application of this method at that time. Since BF_3 is unsuitable for the working gas for the separation of boron isotopes in a thermal diffusion tube [13], attempts were made to use methyl borate for this purpose [14]. The experiments showed [13] that this compound cannot be used for separation by thermal diffusion, but methyl borate was found to have a very high thermal stability.

We investigated isotope effects in the liquid–vapor equilibrium with methyl, ethyl, and n-butyl borates. Rayleigh distillation was used to determine the separation factor α [15]. The experimental procedure was analogous to that described in [3]. The isotope effect of butyl borate could not be determined by Rayleigh distillation. For determining the separation factor, we used a fractionating column 12 mm in diameter with a bed of packing 1000 mm high. The packing consisted of three-turn spirals 1.2-1.3 mm long of silver wire 0.2 mm in diameter. In the distillation of the complex of BF_3 with ethyl ether at 20 mm Hg and 60°C with a liquid flow rate of 0.6 ml/min, the efficiency of the column corresponded to 25 theoretical plates with a separation factor of 1.028 [4]. The change in isotopic composition during the distillation of methyl and ethyl borates was also determined under the previous conditions at 740 mm Hg. The enrichment factor was calculated from the enrichment equivalent to 25 theoretical plates for each system: $\alpha = A^{1/25}$.

The alkyl borates were prepared by the method described in [16]. The azeotropic mixture of methyl borate and methanol was separated with the aid of $CaCl_2$ and LiCl. The physical constants of the materials corresponded to values given in the literature.

The isotopic composition of the boron in the various fractions was determined on an MS-1305 mass spectrometer. The spectra of the alkyl borates were very complex. Peaks of individual ions were superposed on each other, for example, 42 ($B^{10}O_2^+ + B^{11}OCH_3$) or 58 ($B^{10}O_3 + B^{11}O_2CH_3$), and the peaks of ions containing B^{11} without one proton

were superposed on peaks of ions containing B^{10}, etc. B^+ ions were obtained with electrons with an energy of ~100 ev, but they had a low intensity. Therefore it was advantageous to obtain BF_3 from the esters and determine the isotopic ratio in it. In this case, the ratio was readily determined by a comparison of the peaks from BF_2^+ or B^+ [17]. The error in the determination of the isotopic ratio B^{11}/B^{10} was ±0.01.

The BF_3 was obtained from the boric esters in the following way. The ester was hydrolyzed with water and H_2F_2 and NH_4OH were added to the boric acid liberated. A solution with pH 8 was obtained and evaporated to dryness. The addition of H_2SO_4 to the compound $(NH_4)_2O(BF_3)_4$ and heating the mixture liberated gaseous BF_3. These reactions proceed almost to completion.

The results of experiments with the three esters are given in Table 2.

Table 2. Separation of Boron Isotopes in Trialkyl Borates

Compound	Pressure, mm Hg	Temp., °C	Enrichment on column A	Separation factor by Rayleigh's method α	Separation factor determined on a column with 25 plates
$B(OCH_3)_3$	740	56	1.0725	1.0035±0.0005	1.0028
$B(OC_2H_5)_3$	740	56	1.0420	1.0023±0.0008	1.0017
$B(OC_4H_9)_3$	20	128	1.0170	—	1.0007

The table shows that as in the distillation of boron halides, in the distillation of alkyl borates the distillate was enriched in the heavier isotope. This change in the isotopic composition might be expected from a comparison of the structure of boron halides and borates. The structures of the two types of compound are similar: the boron atom lies at the center of the plane of a right triangle formed by halogen or oxygen atoms.

The separation factor falls with a decrease in the size of the molecules. It is interesting to compare this phenomenon with an experiment in [18]. The separation factors B^{10}/B^{11} in ether–BF_3 and thioether–BF_3 complexes hardly decreased or even increased with an increase in the molecular weight of the complex:

Complex	Separation factor
$(CH_3)_2O \cdot BF_3$	1.025
$(C_2H_5)_2O \cdot BF_3$	1.027
$C_6H_5OH \cdot BF_3$	1.027
$C_6H_5OCH_3 \cdot BF_3$	1.030
$(C_4H_9)_2S \cdot BF_3$	1.033
$(CH_3)_2S \cdot BF_3$	1.036
$(C_2H_5)_2S \cdot BF_3$	~1.040

During the distillation of complex compounds of BF_3 with ether there is chemical exchange between BF_3 bound in the complex and gaseous BF_3 passing into the vapor phase on dissociation of the complex. In this case the separation factor is determined primarily by the exchange equilibrium and the reason for the isotopic effect we observed in the distillation of alkyl borates is the difference in the vapor pressure of the two different isotopic molecules.

The degree of isotopic exchange during the distillation of methyl borate approximately equals that during the distillation of BF_3 and BCl_3. The advantages of esters are their thermal stability, low affinity for water, and the simplicity of their recovery. The distillation may be carried out at low temperature and atmospheric pressure. Boric esters and their decomposition products do not corrode glass or metal. Very diverse compounds of boron may be obtained in high yield from methyl borate.

On the basis of all that has been stated above, it may be considered that boric esters are of practical use in the separation of boron isotopes.

LITERATURE CITED

1. I. Mühlenpfordt et al., Proc. Internat. Symposium on Isotope Separation. Amsterdam, North-Holland Publ. Co., 1958, p. 408.
2. M. Green and G. Martin, Trans. Faraday Soc., 48, 416 (1952).
3. N. N. Sevryugova, O. V. Uvarov, and N. M. Zhavoronkov, Atomnaya Énergiya, 4, 113 (1956).
4. K. Holmberg, Proc. Internat. Symposium on Isotope Separation. Amsterdam, North-Holland Publ. Co., 1958, p. 201.
5. G. M. Panchenkov, V. V. Moiseev, and A. V. Makarov, Doklady Akad. Nauk SSSR, 112, 659 (1957).
6. I. Kiss, and I. Opauszky, Magyar kém. folyòirat, 64, 267 (1958).
7. A. Palko, R. Healy, and L. Landau, Chem. Phys. 28, 214 (1958).
8. P. Baertschi, W. Kuhn, and H. Kuhn, Nature 171, 1018 (1953).
9. T. Johns, Proc. Internat. Symposium on Isotope Separation. Amsterdam, North-Holland Publ. Co., 1958, p. 74.
10. I. V. Rabinovich, N. A. Sokolov, and P. I. Artyukhin, Doklady Akad. Nauk SSSR, 105, 762 (1955).
11. A. Palko, Industr. and Engng Chem. 51, 121 (1959).
12. H. Durande, L' Age Nucl., No. 11, 194 (1958) (Murphy: Separation of Boron Isotopes, Oak Ridge, 1952).
13. B. Cooke, I. Hawes, and H. Mackensie, J. S. Afric. Chem. Inst., 7, 11 (1954).
14. S. Makishima, Y. Yoneda, and T. Tajima, J. Phys. Chem., 61, 1618 (1957).
15. A. I. Brodskii, Chemistry of Isotopes [in Russian] (Izd. AN SSSR, Moscow, 1957).
16. H. Schlesinger and H. Brown, J. Amer. Chem. Soc., 75, 213 (1953).
17. G. M. Panchenkov and V. D. Moiseev, Zhur. Fiz. Khim., 30, 1118 (1956).
18. A. Palko, J. Chem. Phys., 30, 1187 (1959).

EXPERIMENTAL DETERMINATION OF AXIAL SELF-ABSORPTION IN CYLINDRICAL Co^{60} SOURCES

K. K. Aglintsev, G. P. Ostromukhova, and E. A. Khol'nova

Translated from Atomnaya Énergiya Vol. 10, No. 1,
pp. 75-76, January, 1960
Original article submitted August 18, 1960

Co^{60} sources are widely used in various branches of science and technology as sources of γ-radiation, and frequently have relatively large dimensions so that they cannot be looked upon as point sources. The dose rate due to such sources is usually calculated from the relationship

$$P=\frac{A}{r^2}\Gamma f e^{-\mu_0 r} p/r, \qquad (1)$$

where μ_0 is the linear absorption coefficient of the γ-radiation in air, r is the distance from the source in cm, A is the activity of the source in mc, Γ is the γ-constant of the isotope which is numerically equal to the dose rate (r/hr) at a distance of 1 cm from a specimen having an activity of 1 mc, and f is the self-absorption coefficient which takes into account the absorption of γ-radiation in the source itself. The latter coefficient indicates the difference between the γ-radiation outside the source and the total γ-radiation which is determined by the activity and the spectral characteristics of the isotope.

Measured Values of the Self-absorption Coefficient f

Length of source, mm	Diameter of source, mm	f
2	2	0.96
4	5	0.92
5	5	0.908
10.8	5	0.836
15	5	0.826

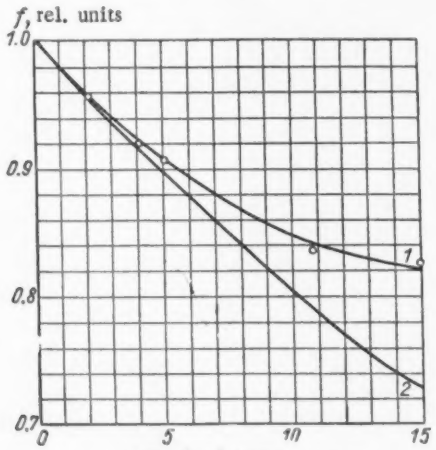

Dependence of the self-absorption coefficient on the length of Co^{60} sources: 1) experimental, 2) calculated.

The correction for self-absorption of the radiation leaving a cylindrical source along its axis is usually calculated (separately for each γ-line) from the formula [1]

$$f=\frac{1-e^{-\mu l}}{\mu l}, \qquad (2)$$

where μ is the linear absorption coefficient of the γ-radiation of cobalt and l is the length of the source in cm. However, the calculation of f from Eq. (2) cannot be considered as entirely correct since the derivation of this formula is based on the assumption that the radioactive isotope is uniformly distributed in the source [2] and that the radiation scattered within the source does not give rise to additional ionization. These two effects are neglected in the calculation.

In order to improve the value of the correction for self-absorption, an attempt was made to determine f for Co^{60} sources experimentally. This was done by measuring the dose rate and the absolute activity of sources of various lengths (between 2 and 15 mm). The dose rate was measured at the end of the specimen, using a narrow collimated beam and a standard apparatus incorporating a free-air chamber [3]. The absolute activity of the sources was measured with the aid of a differential γ-calorimeter [4]. The results obtained are shown in the table and figure (curve 1). Curve 2 shows the values of f based on Eq. (2).

Comparison of the two curves shows that Eq. (2) is correct for sources whose length does not exceed 2-4 mm. As the length increases, the discrepancy between the ex-

perimental and calculated data also increases. This can apparently be explained by the effect of radiation scattered within the source [5, 6].

In order to avoid errors in calculations of the dose rate P, the coefficient f should be determined from the experimental curve (curve 1).

LITERATURE CITED

1. V. G. Gorshkov, γ-radiation of Radioactive Bodies [in Russian](Leningrad State University, 1956).
2. J. Levin, and D. Hughes, Nucleonics 11, No. 7, 8 (1953).
3. K. K. Aglintsev, et al., Atomnaya énergiya, No. 2, 55 (1956).
4. K. K. Aglintsev and E. A. Khol'nova, Tr. Vsesoyuz. n.-i. in-ta metrol., No. 30 (90), 25 (1957).
5. W. Bernstein and R. Schuler, Nucleonics, 13, No. 11, 110 (1955).
6. D. Cormack and H. Johns, Brit. J. Radiol., 31, No. 369, 497 (1958).

ATTENUATION OF GAMMA-RADIATION BY CONCRETE AND SOME NATURALLY OCCURRING MATERIALS

P. N. V'yugov, K. S. Goncharov, V. S. Dementii, and A. M. Mandrichenko

Translated from Atomnaya Énergiya, Vol. 10, No. 1, pp. 76-79, January, 1960
Original article submitted September 5, 1960

The problem of shielding of the personnel and the general population from dangerous radiation is of great importance in the design of linear accelerators. Owing to the considerable length of these accelerators, the shielding structure is relatively expensive, and hence it has become customary to replace concrete by earth (for example, in the case of the large linear electron accelerator at Orsey, France) or other less expensive materials.

The shielding properties and the cost of various types of concrete are well-known [1], while for other building materials there is practically no published data [2]. The present paper reports results of studies of the attenuation of Co^{60} γ-rays by materials whose chemical composition and density are shown in Table 1.

TABLE 1. Characteristics of Shielding Materials

Material	Losses on calcination, %	Composition, %								Density, g/cm³*
		SiO_2	Al_2O	TiO_2	Fe_2O_3	CaO	MgO	Alkalies	SO_3	
Earth	6.02	78.85	11.94		3.86	1.54	1.00	2.42	0.25	1.46
Sand	0.64	96.16	1.48		0.50	0.46	0.10	0.50	0.20	1.64
Clay	7.90	64.40	12.92	0.90	5.00	4.30	1.48	2.90	0.22	1.39

*Refers to freshly deposited materials.

Design of the experiment. The geometry of the experiment is illustrated by Fig. 1. A square-shaped aperture (1.04 m^2) in a concrete wall 2 m thick was employed. A spherically symmetric Co^{60} source having an activity of 0.57 C was placed on the axis of the aperture and in the plane of the wall. The detectors, which were in the form of stilbene crystals mounted on FEU-19M photomultipliers, were located on the axis of the aperture at 2 and 4 m from the source, respectively. All the measurements were thus carried out under wide-beam conditions.

Tin boxes and concrete blocks 1 × 1 × 0.1 m in size were employed. In the case of loose materials, the boxes were inserted into the channel in the wall, and the absorption was determined with and without the materials so that the effect due to the wall of the box could be eliminated. The gaps between the boxes and the walls of the aperture were filled with the material under investigation. No attempt was made to ram the material into the boxes. The thickness of the absorber was increased in the direction towards the source until the indications of the detector placed at 2 m from the source were of the order of the background, which corresponded to 120 cm of concrete and 170 cm for the other materials.

The results obtained with the detector at 2 m from the source are shown in Fig. 2. A similar graph was obtained with the detector at 4 m from the source. For comparison, Fig. 2 also shows the attenuation curve for 1.25 Mev γ-rays by concrete having a density of 2.3 g/cm³. This curve was plotted on the basis of the data given in [3].

The attenuation curves can be used to calculate the absolute absorption coefficients of freshly deposited materials for Co^{60} γ-rays. For absorber thicknesses in excess of 0.3-0.4 m, the attenuation coefficients remain practically constant.

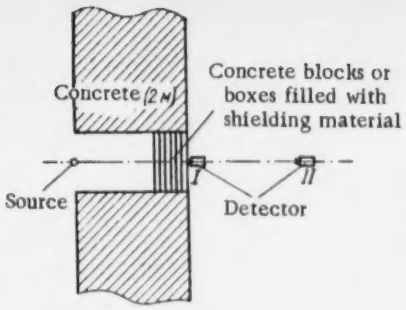

Fig. 1. Experimental arrangement.

The data now reported can be used to estimate the thickness of earth, sand or clay which will be as effective as concrete in reducing the level of radiation to a given figure. Thus, for example, 1 m of concrete is equivalent to 1.36 m of sand, 1.52 m of earth, and 1.61 m of clay.

Discussion of results. It is known that the γ-ray absorption coefficients for Co^{60} γ-rays are proportional to the atomic number Z, while for γ-rays in the region of 15 Mev they are proportional to Z^2. For concrete and the other materials investigated, Z_{eff} is very clearly constant.

The energy spectrum of the lateral radiation from linear accelerators has not as yet been investigated although it is to be expected that relatively low-energy γ-rays (10 Mev or less) should be present at large angles to the beam.

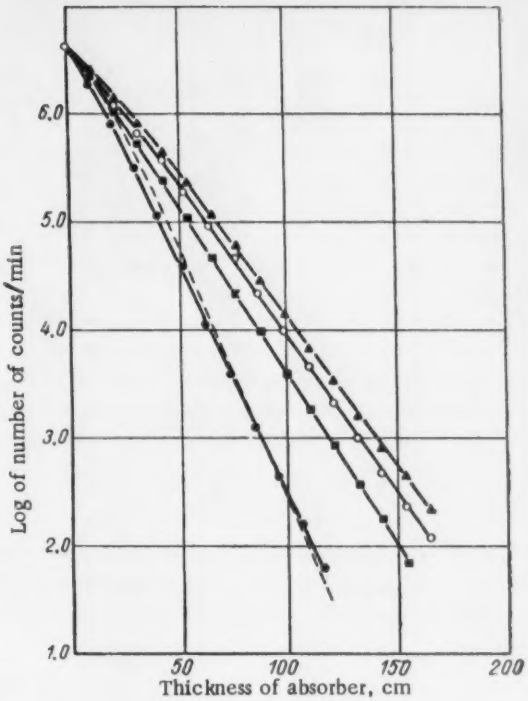

Fig. 2. Attenuation curves for Co^{60} γ-rays for concrete, sand, earth and clay. Source to detector distance 2 m. ● – Concrete, ■ – coarse-grained sand, O – earth, ▲ – clay, – – – curve computed on the basis of data given in [3].

TABLE 2. Calculations of the Cost per 1 m^2 of Shielding

Character and construction of shielding	Cost per 1 m^2 of shielding equivalent to 2 m of concrete		Cost per 1 m^2 of shielding equivalent to 5 m of concrete	
	rubles	%	rubles	%
Solid continuous concrete wall	515	100	1285	100
Two reinforced-concrete walls separated by ordinary earth	315	61	425	33
Two reinforced-concrete walls separated by sand*	320	62	435	34
Reinforced-concrete supporting wall with a bank of earth on one side covered by turf:				
to a height of 5 m	250	49	320	25
to a height of 7 m	260	50	335	26
Shielding wall made of M-25 earth blocks**	375	71	900	70

*3 km from the pit.

**The attenuation coefficient for earth blocks was assumed to be the same as for freshly deposited soil, which in the present case leads to an overestimate of the cost. The building of the shielding wall from earth blocks ensures complete industrialization of the operation. Constructional difficulties are reduced by a factor of 2.3-2.5 as compared with all the other cases.

TABLE 3. Estimated Cost of the Shielding for a 2 Bev Linear Accelerator

Character and design of the shielding	Cost of shielding, %	Consumption of cement, %	Consumption of metal, %
Solid continuous concrete walls with prefabricated reinforced-concrete covering of the accelerator tunnel	100	100	100
Inner (between the accelerator tunnel and working space) screening wall made in the form of two reinforced-concrete walls separated by earth; the outer wall made in the form of a reinforced-concrete support covered from outside by a earth-bank and turf; accelerator tunnel covered with M-50 earth-blocks on a prefabricated reinforced-concrete plate .	47	35	58
The same, with sand replacing the earth*	47	35	58
Shielding made up of soil blocks M-25; accelerator tunnel covered by M-50 soil blocks on a prefabricated reinforced-concrete plate**	78	72	18

*3 km from the pit.

**The attenuation coefficient for earth blocks was assumed to be the same as for the freshly deposited soil, which in the present case leads to an overestimate of the cost. The building of the shielding wall from earth blocks ensures complete industrialization of the operation. Constructional difficulties are reduced by a factor of 2.3-2.5 as compared with all the other cases.

In the present measurements the shielding materials were not compressed since this would only improve their shielding properties. It follows that the difference between the attenuation of γ-rays by concrete, sand and earth at energies corresponding to the Co^{60} γ-rays should not be appreciably greater when the shielding concrete walls are replaced by walls made of sand and earth.

Such a replacement should improve the neutron shielding properties of the walls, owing to the lower Z_{eff} and greater thickness and moisture content.

Costing problems. An estimate was made of the change in the cost of the shielding when the concrete walls of a linear accelerator are replaced by sand and earth in the middle parts of the USSR. The cost of sand and earth includes the cost of ramming [4].

Table 2 gives the estimated cost per 1 m^2 of the shielding for different materials. Table 3 gives the estimated cost for a 2 Bev linear accelerator.

As can be seen from Tables 2 and 3, replacement of the concrete by earth and sand leads to a considerable reduction in the cost of the shielding of a linear accelerator.

In conclusion the authors wish to express their gratitude to V. V. Katrich and V. S. Poryatui for assistance in this work.

LITERATURE CITED

1. A. N. Komarovskii, Building Materials for Shielding of Nuclear Reactor and Accelerators [in Russian] (Moscow, Atomizdat, 1958).
2. G. Guében, Bull. Soc. Roy. Sci., No. 1, 11 (1953).
3. N. G. Gusev, Radiation and Shielding Handbook [in Russian] (Moscow, Medgiz, 1956).
4. Collection of wage-rates in one region for structural work. Nos. 1,6 (Gosstroizdat, 1956).

NEWS OF SCIENCE AND TECHNOLOGY

TENTH INTERNATIONAL CONFERENCE ON HIGH-ENERGY PHYSICS

A. A. Tyapkin

Translated from Atomnaya Énergiya, Vol. 10, No. 1,
pp. 80-83, January, 1961

The Tenth International Conference on High-Energy Physics was held from August 25 to September 1, 1960 in Rochester (USA). Three hundred fifty physicists from 29 countries took part in the Conference.

On the first days of the Conference, simultaneous sessions were conducted on four separate branches of high-energy physics. In these sectional sessions new experimental and theoretical results obtained in various laboratories during the preceding year were reported and discussed in detail. In plenary sessions, reports on specific branches of high-energy and elementary-particle physics were given. In these reports the results presented in the Conference were generalized and systematized, and on this basis, a general view was given of the present state of problems in the respective branches of high-energy and elementary-particle physics.

In one of the sections of the Conference, experimental investigations of strong interactions of nucleons and pions were discussed. Material on this subject was summarized in the papers of J. Ashkin (Pittsburgh, USA) and O. Chamberlain (Berkeley, USA).

In certain laboratories (Dubna, Berkely, CERN) work has been carried out concerning the precision with which the law of conservation of isotopic spin is satisfied. The most precise data have been obtained at Dubna in studying the forbidden reaction in which a neutral pion and an alpha particle are created in d-d collisions. The cross section of the reaction was found to be less than $2 \cdot 10^{-32}$ cm^2 and practically equal to the cross section of the electromagnetic process $d + d \rightarrow \alpha + \gamma$.

The first experimental information was obtained on the very important problem of pion-pion interactions. The group working at Berkely with the large liquid-hydrogen chamber according to the method proposed by Chew and Low obtained data on the cross section of the $\pi^- - \pi^0$ interaction. For relative meson energies of three and five pion masses, the cross sections obtained were equal to ~150 and ~300 mb, respectively.

Another group at Berkely studied the momentum spectrum of He^3 from the reactions

$$p + d \rightarrow \begin{cases} He^3 + \pi^0 \\ He^3 + \pi^- + \pi^+ \\ He^3 + \pi^0 + \pi^0 . \end{cases}$$

Very interesting preliminary data were reported by Crowe. In the high-energy part of the spectrum a sharp maximum with a width close to that of the apparatus was found. If the data on the maximum and its width are confirmed by further measurements, this will indicate the existence of a new particle with a mass of about 2.3 pion masses.

A value of (4^{+6}_{-4}) mb was obtained at Dubna for the cross section of the process $\pi^+ + \pi^- \rightarrow \pi^0 + \pi^0$ at zero energy of interacting π^--mesons.

The most precise data on the scattering of pions by nucleons was obtained this year at Saclay (France). In particular, for the scattering cross section of negative pions by hydrogen, the values of 45.8 ± 1.8 and 58.0 ± 1.8 mb were obtained as maxima at 600 Mev and 900 Mev, respectively. R. Glasser, et al. (Washington) carried out direct measurements of the lifetime of the neutral pion. The measurements were performed in photoemulsions by observing Dalitz pairs from π^0-mesons created together with π^+-mesons in the decay of positive K-mesons. The mean life of π^0-mesons was found to be $(2.3 \pm 0.8) \cdot 10^{-16}$ sec.

The laboratories at Rochester, Dubna, Harwell, and Harvard presented new data on elastic scattering of nucleons by nucleons which were carried out with the purpose of establishing the scattering amplitude.

In Rochester, the depolarization factor D for angles of 30° and 60° in the center of mass system (CMS) and the triple scattering parameters R and A for seven angles in the interval from 30° to 90° (CMS) were measured for p-p scattering with 210-Mev protons. For p-n scattering, measurements of polarization were performed for 12 angles in the interval from 30° to 90° (CMS).

The correlation coefficient of polarization C_{pp} (90°) in p-p scattering was measured at Dubna for proton energies of 315 and 630 Mev.

The results of phase analysis of p-p scattering at energies of 95, 150 and 310 Mev were reported at the Conference by the Moscow group.

Several experiments on elastic scattering of nucleons by nucleons were performed at Liverpool, Berkely and Dubna in order to determine the constants of pion-nucleon interaction.

The Conference gave its approval to the program of the Photomeson Laboratory of the P. N. Lebedev Institute of Physics, Academy of Sciences, USSR (FIAN). This program, which was presented in the paper of A. M. Baldin, involves the analysis of experimental data on the photoproduction of mesons in the near-threshold region.

In the field of photoproduction of mesons, a great deal of research has been done on the second and third resonances of the meson-nucleon interaction. Measurement of proton polarization in the reaction $\gamma + p \rightarrow p + \pi^0$ was done in Frascati (Italy). The differential cross section for the photoproduction of positive pions in the resonance region was studied at Frascata and at the California Institute of Technology (USA). The data obtained agree well with the assumption that the second resonance is due to a dipole transition in the $d_{3/2}$ -state and the third resonance, to an electric quadrupole transition in the $f_{5/2}$ -state. Both resonances correspond to the isotopic spin state $T = \frac{1}{2}$.

Some work on the strong interaction of nucleons and pions was performed at energies greater than 1 Bev. Measurements of proton polarization elastic p-p and p-Be collisions were made with the accelerator at Saclay for proton energies of 1.7 Bev.

The double scattering of antiprotons with momenta 1.5-2.0 Bev/c was investigated by the group at Berkely with the 72-in liquid hydrogen chamber. The magnitude of antiproton polarization averaged over the angular range 6° - 25° (CMS) was found to be 0.51 ± 0.09 under the assumption that the antiproton magnetic moment is equal in magnitude and opposite in sign to that of the proton. Study of the annihilation of antiprotons in the chamber showed that the fraction of annihilations leading to two pions or to two K-mesons does not exceed 1/400 and 1/1000, respectively, of the total probability of annihilation.

The scattering of antiprotons by protons and neutrons at an energy of 1.2 Bev was investigated by Wenzel's group (Berkeley). In this work, the cross sections (elastic and inelastic) for these collisions were shown to be equal.

The reports of the Joint Institute for Nuclear Research (OIYaI) (V.Petrzhilka, V. I. Veksler) contained a large amount of material on the study of pion and nucleon interactions in the energy region from 3 to 9 Bev. From a comparison of experimental data obtained on the synchrophasotron with theoretical investigations at OIYaI (D. I. Blokhintsev et al.) and FIAN (D. S. Chernavskii) it was concluded that the interaction of nucleons and pions occurs mainly in the pion shells of nucleons.

Using the large CERN accelerator, von Dardel's group measured the total cross section for the interaction of pions, protons, and antiprotons with protons in the energy range from 3 to 10 Bev. The pion-proton cross sections in this range have values of the order of 30 mb. The proton-proton cross sections decrease with increasing energy, having at 10 Bev a value of about 42 mb. The cross section for p-p scattering at 10 Bev exceeds the cross section for p-p scattering by 20 mb.

A separate plenary session was devoted to the structure of elementary particles. New experimental data on the electromagnetic structure of nucleons were reported in the papers of R. Hofstadter (Stanford, USA) and R. Wilson (Cornell, USA). New measurements of form factors were made for $q^2 = 25$ (in reciprocal fermis). The difference between magnetic and electric form factors for the proton was established. With increasing energy, the magnetic form factor decreases and the electric form factor approaches a constant value. In all earlier work the equality of these form factors had been assumed. The experimental data on electron scattering by the neutron continue to be compatible with the assumption that its electric radius is zero.

A great deal of experimental material on strange particles was presented at the Conference. In the section dealing with this subject, 27 papers were given.

The paper of E. Turkot (Cornell University) was devoted to the photoproduction of strange particles. Study of the reaction $\gamma + p \rightarrow \Lambda^0 + K^+$ at energies of 910-1040 Mev showed that the differential cross section for this reaction is isotropic in the CMS and amounts to about $1 \cdot 10^{-31}$ cm^2/sr. In an investigation of the reaction $\gamma + p \rightarrow \Sigma^0 + K^+$ it was found that the excitation curve is proportional to the cube of the momentum of the K^+-meson. The photoproduction of K^+-mesons in deuterium for two values of the γ-quantum was also studied. It was found that within the limits of error of measurement the cross section for production of K^+-mesons with a neutron is equal to that with a proton.

The group working with the 72-in liquid-hydrogen chamber at Berkeley studied the generation of strange particles in π^--p collisions in the near-threshold region. In this work, in order to determine the relative frequency of hyperons, the peculiarities in behavior of different terms in the expression for the differential cross section for the reaction $\pi^+ + p \rightarrow \Lambda^0 + K^0$ were investigated in their dependence on the threshold energy of the reactions:

$$\pi^- + p \rightarrow \begin{cases} \Sigma^0 + K^0 \\ \Sigma^- + K^+. \end{cases}$$

M. I. Solov'ev reported on new data (obtained by the Dubna group with the propane chamber) on the generation of strange particles in pion-nucleon collisions at an energy of 8 Bev. I. V. Chuvilo (Dubna) reported on the generation of strange particles by 3-Bev negative pions. Considerable interest was aroused by data obtained here on an asymmetry in the decay of Λ-hyperons, which indicated the possibility of nonconservation of parity in strong interactions.

Investigations carried out at Dubna showed that the picture presented at the Kiev Conference of the generation of unstable particles by 7-Bev π-mesons can be explained fully without assuming the existence of a new particle.

The first results on the creation of strange particles by 16-Bev π^--mesons were presented at the Conference (obtained at CERN with the 32-cm hydrogen bubble chamber). In this work, a value of ~1 mb was obtained for the cross section for generation of Λ-hyperons and ~3 mb for K^0-mesons. In the CMS the Λ-hyperons created are strongly directed backward. This result indicated that in the 16-Bev region the same laws hold as at energies investigated earlier at Dubna.

In the propane chamber at Saclay, 81 cases of the production of Σ^+-K^+ pairs by hydrogen were obtained in a beam of positive pions with a momentum of 1.15 Bev/c. The cross section for this reaction was found to be 0.26 $\pm$ 0.05 mb. The resulting angular distribution of particles produced in this reaction does not agree with the distribution required by isotopic invariance. However, the statistical accuracy does not permit a final conclusion.

M. Good (University of Wisconsin, USA) reported on research on the interactions of 1.15-Bev/c K^--mesons in a hydrogen bubble chamber. In this work the analysis of momentum spectra of π^+-mesons produced in the reactions $K^- + p \rightarrow \Lambda + n\pi$ suggests the existence of excited states of hyperons.

The experimental work on weak interactions presented at the Conference was concerned mainly with research on the properties of μ-mesons.

V. A. Lyubimov (Institute of Theoretical and Experimental Physics, Academy of Sciences, USSR) reported on measurements of the helicity of μ-mesons. It was found that in $\pi \rightarrow \mu$ decay the negative μ-meson has a right-hand helicity ($P_- = +0.65 \pm 0.22$) and the positive one has left-hand helicity ($P_+ = -0.15 \pm 0.21$).

The first results were obtained in experiments to measure the difference in precession and cyclotron frequencies for μ-mesons. At Columbia University it was found that

$$\frac{g-2}{2} = \begin{pmatrix} 1.0 + 0.10 \\ -0.14 \end{pmatrix} \cdot \frac{\alpha}{2\pi}.$$

According to preliminary data obtained at CERN, this quantity equals

$$\frac{g-2}{2} = (1.8 \pm 0.3) \cdot \frac{\alpha}{2\pi}.$$

At Berkeley, experiments were conducted to determine the probability of a neutrinoless transition from μ-meson to electron. It was found that the probability of this transition amounts to less than $4 \cdot 10^{-6}$ of the probability of the neutrino transition.

A. I. Mukhin reported on research carried out with the synchrocyclotron at Dubna on the intensity of radiationless transitions in the mesic atoms of Pb, Bi, Th, U^{235} and U^{238}. The experimental results of this work are satisfactorily explained by assuming the presence of a mechanism of energy radiation analogous to Raman scattering in optics.

The asymmetry in angular distribution of neutrons emitted by nuclei of Mg and S in the capture of polarized μ^--mesons was subjected to several investigations. In Chicago, measurements were made of the probability of μ^--meson capture in the isotopes Cl^{37} and Cl^{35}. The relative probability of these captures was found to be 0.694 ± 0.034. The ratio calculated by the formula of Primakov is equal to 0.82. At Columbia University, work was successfully completed on the observation of muonium (μ^+e^-). It was found that the degree of polarization of muonium in argon depends strongly on admixtures of other gases. For the first time, scattering of μ-mesons was studied with an accelerator. Mu mesons with a momentum of 1.95 Bev/c obtained with the Bevatron (Berkeley) were scattered by lead. Anomolous scattering was not observed. At Liverpool, measurements were made of the mean life of the μ-meson in connection with the discrepancy of results obtained earlier at Chicago and at CERN. The value found was $\tau = 2.230 \pm 0.006$ μ sec.

A large number of theoretical papers were presented at the Conference. A great deal of interest was elicited by the reports of R. Eden (Berkeley) and J. Polkinghorne (Cambridge University, Great Britain), which were devoted to proof of the double dispersion relations of Mandelstam. An important contribution to the study of the analytic structure of matrix elements was made in the report of A. A. Logunov (Dubna). The papers of A. P. Rudik (Institute of Theoretical and Experimental Physics) on singularities of scattering amplitude in perturbation theory should be mentioned, as should his reports on the work of V. N. Gribov (LFT), V. B. Berestetskii and I. Ya. Pomeranchuk (ITEP) on the asymptotic values of cross section in the very high energy region.

The following papers were concerned with practical application of the dispersion relations: G. Chew (Berkeley) on pion-pion scattering, M. Cini (Italy) on new numerical results obtained at CERN on pion-nucleon scattering, and A. M. Baldin (FIAN, USSR) on a new treatment of data on photoproduction based on the relativistic dispersion relations. The report of D. V. Shirkov (Dubna) on a new method of obtaining equations for partial waves contained a series of numerical data on π-π and π-N scattering at threshold.

Problems of elementary-particle theory were discussed at a special session presided over by W. Heisenberg (Munich). Considerable interest at this session was aroused by the paper of Y. Nambu (Chicago), in which the mathematical methods developed by the Soviet scientist N. N. Bogulyubov in the theory of superconductivity was successfully applied to field theory. Bogolyubov reported on the interesting results of the work of A. N. Tavkhelidze (Dubna), in which the methods of superconductivity theory were applied to field theory.

In the paper of Heisenberg, some general properties of equations obtained earlier by him were investigated.

D. I. Blokhintsev (Dubna) reported on attempts, based on the mathematical work of Lapo-Danilevskii, to solve some problems of elementary-particle theory without the use of the expansion in the interaction constant.

Several papers were concerned with semiphenomenological theories. S. Drell (Stanford, USA) showed that at high energies γ-quanta give a more effective method of obtaining high-energy pions than do nucleon-nucleon collisions, which lead to a high multiplicity of the mesons produced.

The papers of M. A. Markov (Dubna) and T. Lee were devoted to processes involving high-energy neutrinos. These reports discussed the question of the possible existence of intermediate mesons in weak interactions and also the question, raised earlier by B. Pontecorvo, of the possible nonidentity of neutrinos involved in β-processes and neutrinos formed in the decay of mesons. The papers of R. Feynman and M. Gell-Mann (Cal. Tech.) discussed problems associated with the conservation of vector current.

The Conference, which proceeded in a friendly and business-like atmosphere, certainly played a significant role in uniting the efforts of scientists of various nations who are occupied with the study of the most important field of contemporary physics. The Proceedings of the Conference will be published by the University of Rochester early in 1961.

After the Conference the Soviet delegation visited and inspected many American laboratories which are doing reseach in the field of high-energy physics. The delegates became familiar with the 240-Mev synchrocyclotron at the University of Rochester; the 1.2 Bev, strong-focusing electron accelerator at Cornell University; the 380-Mev synchrocyclotron at Columbia University; the 3- and 30-Bev proton accelerators at the Brookhaven Laboratory; the 3-Bev, high-precision proton accelerator with weak focusing, under construction at Princeton; the 6-Bev, strong-focusing electron accelerator under construction in Boston; and also with the laboratories of the Massachusetts Institute of Technology. The Soviet delegates taking part in the International Conference on Instrumentation for High-Energy Physics became familiar also with the 960-Mev linear accelerator at Stanford University and with the 730-Mev synchrocyclotron and 6.3 Bev Bevatron at Berkeley.

The delegates from the Soviet Union were given a warm reception everywhere, both from the officials who conducted this Conference and from the American physicists. It should be mentioned also that there in a great deal of interest in the USA in Soviet physics. At the request of American physicists, D. I. Blokhintsev, V. I. Veksler, V. P. Dzhelepov, S. Ya. Nikitin, and A. S. Belousov gave survey reports at Brookhaven and at Stanford on research which has been done in the Joint Institute for Nuclear Research, the Institute of Theoretical and Experimental Physics, and the P. N. Lebedev Institute of Physics, Academy of Sciences, USSR.

At the meeting of the Committee on High-Energy Physics of the Union of Pure and Applied Physics, it was decided to increase the interval between conferences to two years in order to permit more complete investigations.

The Eleventh International Conference on High-Energy Physics and the Conference on Instrumentation is planned for July, 1962 in Geneva. The next conference on accelerators is planned for September, 1961 at Brookhaven.

INTERNATIONAL CONFERENCE ON INSTRUMENTATION FOR HIGH-ENERGY PHYSICS

A. A. Tyapkin

Translated from Atomnaya Énergiya, Vol. 10, No. 1,
pp. 83-85, January, 1961

The International Conference on Instrumentation for High-Energy Physics took place in Berkeley (USA) from September 12 to 14, 1960. Two hundred forty persons from 13 countries took part in the Conference.

Seventy-three papers on new developments of methodology were given. The Soviet delegation presented eight papers covering part of the important work which has been done in the field of high-energy physics.

The first session was devoted to problems of separation and focusing of high-energy particles. J. Murray (Berkeley) reported important results in the use of glass electrodes in electrostatic separators. Tests showed that the use of glass plates made it possible to double and even triple the regularly used electric field strength. At Berkeley, separators with glass plates have already been used with fields of 150 kv/cm instead of the usual 60 kv/cm.

In the paper of M. Good (University of Wisconsin) the problem of an energy limit for electromagnetic separators was discussed. In the speaker's estimation this limit for the separation of K-mesons lies at about 10 Bev/c.

Several reports were devoted to the production of large magnetic field. H. Furth (Berkeley) described impulse coils for obtaining magnetic fields up to 160 kilogauss in small volumes. The report of R. Post (Berkeley), which was received with great interest, presented a detailed discussion and also experimental data on obtaining constant, high-intensity magnetic fields in large volumes using sodium or aluminum coils cooled with helium. The electrical resistivity of these metals over a wide range is independent of the magnetic field strength. As an example, the speaker presented calculations of a coil, cooled by helium to 10°K, for producing a constant field of 60 kilogauss in a volume of 1 m^3.

A large amount of material on electronic methods of recording particles was presented at the Conference. A central place in this subject was set aside for new detectors of charged-particle tracks—spark, discharge, and luminescent chambers. The survey paper of M. S. Kozodaev on spark chambers developed in the Soviet Union was met with great interest. A. A. Tyapkin reported on research at OIYaI and MIFI on the conditions under which the discharge develops along the particle track in the chamber.

An interesting report was given by S. Fukui (Japan) on the results of tests of a high-frequency discharge chamber. The 150 × 100 × 20 mm chamber was filled to atmospheric pressure and neon and a half-percent admixture of argon. A 3.7-kv/cm, 2.8 × 10^{10}-cycle field from a magnetron is applied for about 10^{-7} sec with a delay of 0.5 μsec after passage of the charged particles through the chamber. Along the track of the particle, a luminosity of the gas arises which diminishes more slowly than in the case of a spark chamber.

The papers of J. Cronin (Princeton) and B. Cork (Berkeley) attested to the successes achieved in the development of spark chambers. The Princeton chamber contains 19 aluminum electrode-plates about 6 mm thick, situated 10 mm one from another and having a sensitive area of 18×18 cm^2. The chamber is filled with neon. This chamber has already been used for measuring the proton polarization. Figure 1 shows a photograph of two projections of the track of a proton which has undergone scattering in one of the plates of the chamber.

An analogous spark chamber was developed at Berkeley and was tested with both neon and argon. An efficiency of 99% was attained with pulses of 10 kv amplitude in the case of neon and 15 kv in the case of argon (the interelectrode spacing in this chamber was about 6 mm). The recovery time of the chamber after a discharge is about 10 msec. The sensitivity time of the chamber without a clearing field is 10 μsec, and with a field of 160 v/cm it decreases to 0.5 μsec. Interesting results were obtained when the chamber was tested in a magnetic field of 13,000 gauss parallel to the plane of the electrodes. In conclusion, the speaker showed electrodes made of graphite for a new chamber to be used in measuring the polarization of protons. D. Meyer (Michigan, USA) reported on a discharge chamber whose electrodes were made of a thin foil. A chamber with such an electrode system is useful in the study of the angular distribution of particles liberated from a liquid hydrogen target.

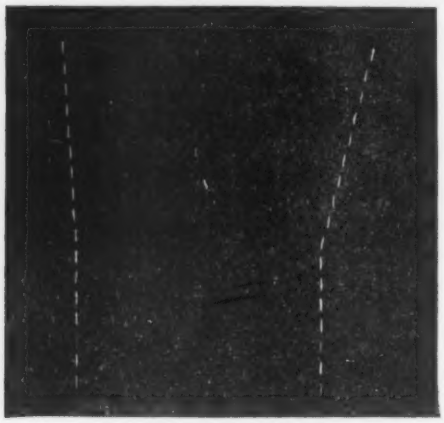

Fig. 1. Projections of the spark track of a proton

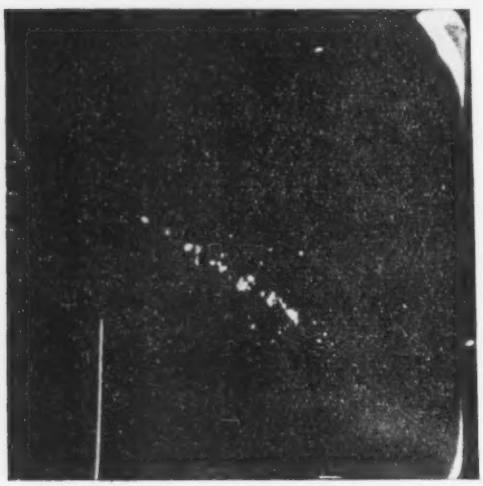

Fig. 2. Track of a cosmic ray particle

Considerable success was achieved in several laboratories in the USA during the past year in the development of luminescent chambers, which were proposed earlier by E. K. Zavoiskii (USSR). Extensive work on the creation of scintillation chambers became possible thanks to the appearance in laboratories of reliably effective electron-optical converters. Each stage of an electron-optical converter insures a 30-fold amplification for a voltage of 15 kv. Three such stages are usually used in amplifying light from a scintillator.

A paper presented by the Berkeley group reported on luminescent chambers intended for investigation of elastic and inelastic scattering of negative pions by hydrogen in the energy range 1.5-2.5 Bev. A crystal of sodium iodide is used as the scintillator. In studying inelastic scattering the use of two luminescent chambers is recommended.

Lande (University of Pennsylvania) reported on a chamber whose scintillator is built up of fine fibers made of scintillating plastic. Total internal reflection in the fibers insures an effective collection of light at the photocathode of an electron-optical converter. This type of scintillator has been chosen by several laboratories in the USA, in particular at Princeton University and Massachusetts Institute of Technology. The construction of the chambers is practically identical. The diameter of the scintillating fibers is 0.5 and 0.7 mm. The fibers are arranged in uniform rows in two mutually perpendicular directions and are fastened in a single unit with the aid of Epoxy resin. An independent light-amplification system is used for the fibers of each direction. The first stage of the electron-optical converter insures image reproduction on a fluorescent screen with an emission time of about 1 μsec. The control system for this time includes the second stage of amplification. For convenience of observation and photography, after the third stage of amplification, the image is focused on the photocathode of a television kinescope. Dr. Hill at MIT created a special scintillation chamber of dimensions of $12 \times 12 \times 24$ cm which can be operated in a magnetic field of 50 kilogauss for measuring the magnetic moment of the Λ^0-particle. A photograph of the track of a cosmic ray particle passing through a fiber scintillator is presented in Fig. 2.

A great deal of attention at the Conference was paid to gas Cerenkov counters. The most important paper in this field was given by A. Roberts (Argonne National Laboratory, USA), who told of a new type of Cerenkov counter which permits precise measurement of the speed of a particle within a wide range of speeds and also determination of the direction of motion of the particle with high precision. In this detector, the Cerenkov light from the gas radiator is amplified using four photomultipliers, and the speed of the particle is determined from the diameter of the illuminated ring on a television screen. The direction of motion of the particle is determined by the position of the center of the ring. The relative precision of the velocity measurement is estimated to be $\sim 10^{-3}$-10^{-4}.

The paper of R. Schluter (Argonne National Laboratory) was devoted to the same problem of combining precision of velocity measurement with wide measureable angle. In this detector, the Cerenkov light from the separate angular intervals is collected by fiber light-guides at the photocathodes of separate photomultipliers.

I. V. Chuvilo gave a report on the gas Cerenkov counter used for the separation of K^+-mesons at the synchrophasotron of the Joint Institute for Nuclear Research.

New ionized-particle detectors based on p-n junctions in semiconductors are of significance. The paper of L. Yuan (Brookhaven National Laboratory), which was received with much interest at the Conference, discussed ionization losses in the sensitive layer of a silicon detector. This work showed the possibility of clearly separating positive pions of momentum 700 Mev/c from protons of the same momentum on the basis of amplitude analysis. The energy of liberation for pions and protons of this momentum amounts to 110 and 200 kev, respectively.

C. Wiegand reported on a very complete multichannel system of scintillation counters developed at Berkeley, the impulses from whose photomultipliers are fed directly to the memory of a computer. This apparatus is especially constructed to obtain information on the π-π interaction on the basis of a study of the processes $\pi^- + p \rightarrow \pi^- + \pi^+ + n$ and $\pi^+ + p \rightarrow \pi^+ + \pi^+ + n$. The determination of neutron energies up to 50 Mev is accomplished by time-of-flight measurements. In the future, similar systems of scintillation counters directly connected to computers will undoubtedly replace the usual counting systems utilized in coincidence and anticoincidence circuits.

At one of the sessions, proposed neutrino experiments were discussed in the presentations of C. Cowan (Washington), K. Greisen (Cornell University), L. Lederman (Columbia University), and others. Theoretical problems requiring experimental tests with neutrinos were reported by C. Yang (Princeton). D. I. Blokhintsev told about work in this field that has been carried out in the Soviet Union. Particle detectors planned for neutrino experiments have grandiose dimensions. For example, at Columbia University, a spark chamber of dimensions $2 \times 2 \times 1$ m is being developed for the study of scattering of neutrinos by electrons. The electrodes of this chamber will be made of iron one cm thick, and the total weight of this system will exceed 15 tons.

Specialists in bubble chamber technique discussed experiments in two separate sectional meetings. At these sessions, reports from the Radiation Laboratory in Berkeley were presented on a xenon bubble chamber, on experiments with a large hydrogen chamber (L. Alvarez), and on a combination of a bubble chamber with a hodoscopic counting system. A paper by Glaser (Berkeley) compared various types of bubble chambers.

V. P. Dzhelepov told of a meter propane chamber in a magnetic field developed at Dubna. The report of I. V. Chuvilo was devoted to the identification of particles in a xenon chamber without a magnetic field. A report from the Brookhaven Laboratory was presented on the construction of a 20-inch liquid-hydrogen bubble chamber. A report from Princeton University was devoted to a rapid-cycling bubble chamber with propane and hydrogen. C. Ramm told of the propane chamber developed at CERN.

The fruitful exchange of information on the newest technological developments that took place at this Conference will undoubtedly benefit the growth of the experimental basis of high-energy physics in the next few years. Also very important is the establishment of personal contacts between physicists and engineers working in various countries on the creation of the most complex apparatus for high-energy physics research.

The Conference material will be published by the University of California at the beginning of 1961.

A DEVICE FOR THE MEASUREMENT AND AUTOMATIC CONTROL OF LIQUID DISCHARGE BY MEANS OF RADIOACTIVE RADIATION

N. N. Shumilovskii and Yu. V. Gushchin

Translated from Atomnaya Énergiya, Vol. 10, No. 1,
pp. 93-94, January, 1961

The solution of many problems in modern technology necessitates the development of new methods for measuring and controlling various technological parameters. Among such problems are the development of methods for the automatic control of various industrial processes that are connected with the motion of highly aggressive and explosive liquids as well as liquids that are at high temperatures and under high pressures.

From among the new methods, the contactless method of automatically controlling liquid discharge by using radioactive radiation deserves attention. One of the methods of measuring the discharge of liquids by using radioactive isotopes has been developed at the Institute of Automation and Remote Control, Academy of Sciences, USSR. This method is based on mechanical modulation of radioactive radiation. A multivane wheel, which is placed in the liquid flow, serves as the sensing element. One or several vanes of the wheel contains a radioactive isotope, which is pressed into the vane in such a manner that it cannot come into contact with the liquid. A lead collimator, where the radiation from the radioisotope is partially absorbed over a certain segment of its rotation path, is mounted on the outisde of the pipe wall. The radioactive radiation receiver, which is connected to the measuring device by means of a cable, is located behind a screen. The Co^{60} isotope is used as the radioactive radiation source. Instead of this one, any other γ-source whose γ-quanta energy is sufficient to secure the necessary penetrability through the piping walls can be used. Of the radioisotopes that are most widely used at the present time, Cs^{137}, Eu^{154}, Sn^{113}, etc. can be used. In the case of a different data transmitter design (with a lighter wall), β-sources can be used: Sr^{90}, Tl^{204}, etc.

As the vane wheel rotates in the liquid flow, the amount of radiation falling on the receiver per single vane wheel revolution changes from a given minimum to a certain maximum value due to the presence of the absorbing collimator in the device. The thus modulated radioactive beam falls on the receiver, for which a counter is used. The counter transforms the energy of γ-quanta into electric energy in the shape of pulses. Through a cable, whose length can be equal to several hundreds of meters, electrical pulse packages arrive at the electrical measuring device input. The electrical measuring device serves for counting the number of pulse packages arriving from the receiver and for determining the total liquid discharge with respect to this count as well as for measuring the arrival frequency of packages, which makes it possible to determine the instantaneous liquid discharge. An electronic self-recorder can be connected to the measuring device.

An experimental model of the radioactive liquid flowmeter (see figure), which was constructed at the Institute of Automation and Remote Control, Academy of Sciences, USSR, was investigated at the All-Union Scientific Research Institute of Glass in measuring black oil flow. In these experiments, a mechanical volume-type flowmeter with the counting mechanism removed, which was developed at the All-Union Scientific Research Institute of Glass, was used as the primary converter of black oil flow; instead of using packing glands, the device was made completely airtight. The tests were performed for discharges from 0.1 to 1.0 m^3/hr. The total discharge accuracy was maintained within $\pm 0.5\%$. The maximum error in measuring the instantaneous discharge value was $\pm 1.5\%$ of the scale upper limit. The new method made it possible to reduce the operational sensitivity threshold of mechanical flowmeters to a great extent, and to improve the measurement accuracy.

At the present time, in collaboration with the Institute of Physics, Academy of Sciences, Latv. SSR, the All-Union Scientific Research Institute of Glass, and the Special Design Office (SKB) of the Avtoelectropribor Plant, the Institute of Automation and Remote Control, Academy of Sciences, USSR, is engaged in the development of a standarized design of the RZhr-1 device for the measurement and automatic control of the discharge of liquids flowing through a closed piping system as well as for the dosing of liquids. The device measuring section is based on standardized URAP units. The device design will make it possible to measure the total and the instantaneous discharge, to dose a required amount of liquid with the possibility of adjustment to the assigned value, and to record the

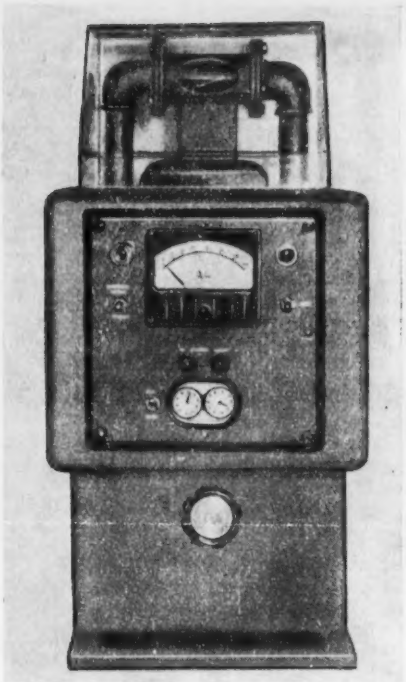

Experimental model of the radioactive liquid flowmeter.

readings by means of a self-recorder. The complete assembly of the standardized units, each of which performs the above-indicated functions, constitutes the measuring unit of the RZhR-1 device. In the first variant of the RZhR-1 device (the design of which was developed at the Special Design Office (SKR) of the Avtoelectropribor plant), which is designed for measuring black oil discharge, a specially constructed volume-type flowmeter using β-radiation is utilized as the discharge data transmitter. The data transmitter makes it possible to measure the discharge of black oil under pressures in excess of 6 kg/cm^2 in the discharge range from a few liters per hour to 4000 liters/hour. If a suitable data transmitter that is designed for measuring the discharge of different liquids is connected to the measuring device, no additional modifications of its measuring unit are necessary.

The described method and the measuring equipment of the RZhR-1 device can also be used for contactless tachometry, i. e., for measuring the number of revolutions of rotating parts, shafts, etc. in locations that are not readily accessible. For this purpose, only a specially constructed data transmitter (primary transducer) can be used.

BRIEF COMMUNICATIONS

Translated from Atomnaya Énergiya, Vol. 10, No. 1,
p. 95, January, 1961

USSR. The Ninth Session of the Scientific Council of the Joint Institute of Nuclear Studies was held at the end of November in Dubno. Prominent scientists from 12 countries which are members of the Institute participated in the work of this session.

The Scientific Council heard reports concerning the most important results obtained in 1960 by Soviet and foreign scientists working in Dubno.

The personnel of the High-Energy Laboratory succeeded in considerably improving the 10-Bev synchrophasotron.

USSR. On the initiative of UNESCO and the Academy of Sciences, USSR, an international symposium on primary and initial processes occurring in living cells under the action of ionizing radiation was held in September in Moscow. Eminent biologists from USA, Great Britain, France, Belgium, Czechoslovakia, and the USSR took part in this symposium.

The participants at the symposium brought forward a new point of view concerning the processes of radiation action on living cells while paying attention to injuries sustained by internal cell structures. In the reports by P. Alexander (Great Britain), Z. M. Bach (Belgium), and A. G. Pasynskii (USSR), it was emphasized that injuries to internal cellular membrane structures greatly affect the metabolism process. The ionizing radiation action results not only in direct injuries to the cell nucleus, as was maintained for a long time by biologists, but also to other cellular organic components.

Two basic methods for radiation protection were proposed recently. The first (prophylactic) method consists in introducing special protective substances into the organism before irradiation. These substances receive the main radiation shock and protect the organism. For instance, Prof. Z. M. Bach recommends a substance which reduces the action of radiation by 50%. The other method is the so-called substitutiontherapy, which consists of introducing into the organism unirradiated tissue which is most affected by the action of radiation. However, these two methods have not yet been sufficiently studied, and they do not always yield satisfactory results.

USSR. A group of collaborators of the Central Scientific Research Laboratory of the Construction Ministry of the Latv. SSR succeeded in producing heavy concrete which is characterized by great density.

This shielding material has been successfully used in the nuclear reactor under construction in Salaspils.

USSR. Radioactive devices for measuring the thickness of pastes that are applied to various materials are now being utilized at the Kalinin Iskozh combine.

These thickness meters provide the possibility of accurately controlling the paste layer thickness, which provides a yearly saving of several millions of rubles. Until recently, paste layers of maximum thickness had to be applied if the quality of leather substitutes was not to suffer. Equipment for such measurements was not available before the development of radioactive thickness meters.

BIBLIOGRAPHY

NEW LITERATURE

Translated from Atomnaya Énergiya, Vol. 10, No. 1,
pp. 99-110, January, 1961

Books and Symposia

Issledovanie kriticheskikh parametrov reaktornykh sistem [A Study of critical parameters of reactor systems]. Symposium. Moscow, Gosatomizdat, 1960. 118 pages, 36 kopeks *

The symposium contains original articles not previously appearing in printed form and dealing predominantly with theoretical calculations and critical parameters in various reactor systems.

Graphs and tables are given to establish the dependence of the critical parameters on the relative concentration and nature of fissionable material and moderator, as well as on fuel enrichment for a wide range of neutron energy spectra.

The book is compiled for engineers and physicists working in the field of reactor system design, for experimental physicists, and for specialists in the related fields dealing with processing of uranium- and plutonium-containing products.

M. Gauzy, T. Kahan. Upravlenie yadernymi reaktorami [Nuclear reactor control]. Translated from the French. Moscow, Atomizdat, 1960. 174 pages, 88 kopeks.

The book contains the first two chapters of volume II of the French three-volume edition "Introduction a la Physique Nucleaire."

The first chapter (chapter VII in the original) presents a survey of the basic characteristics of different particle detector types. The general physical operating principles of detectors are explained, and a concise description of accessories is given.

The second chapter (chapter VIII in the original) takes up the problem of control of nuclear reactors. Techniques of reactor power measurement, control devices, steady state control, reactor start-up, and emergency scram systems are discussed.

The translation will be found useful by engineering and technical workers in nuclear industry.

Spravochnik po korrozii i iznosu v yadernykh reaktorakh s vodyanym okhlazhdeniem [Handbook of corrosion and wear in water-cooled reactors]. Translated from the English. Moscow, Atomizdat, 1960. 402 pages, 1 ruble, 89 kopeks.

The handbook is devoted to corrosion and wear of structural materials where water is used as coolant in nuclear power reactors.

The handbook consists of three parts. Part I presents general information on iron and steel corrosion effects, friction and wear, and takes up questions related to water technology. Part II describes techniques for testing resistance to wear and corrosive attack on the part of some materials and combinations of materials, with tabulated data and discussion of various factors affecting corrosion and wear. Part III is devoted to special research on materials selection and development of concrete reactor designs.

The handbook is compiled to service a broad readership of scientific workers, engineers, and technicians interested in reactor design.

Yu. M. Dymkov. Uranovaya Mineralizatsiya rudnykh gor [Uranium mineralization in the Krušné Hory (Erzgebirge)]. Moscow, Atomizdat, 1960. 104 pages, 34 kopeks.

---

* Translator's note: all prices listed are given in terms of the new "heavy ruble."

The book is based on an analysis of factual material and theoretical concepts published in the Soviet and foreign press. Information on vein formations and mineral associations of endogenic occurrences is presented for one of the world's oldest mining regions, the Krusné Hory [or Erzgebirge, between Saxony and Bohemia, SE of Dresden, NW of Prague – translator's note].

The book deals mainly with the genesis of uranium occurrences and first of all with the evolution of the hypogenetic mineralization of the Krušné Hory. A good deal of space is given to the mineralogical characteristics and geochemical analysis of discrete stages of mineralization of various endogenic occurrences in the Krušné Hory.

Literature data embracing some 160 titles are supplemented by findings from the author's investigation of extensive mineral collections. The text is illustrated with original sketches and microphotographs.

The book is written for geologists, mineralogists, and geochemists engaged in the study of uranium deposits, and for a wide audience of specialists interested in the theory of ore formation.

Sbornik rabot po nekotorym voprosam dozimetrii i radiometrii ioniziruyushchikh izluchenii [Symposium of papers on some aspects of dosimetry and radiometry of ionizing radiations]. Moscow, Gosatomizdat, 1960. 188 pages, 1 ruble.

The symposium contains 23 articles all by Soviet authors. Part I considers particular problems in the dosimetry of gamma and beta radiations. Part II deals with neutron dosimetry, primarily with neutron dosimetric instruments. Part III discusses the general problems encountered in the radiometry of aerosols and gases, plus some particular problems of interest in the area of radiometric monitoring.

A. V. Bibergal', V. U. Sinitsyn, N. I. Leshchinskii. Izotopnye gamma-ustanovki [Isotope gamma facilities]. Moscow, Atomizdat, 1960. 156 pages, 45 kopeks.

The book deals with basic questions in irradiation techniques. It discusses sources of ionizing radiations for isotope gamma radiation facilities, presents examples of various types of gamma facilities, and specifies the requirements applying to them. Structural components of gamma facilities, such as irradiators, systems for positioning objects and irradiator units, radiation shielding, charging of irradiators, controls, etc. are described. Techniques used in calculating the dose field of sources of different geometry are explained. Design requirements affecting gamma facilities are listed, and examples of shielding calculations for gamma facilities are given. A list of reference literature appears at the end of each chapter.

The book is written for engineering and technical workers interested in problems of irradiation techniques.

Pribory i metody analiza izluchenii, No. 2 [Instruments and techniques in radiation analysis]. Moscow, Atomizdat, 1960. 168 pages, 49 kopeks. (Moscow Engineering and Physics Institute.)

17 papers by the faculty and graduate students at the Moscow Engineering and Physics Institute, delivered at the 1957 conference of the Institute, are published in the symposium. Of these, four papers are devoted to questions directly related to the design of shielding devices. Four papers take up dosimetry problems regarding ionizing radiation. The last four articles describe a facility based on delayed coincidences designed to measure 10^{-10} to 10^{-7} sec time intervals; other topics are the determination of small phases in pion-nucleon scattering and problems involving attempts to increase the dispersion and resolving power of magnetic analyzers.

Articles from the Periodical Literature

I. Nuclear Power Physics

Neutron and reactor physics. Physics of hot plasmas and controlled fusion. Physics of charged-particle acceleration

Voprosy istorii estestvoznaniya i tekhn., No. 9 (1960)

––, p. 18-27. Reminiscences of Frederic Joliot-Curie. (Remarks at the reunion of scientists with participants of the session of the Bureau of the World Peace Council, devoted to the memory of Frederic Joliot-Curie: A. N. Nesmeyanov, D. V. Skobel'tsyn, John Bernal).

N. A. Figurovskii, 28-37. Reminiscences of Frederic Joliot-Curie (on the anniversary of his death).

Doklady akad. nauk SSSR, 133, No. 3 (1960)

A. G. Ershov et al., 554-57. Experimental investigations of constriction of an electron bunch in the 280 Mev synchrotron.

Zhur. tekhn. fiz. XXX, No. 9 (1960)

A. I. Anisimov et al., 1009-18. A method for investigating the spatial distribution of electrons in a plasma.

V. V. Yankov, 1019-23. On the stabilization of localized and flying plasmoids by electromagnetic waves.

S. N. Breus, 1030-34. On the stability of a fluid current cylinder at finite conductivity.

A. I. Gubanov, Yu. P. Lun'kin, 1046-52. Equations of magnetic plasma dynamics.

A. I. Morozov, L. S. Solov'ev, 1104-08. On acceleration of a plasma in a coaxial tract.

Zhur. eksptl. i teoret. fiz. 39, No. 2 (1960)

Li Ha-Yuan et al., 225-229. Study of the $He^3 + H^3$ reaction.

I. M. Samoilov, A. A. Sokolov, 257-259. Contribution to the problem of azimuthal instability of circulating currents.

S. M. Osovets, 311-16. Dynamic stabilization of a plasmoid.

I. Sh. Vashakidze et al., 393-96. Investigation of the (n, p) reaction on the Li^6 nucleus.

A. V. Timofeev, 397-99. Buildup of ion acoustic oscillations in an anisotropic plasma.

V. P. Dokuchaev, 413-15. On the buildup of magnetohydrodynamic waves in a stream of plasma moving through an ionized gas.

R. V. Polovin, 463-70. Contribution to the theory of simple magnetohydrodynamic waves.

Zhur. eksptl. i teoret. fiz. 39, No. 3 (1960)

A. P. Akhmatov et al., 536-44. Magnetoacoustic resonance in a plasma.

V. N. Dmitriev, et al., 556-62. Energy distribution of threefold-fission fragments of U^{235}.

R. V. Polovin, 657-61. On the escape of a plasma into a vacuum in the presence of a magnetic field.

D. A. Frank-Kamenetskii, 669-79. On the natural oscillations of a bounded plasma.

E. P. Sirotina, S. I. Syrovatskii, 746-53. Structure of low-intensity shock waves in magnetohydrodynamics.

V. F. Aleksin, V. I. Yashin, 822-26. Study of plasma stability by means of the generalized energy principle.

V. M. Strutinskii, 781-93. Angular distribution of fission fragments in fission induced by low-energy neutrons.

O. V. Konstantinov, V. I. Perel', 862-71. Collisions between particles in a high-temperature plasma.

Pribory i tekhnika eksperimenta No. 4 (1960)

B. B. Gel'perin, et al., 13-17. Techniques for adjusting betatrons to peak intensity.

I. A. Grishaev, et al., 17-23. Measurement of position and beam current for a pulsed charged-particle beam in flight.

A. N. Kabanov, 23-28. A general-purpose high-resolution electrostatic electron spectrograph for electrons at 75 kev.

A. N. Pisarevskii, et al., 29-35. A portable automatic single-channel transistorized scintillation gamma-ray spectrometer.

E. A. Zherebin, E. A. Tamanov, 40-45. Time-of-flight fast neutron spectrometer.

G. S. Malkiel', B. I. Sukhanov, 46-50. A pulsed neutron source.

Yu. G. Abov, et al., 51-55. Production of polarized neutrons by reflection from a cobalt reflector.

A. T. Vasilenko, et al., 56-63. A semiautomatic comparator for processing stereophotographs.

G. V. Koshelyaev, 63-66. Nomographs for calculating particle tracks in emulsion stacks.

A. I. Abramov, 66-71. On calculating the pulse spectrum shape for ionization chambers.

P. K. Oshchepkov, et al., 89-91. Continuous secondary-electron multiplication is used to amplify small currents.

W. Schütze, et al., 92-98. A mass spectrograph capable of two-directional focusing over the entire scale, for measuring isotopic masses.

L. F. Kondrashev, et al., 102-105. Thin vacuum-tight walls.

V. Ya. Dudarev, 123-26. Measurement of the thickness of thin coatings overlying thick substrates.

A. B. Fradkov, 126-30. Equipment for low-temperature research on bottled liquid helium.

E. A. Koltypin, 130-31. Design of solid deuterium and tritium targets for an electrostatic generator.

V. V. Sidorenko, G. A. Utkin, 133-34. Automatic measurements of the counting characteristics of gas-discharge counters.

V. N. Dmitriev, et al., 135. Teflon insulators for ionization chambers and counters.

Príroda No. 8 (1960)

Ting Ta-Tsao, E. N. Kladnitskaya, 17-18. The new antiparticle antisigma minus hyperon $\bar{\Sigma}^-$.

Tekhnika molodezhi No. 8 (1960) (Science for the Young)

I. E. Tamm, 7-11. Three intriguing problems in physics (controlled thermonuclear reactions, the quantum theory of elementary particles, and new physical methods in biological research).

S. Sokolov, 17. The first few anti-hyperons.

Uspekhi fiz. nauk LXXI, No. 4 (1960)

Ya. B. Zel'dovich, S. S. Gershtein, 581-630. Nuclear reactions in cold hydrogen. 1. Mesonic catalysis.

Uspekhi fiz. nauk LXXII, No. 1 (1960)

R. V. Polovin, 33-52. Shock waves in magnetohydrodynamics.

Canad. J. Phys. 38, No. 9 (1960)

R. Bourret, 1213-23. Autocorrelation functions of charged-particle velocities in a magneto-ionic medium, and turbulent diffusion.

Industries Atomiques IV, No. 5/6 (1960)

B. Henry, J. Rastoin, 55-59. The age of neutrons emitted by the $T(p,n)He^3$ for the indium resonance.

A. Decae, J. Gervaise, 61-73. The CERN proton synchrotron: high-precision assembly of the magnets.

Industries Atomiques IV, No. 7/8 (1960)

E. Schatzman, 41-51. Nuclear reactions in the stars.

Kerenergie 3, No. 7 (1960)

H. Hessel, 613-17. Boundary conditions in calculating neutron flux in a unit cell in the two-group approximation.

Kernenergie 3, No. 8 (1960)

M. Ardenne, K. Steinfelder, 717-21. Vapor under study removed from the charge cathode in new ion source.

Nucl. Engng. No. 5, 53 (1960)

F. Ribe, 445-46. U. S. fusion research.

Nukleonika V., No. 7/8 (1960)

Z. Wilhelmi, 469-80. Research on the structure of atomic nuclei as part of the program of the EWA reactor.

K. Blinowski, 481-93. Neutron diffraction studies in solid state theory.

J. Janik, et al., 494-500. On scattering of thermal neutrons by hydrogen-containing molecules.

Nuovo Cimento XVII, No. 3 (1960)

F. Bisi, B. De Michelis, 343-54. Radiofrequency discharges in a magnetic field.

Nuovo Cimento XVII, No. 4 (1960)

S. Corno, 580-98. Heterogeneous theory of cylindrical structures used for neutron multiplication.

II. Nuclear Power Engineering

Nuclear reactor theory and calculations. Reactor design. Operation of nuclear reactors and nuclear power stations.

Izvestiya akad. nauk SSSR, Otdel, tekhn. nauk. Energetika i avtomatika No. 4 (1960)

B. Ya. Kogan, 36-47. Analog computer simulation of nuclear reactor transients.

Pod'em No. 4 (1960)

I. Skopin, A. Gridchin, 88-100. An atomic giant (construction of the nuclear power station at Novo-Voronezh; brief note).

Pribory i tekhn. eksper. No. 4 (1960)

G. A. Nichiporovich, 84-87. Leak detector works on sorption.

Teploenergetika 7, No. 10 (1960)

T. Kh. Margulova, 3-5. Some problems in the development of nuclear electric power stations with reactors using water, steam, and water-steam mixtures as heat-transfer medium.

Tekhnologiya sudostroeniya No. 4 (1960) (Shipbuilding technology)

V. P. Bogdanov, 72-80. Maritime nuclear steam generating units (survey of the foreign literature).

Atomkernenergie 5, No. 7/8 (1960) .

J. Schmidt, 245-56. Study of infinite unmoderated homogeneous critical systems.

H. Benzler, 256-62. Reversal of coolant flow in gas-cooled reactors.

W. Kliefoth, 287-99. Reactor designs for nuclear electric power stations.

Atomwirtschaft 5, No. 7/8 (1960)

W. Schütz, 295. The Julich research center.

K. Bohmer, 296-300. Design and Construction

G. Seiler, H. Speicher, 301-302. Problems and organization of the Society for the Development of Nuclear Physics Research.

--, 302-307. Institutes and their problems.

W. Cautius, C. Marnet, 307-14. Problems and activities of groups on reactor design and operation.

M. Keller, W. Schröck-Vietor, 315-21. Safety problems and radiation shielding.

L. Futterer, 321-23. Architectonics problems.

W. Martens, 323-25. Water management.

W. Cautius, C. Decken, 329-32. The Braun-Boweri-Krupp reactor.

L. Hiesinger, et al., 333-39. Design and construction of the MERLIN and DIDO reactors.

C. Marnet, 339-45. Ancillary projects in the construction of the MERLIN and DIDO reactors.

J. Strobel, 343-45. Equipment for the MERLIN and DIDO research reactors.

– –, 347-58. Major equipment systems and assembling of the MERLIN and DIDO reactors.

J. Impe et al., 359-63. Laboratories for testing radioactive samples.

H. Speicher, W. Zimmermann, 363-64. Design principles in planning research institutes.

K. Rattay, 365-68. A system for processing radioactive wastes.

J. Fassbender, W. Porschen, 368-70. Start-up operations in the MERLIN and DIDO reactors.

Energia Nucleare 7, No. 9 (1960)

T. Leardini, et al., 597-610. Testing facility for determining temperature and pressure transient behavior in simulation of reactor damage resulting from considerable coolant losses.

R. Bonalumi, et al., 611-29. Measurements of diffusion length of thermal neutrons in diphenyl-impregnated graphite.

Industries Atomiques IV, No. 5/6 (1960)

C. Meunier, 74-82. Activities of the Grenoble nuclear research center in connection with the MELUSINE reactor.

R. Lamarche, 83-96. Review of recent trends in the design of reactors with neutron flux levels.

Jaderná Energie IV, No. 9 (1960)

A. Blāha, 289-93. Vacuum pressure gages detect leaks in industrial installations and nuclear power stations.

Kernenergie 3, No. 8 (1960)

A. Rau, G. Schumann, 707-716. Calculations of activation of the primary loop in a pressurized-water reactor.

Nucl. Energy 14, No. 148 (1960)

G. Herzet, et al., 403-407. Containment shells for the BR-II and BR-III at Mol (Belgium).

– – – , 408-409. Building of the Dungeness nuclear power plant.

– – – , 412-13. Nuclear research costs.

– – – , 416-18, 24. The Indian program for nuclear energy development.

– – – , 419-20. Measurements of gamma-radiation intensity inside of buildings.

Nucl. Engng. 5, No. 53 (1960)

F. Pittman, 430-31. The U.S. program of power reactor development.

C. Starr, 431-32. Industrial development of nuclear power.

G. Stathakis, K. Paulovich, 432-33. Exports.

A. Hitchman, 433. Collaboration between the USA and the United Kingdom.

– – – ,434-36. The Dresden nuclear electric power station (USA).

V. Nixon, 436-38. Planning of the Dresden power station.

V. Nixon, 438-39. Safety problems in the Dresden project.

– – – , 440-41. Bringing the Dresden reactor up to full power.

F. Hittman, 442-44. Military portable power facilities.

– – – , 447-52. The Savannah nuclear-powered ship.

– – – , 452-54. Reactor control rod system.

J. McDaniels, 455-59. Fuel transfer.

G. Anderson, F. Featherston, 460-63. Development of auxiliary nuclear power facilities for space use.

A. Weinberg, 463-65. Some promising power reactor systems.

J. Kilpatrick, 466-68. The Yankee Atomic power station.

P. Haga, 468-70. The reactor pressure vessel

A. Thorp, 470-72. The first core loading in the Yankee Atomic reactor.

T. Widmer, 472-74. The control rod drive system.

C. Obermesser, 474-75. The Yankee Atomic reactor control system.

H. Smith, 476. Fuel transfer in the Yankee Atomic reactor.

Nucl. Power 5, No. 54 (1960)

J. Burkett, 77-80. Review of nuclear reactor accidents.

---, 81. Nuclear power plant for space applications.

---, 87. Costs analysis of nuclear reactors.

W. Thomas, R. Lorge, 88-91. Power reactor steam cycles. 2.

R. Berenbaum, et al., 92-96. Temperature analog of neutron flux distribution.

N. Chrimes, 97-98. Brazing of fuel elements for organic-moderated reactors.

A. Hughes, 99-101. Conference on training reactors.

Nucl. Sci. and Engng. 8, No. 2 (1960)

A. Akcasu, A. Dalfes, 89-94. Study of nonlinear dynamics of a nuclear reactor.

J. Lewins, 95-104. Variational representation in reactor physics derived from a physical principle.

W. Blessing, 105-11. Techniques for the irradiation of ceramic fuels in a moderate thermal neutron flux.

R. Block, 112-21. Measurements of thermal neutron cross sections for U^{233}, U^{235}, Pu^{240}, U^{234}, I^{129} with a fast-chopper time-of-flight neutron spectrometer.

W. Rothenstein, 122-27. Some Monte Carlo and analytical results for resonance capture in lattices.

S. Gunst, J. Connor, 128-32. The stability of "stable" fission product poisoning.

J. Weeks, C. Klamut, 133-47. Reactions between steel surfaces and zirconium in liquid bismuth.

D. Foster, 148-56. Measurement of age of Na-Be neutrons in water and kerosene.

J. Koppel, 157-63. Time-dependent neutron spectra.

E. Wachspress, 164-70. Numerical technique for solving group diffusion equations.

Nucleonics 18, No. 9 (1960)

E. Albenesius, R. Ondrejcin, 100. Nuclear fission produces tritium.

---, 104. WTR fuel element failure.

T. Beresovski. 106, 108, 111-112, 114-116, 118. Safe design of in-pile tests.

E. Irwin. 118, 120, 122, 125. Fabricating inconel piping systems for TF-65 loop and DIG prototype.

Nucleonics 18, No. 10 (1960)

---, 52-53.Special issue on nuclear energy in Canada.

W. Lewis. 54-59. Competitive nuclear power for Canada

A. Mooradian, J. Robertson, 60-65, 122. CANDU reactor fueling costs analysis.

J. Foster et al., 66-68. On-power refueling.

A. Ward, 69-72. Reactivity life of natural uranium (CANDU).

G. Laurence, 73-77. Reactor safety in Canada.

I. MacKay, 78-80. Organic-cooled, deuterium-moderated reactors.

C. Lennox, A. Pearson, 82, 84, 132. Versatile data displays for reactors.

W. Wolfe, 96, 98, 100. Burst tests help set design stress for NPD pressure tubes.

F. Hume, 102, 104. Spray technique applies shielding concrete.

Nukleonik 2, No. 5 (1960)

F. Stummel, 178-92. Numerical calculations for a heterogeneous reactor.

R. Frohlich, 192-98. Two-group technique for determining the worth of control rods for a thermal reactor.

A. Özemre, 213-14. Elementary studies of time-dependent material buckling.

Nukleonika V. No. 7/8 (1960)

---, 383-84. Conference on reactors in the socialist countries (Rossendorf, June 13-18, 1960).

E. Aleksandrowicz, 385-414. The second year of operation of the WWR-S reactor in Poland.

W. Dabek, 415-37. Research in experimental reactor physics.

R. Zelazny, 435-59. Applied reactor theory at the Institute of Nuclear Research of the Polish Academy of Sciences.

III. Nuclear Fuel and Materials

Nuclear geology and primary ore technology. Nuclear metallurgy and secondary ore technology. Chemistry of nuclear materials.

Vestnik akad. nauk SSSR XXX, No. 9 (1960)

K. V. Chmutov, V. M. Luk'yanovich, 73-74. Structure of graphite and its reaction kinetics.

Voprosy estestvoznaniya i tekhn. No. 9 (1960)

L. L. Zaitseva, 120-24. The beginnings of the systematic study of deposits of radioactive minerals on the territory of pre-revolutionary Russia.

Geologiya i geofizika No. 6 (1960)

E. M. Filippov, 94-105. Foundations of the theory of photoneutron techniques for investigating minerals and ores.

Zhur. anal. khim. 15, No. 4 (1960)

S. B. Savvin et al., 446-51. Photometric assay of clarke amounts of thorium in rocks, using arsenazo II reagent.

---, 452-54. The analytical chemistry of thorium.

Yu. A. Chernikhov et al. Report No. 2. Complexometric determination of thorium in monazite concentrations after separating it out on KU-2 cation exchange resin.

Zhur. neorgan.khim. 5, No. 7 (1960)

I. I. Chernyaev et al., 1454-66. Aquo-oxalato-sulfate uranyl compounds.

V. P. Markov, E. N. Traggeim, 1467-73. Uranyl rhodanide compounds.

I. I. Chernyaev et al., 1481-92. On the complex character of uranates.

V. P. Markov, E. N. Traggeim, 1493-1501. Uranyl thiocyanates.

R. G. Denotkina et al., 1509-15. Determination of composition and dissociation constants of phosphate plutonyl (IV) complexes by the solubility method.

A. E. Klygin, V. K. Pavlova, 1516-21. Spectrophotometric investigation of the complexing reaction of thorium with benzene-2-arsonic acid – (1-azo-2-)-1,8-dihydroxynaphthalene-3,6-disulfo acid (arsenazo).

Zhur. neorgan. khim. 5, No. 8 (1960)

E. A. Kanevskii, G. R. Pavlovskaya, 1738-42. Polarographic investigation of sulfate solutions of hexavalent uranium.

A. I. Alekperov, S. I. Zhdanov, 1743-47. Effect of anions on the reduction of uranyl ions on a dropping-mercury cathode.

A. S. Solovkin et al., 1861-67. Extraction of uranyl nitrate using the di-isoamyl ether of methylphosphonic acid.

V. B. Shevchenko et al., 1911-13. Extraction of plutonium from chloride solutions, with tri-n-octylamine.

Zhur. prikladn. khim. 33, No. 7 (1960)

G. V. Samsonov et al., 1661-64. Preparation of thorium carbides.

Zhur. struckturnoi khim. 1, No. 2 (1960)

L. V. Lipis et al., 135-44. Spectrophotometric study of the complexing processes of tetravalent plutonium in nitrate solutions.

Zavod.lab. 26, No. 8 (1960)

Yu. A. Chernikhov et al., 921-24. Successive chelatometric determination of thorium and sums of rare-earth metals.

R. S. Volodarskaya, 925-27. Chelatometric method for determining thorium in magnesium alloys.

R. S. Veitsman, 927-29. Photocalorimetric determination of zirconium in the form of a phosphoric-molybdenic-zirconium complex.

L. N. Aleksandrov, 975-77. Radiometric determination of thorium in tungsten and molybdenum.

Izvestiya akad. nauk SSSR, seriya geol. No. 7 (1960)

A. A. Smyslov, 32-45. Significance of data on the radioactivity and thermal conductivity of minerals in metallogenetic investigations.

Izvestiya vyssh. ucheb. zaved. Chernaya metallurgiya No. 7, (1960)

V. G. Vlasov, A. G. Lebedev, 5-6. Dissociation of uranium trioxide.

Inzhener. sbornik Inst. mekhaniki akad. Nauk SSSR 28 (1960)

V. S. Lenskii, 97-133. Effect of radioactive radiations on the mechanical properties of solids (literature survey).

Radiokhimiya II, No. 4 (1960)

N. M. Adamskii et al., 400-410. Zirconium distribution in extraction of tri-n-butylphosphate.

A. P. Ilozhev et al., 411-18. Distribution of butylphosphoric acids between aqueous solutions and a tri-n-butyl-phosphate phase.

V. G. Timoshev et al. 419-25. Extractive power of neutral oxygen-containing organic compounds.

V. I. Kuznetsov, T. G. Akimova, 426-30. Organic co-precipitants. XIV. Improved technique for co-precipitating uranium from mineral waters.

S. Z. Roginskii et al., 431-37. Glauconite ion exchange columns separate out radiocesium concentrates.

S. Z. Roginskii et al., 438-45. Concentrates of radioactive cesium isotopes separated out on ferrocyanides of heavy solutions from solutions with high content of salt impurities.

M. V. Vladimirova, Z. V. Ershova, 495-99. Effect of alpha radiation from polonium on concentrated sulfuric acid solutions.

A. A. Grinberg et al., 505-506. Contribution to the problem of instability constants of oxalate complexes of uranium.

Trudy Inst. geol rud. mestorozhd., petrografii, mineral. i geokhim. akad. nauk SSSR No. 42 (1960)

S. A. Brusilovskii, 58-99. Investigation of conditions governing precipitation of uranyl hydroxide from low-temperature aqueous solutions.

Trudy Inst. metallurgii im. Baikova No. 4 (1960)

M. E. Dritz et al., 74-83. Thorium-containing magnesium alloys.

Trudy Inst. metallurgii im. Baikova No. 5 (1960)

B. N. Melent'ev, N. S. Gertseva, 198-201. Polarography of large amounts of uranium.

Trudy po khim. i khim. tekhnol. No. 2 (1959)

N. N. Mironov, 257-60. Determination of thorium from lanthanum and cerium by the oxalate method.

N. N. Mironov, 264-70. Methods for obtaining thorium-containing compounds and some physical-chemical techniques.

Tsvetnye metally No. 8 (1960)

I. L. Perlin, V. A. Fedorchenko, 88-93. Equipment of fabricating reactor fuel elements, and shielding devices (review of the foreign literature).

Fizika metallov i metallovedenie 10, No. 2 (1960)

Sh. Sh. Ibragimov, V. S. Lyashenko, 183-86. Fast neutron effects on properties of metals.

F. P. Butra, 223-25. Neutron irradiation effects on the structure of molybdenum.

Sh. Sh. Ibragimov et al., 316-17. Study of fast neutron effects on the characteristic temperature of iron and copper.

Canad. J. Chem. 38, No. 4 (1960)

A. Kertes, V. Kertes, 612-19. Extraction of mineral acids. Part III. Interaction between solute and solvent in the hydrobromic acid-water-tri-n-butylphosphate system.

Canad. J. Chem. 38, No. 6 (1960)

G. Caldow et al., 772-82. Infrared spectra of some uranyl compounds.

Energia Nucl. 7, No. 9 (1960)

B. Brigoli, 590-96. Up-to-date distillation methods. I.

A. Bassi. C. Corsetti, 638-48. Study of the structure of uranium metal.

Industr. Chemist 36, No. 427 (1960)

G. Miller, 447-53. Tantalum and niobium production.

Industries Atomiques. IV, No. 5/6 (1960)

---, 97-104. Grenoble conference on plutonium metallurgy.

J. Inorg. and Nucl. Chem. 14, No. 3/4 (1960)

J. Korkisch et al., 247-50. Ion exchange in mixed solvents [in German]. I. On the distribution of uranium between alcoholic solutions of mineral acids and strongly basic Dowex-1 resin.

P. Antal, et al., 251-54. Ion exchange in mixed solvents [in German]. II. On the distribution of Th, Zr, and Ti between alcoholic mineral acid solvents and the strongly basic Dowex-1 anion exchange resin.

J. Inorg. and Nucl. Chem. 15, No. 1/2 (1960)

R. Panzer, J. Suttle, 67-70. Uranium tetrachloride solvents with phosphorus oxychloride.

G. Gibson et al., 110-14. Interaction between uranium trioxide and nitrogen pentoxide.

C. Banks, R. Singh, 125-32. Composition and stability of metal complexes with 5-sulfosalicylic acid.

N. Isaac et al., 151-57. Extraction separation of transcurium elements from large amounts of curium.

H. Irving, D.Edgington, 158-70. The synergism phenomenon in the extraction of actinides.

M. Taube, 171-76. The effect of solvent polarity on the extraction separation of neptunium and uranium compounds.

J. Korkisch, F. Tera, 177-81. Ion exchange in mixed solvents III. On the distribution of thorium chloride between strongly basic anion exchange resins and alcoholic chloride solutions.

G. Panson, C. Weill, 184-85. Production and crystalline structure of americium metal.

C. Pistorius, 187-88. Infrared spectrum of $Th(OH)_4$.

M. Lindner et al., 194-95. Half-life of Hf^{181}.

R. Naumann, M. Michel, 195-96. Production of the long-lived isotope Ho^{163}.

A. Aten et al., 198-99. Co-precipitation of astatine iodide with iodine.

J. Nucl. Materials 2, No. 3 (1960)

B. Blumenthal, 197-208. Structure of U-C alloys with low carbon content.

D. Evans, G. Raynor, 209-15. Lattice periods in thorium-yttrium lattices.

R. Blanchard et al., 216-24. Effect of hydrogen in tensile rupture in stainless steels.

S. Gregg et al., 225-33. High-temperature oxidation of beryllium. Part II. Interaction between carbon dioxide and carbon monoxide.

A. Young et al., 234-47. Plastic flow of alpha-uranium.

L. Howe, W. Thomas, 248-60. Effect of neutron irradiation on the properties of Zircaloy-2, under tension.

J. Lehmann, 261-68. A suggestion on the systematics of phases in uranium alloy.

H. Newkirk, 269-73. Electron-microscopic studies of radiation damage in irradiated uranium dioxide.

Nucl. Energy 14, No. 148 (1960)

---, 414-15. Fuel processing technology at the Eurochimique plant at Mol (Belgium).

Nucleonics 18, No. 9 (1960)

D. Leeser, 68-73. Radiation effects on reactor metals.

J. Carroll, R. Bolt, 78. Radiation effects on organic materials.

J. DeMastry, R. Dickerson, 87-90, 132, 134. Niobium, promising high-temperature core materials.

B. Levy, et al., 128, 130. Obtaining hydrazine by irradiation of solid and liquid ammonia.

Nukleonik 2 No. 5 (1960)

R. Kiessling, 198-203. Swedish research on UO_2 from the viewpoint of fuel element applications.

Nucleonika, V, No. 5 (1960)

Z. Zagórski, 253-60. Determination of the G value of gamma-induced reactions by the method of constant-potential polarographic electrolysis.

Nukleonika V, No. 6 (1960)

L. Adamskii et al., 317-27. Simultaneous determinationof trace amounts of sodium and potassium by neutron activation techniques.

W. Długosz, 329-39. Tracer studies of flotation processes.

T. Urabński, 341-53. Some problems in uranium extraction using dodecylphosphoric acid.

IV. Nuclear Radiation Shielding

Radiobiology and radiation hygiene. Shielding theory and techniques. Instrumentation.

Biofizika 5, No. 4 (1960)

B. M. Isaev, 479-87. Physical foundations of radiobiological neutron flux experiments.

Vestnik akad. nauk SSSR XXX, No. 9 (1960)

A. M. Kuzin, 48-51. Hazard of increased C^{14} concentration in the atmosphere.

Voenno-meditsinskii zhur. No. 7 (1960)

L. A. Tiunov, 36-39. Prophylactics of radiation injury, using combinations of drugs and medicines (survey of the literature).

I. V. Fedorov, G. V. Sazykin, 69-71. On feeding cases of acute radiation syndrome.

Vrachebnoe delo No. 8 (1960)

M. A. Khvoinitskaya, V. P. Pugachevskii, 93-94. The public health approach to work safety conditions where radioactive isotopes are in use in the metallurgical industry.

Gigiena i sanitariya No. 7 (1960)

Z. Ya. Gorodishcher, N. I. Mashneva, 56-60. Deactivation of drinking water containing radiophosphorus by the contact coagulation method.

Izvestiya akad. nauk SSSR, seriya geograf. No. 4 (1960)

V. G. Bogorov, B. A. Tareev, 3-10. Ocean depths and the problem of radioactive wastes disposal at sea.

Med. radiologiya 5, No. 7 (1960)

Yu. V. Novikov, I. P. Korenkov, 66-71. Reduction in the radioactivity level of atmospheric air as a result of the cessation of nuclear weapons testing.

M. Ya. Maizelis, 92-95. Problems of medical radiology reviewed at the All-Union Conference on the assimilation of radioactive isotopes and nuclear radiations into the USSR national economy, Riga, April, 1960.

Priborostroenie No. 7 (1960)

M. L. Gol'din, 22-24. On safety techniques in the preparation and use of instruments based on the use of radioactive isotopes.

Pribory i tekhn. eksper. No. 4 (1960)

Yu. K. Akimov et al., 71-77. Separation of particles according to the degree of ionization in some scintillation counters.

Yu. A. Egorov, D. S. Khukhorev, 136-37. On the use of light pipes in scintillation counters.

L. I. Zlobin, Yu. I. Lyubimov, 137-38. Transistorized preamplifier for scintillation counters.

L. D. Soshin, 138. Transistorized multivibrator with millivolt operating threshold.

G. N. Muskhelishvili, G. V. Zakomornyi, 139-41. Electronic voltage stabilizer for transistor circuit power supplies.

Sovetskoe zdravookhranenie Kirgizii No. 2/3 (1960)

I. P. Mashkov, 112-18. The Tashkent conference on the peaceful uses of nuclear energy (review of the medical panel presentation and discussion).

Trudy Ural. otdel. Mosk o-va ispytatelei prirody, No. 2 (1959)

N. V. Gorbatyuk, N. V. Timofeev-Resovskii, 181, 193-4. On critical tolerance norms for radioactive contamination of water and air. I, II.

L. K. Ponomareva et al., 201-05. Determination of cesium-137 in the water of open reservoirs.

Khlopkovodstvo No. 8 (1960)

D. T. Kabulov et al., 48-51. Effect of radioactive isotopes on the growth, development, and crop yield of the cotton plant.

Archives Environmental Health 1 No. 2 (1960)

J. Felton, C. Rozas, 87-95. Deactivation of human skin contaminated by hot spills as an experiment.

Atomkernergie 5, No. 7/8 (1960)

K. Lindackers, 272-77. Design of biological shielding for reactors.

H. Schneider, E. Schwerdtel, 278-81. Portable scintillation counter with differential discriminator.

K. Godt, K. Sommermeyer, 282-85. RaD content in plants, determined by gamma-ray spectroscopy.

K. Pötzl, R. Reiter, 285-87. Quantitative determination of fission-product fallout in the Northern Alps.

Atompraxis 6, No. 8 (1960)

A. Berger, 301-308. Behavior of x-rayed potatoes.

A. Micke, K. Wöhrmann, 308-16. Radiosensitivity of dry seeds.

S. Krawczynski, 320-22. Effect of synthetic purifying agents and complexing agents on deactivation of radioactive waters (deactivation by chemical precipitation).

Canad. J. Chem. 38, No. 6 (1960)

W. Armstrong, D. Grant, 845-50. Aqueous benzoate system as a sensitive dosimeter of ionizing radiations.

Canad. J. Phys. 38, No. 8 (1960)

J. Wolfson, F. Terentiuk, 991-1010. Concentration of fission products in the air at sea level in Canada during the IGY.

Energia Nucleare 7, No. 9 (1960)

E. Cerrai, 581-89. Problems arising in the disposal of liquid hot reactor wastes.

E. Cerrai et al., 630-37. Clean-up of liquid wastes at the CISE radiochemical laboratory.

Jaderná Energie VI, No. 9 (1960)

V. Santholzer, 294-98. Increase in fallout radioactivity as a result of nuclear testing in the Sahara.

F. Běhounek, V. Zelenková, 299-302. Determination of beta activity of liquid wastes.

J. Mackou, 303-11. Designs of automatic radioactivity measuring facilities.

J. Koči, 312. Individual sonic dosimeter warns of gammas, x-rays, and neutrons.

Nucl. Energy 14, No. 148 (1960)

A. Gould, 421-24. Planar film dosimeter and electroscope.

Nucl. Power 5, No. 54 (1960)

R. Owen, 82-86. Scintillation counter review.

Nucl. Sci. and Engng. 8, No. 2 (1960)

W. Pettus, 171. Age of U^{233} fission neutrons in water.

P. Khubchandani, 172. Thermal neutron scattering in graphite.

Nucleonics 18, No. 9 (1960)

G. Hine, J. Cardarelli, 92-94, 96, 100. Conical plastic scintillators show total gamma absorption.

S. Sandler et al., 102-03. Dimethyl styrene yields more efficient scintillators.

Nucleonics 18, No. 10 (1960)

A. Jones, 86, 88, 90, 91. Uses of semiconductor detectors in health-physics monitoring.

R. Tolmie, 92. Dual detectors key to radioisotope identifier.

Nukleonik 2, No. 5 (1960)

W. Pohlit, H. Pohlit, 175-78. Paraffin moderator used for dosimetry in a mixed neutron field.

W. Kern, 203-13. On fragment activity due to fallout.

Nukleonika V. No. 5 (1960)

I. Złotowski, H. Wincel, 261-79. Mass-spectrometric studies of chemical processes occurring in a self-quenching Geiger-Müller counter loaded with heavy hydrocarbons.

J. Liniecki et al., 301-13. Sr^{90} content in bones of humans and animals and in milk in Poland during 1958.

Nukleonika V, No. 6 (1960)

S. Chwasczewski, 355-60. Pulse modulation of a high-frequency ion source.

T. Radoszewski, 361-68. Scintillation counter characteristics.

M. Miazek-Kula, 373-76. Deactivation of a surface contaminated by hot isotopes.

C. Szwacka, 376-77. Deactivation of protective clothing worn in radiochemical plants.

J. Flattau et al., 377-78. Protective clothing for deactivation points.

Radiation Res. 12, No. 1 (1960)

N. Barr, M. Stark, 1-4. Fluorescent compounds in chemical dosimetry. Gamma radiation effects on chinine fluorescence.

M. Berger, D. Raso, 20-37. Monte Carlo computations of background gamma radiation.

Radiation Res. 12, No. 3 (1960)

W. Gordy, I. Miyagawa, 211-29. Electron spin resonance studies of mechanisms for chemical protection from high-energy ionizing radiations.

Radiation Res. 12, No. 4 (1960)

J. Hunt et al. 319-24. Effect of parametric gases on the electron spin resonance signal from activated charcoal.

Radiation Res. 12, No. 6 (1960)

S. Kronenberg, H. Murphy, 728-35. Energy spectrum of protons emitted by a hydrogen-containing substance.

Radiation Res. 13, No. 1 (1960)

W. Jesse, 1-17. Ionization of air by polonium alphas and mean energy of formation of ion pairs.

S. Kondo, M. Randolph, 37-60. Effects of finite dimensions of an ion chamber on measurements of low-level photon sources.

P. McClement, G. Failla, 61-91. Dose measurement in a small volume of tissue surrounding a radioisotope point source.

Radiation Res. 13, No. 2 (1960)

E. Burke, R. Pettit, 271-85. Absorption analysis of x-ray spectra produced by beryllium-window tubes operated at 20-50 kv.

Research XIII, No. 10 (1960)

D. Stevenson, 383-89. Theoretical and practical deactivation problems.

V. Radioactive and Stable Isotopes

Labeled-atoms technique. Uses of radioactive radiations. Direct conversion of nuclear to electrical energy.

Azerbaid. neft. khoz. No. 1 (1960)

A. G. Khanlarova et al., 39-41. Tracer study of the dynamics of formation of a protective corrosion-resistant film on metals by AzNII-7 and TsIATIM-339 additives.

Byull okeanograf. komis. pri Prezidiume akad. nauk SSSR No. 3 (1959)

O. K. Leont'ev, V. N. Afanas'ev, 73-79. Experience in the use of radioisotopes for research on shifting of sand bars.

Vestnik mashinostroeniya No. 8 (1960)

V. I. Postnikov, 78-80. Introduction and assimilation of radioisotopes into machinery manufacture. Based on materials of the All-Union Conference at Riga, April, 1960, on the assimilation of radioactive isotopes and nuclear radiations into the USSR national economy.

Vestnik sel'sko-khoz. nauki No. 7 (1960)

V. N. Silin, 115-18. A powerful tool for the progress of science and industry (on the uses of radioative isotopes in agriculture). Contribution to the balance sheet of the Riga April, 1960 All-Union Conference on the assimilation of radioactive isotopes and nuclear radiations in the USSR national economy.

Vinodelie i vinogradarstvo SSSR No. 5 (1960)

P. I. Litvinov, 37-40. Tracer applications in the study of the regeneration of grapevine roots and in elucidating the relations between separate roots and vine shoots.

Vodosnabzhenie i san. tekhnika No. 7 (1960)

I. I. Mechitov, 1-5. Tracer applications in hydraulics research on the performance of sedimentation tanks.

Geologiya i geofizika No. 3 (1960)

E. M. Filippov, 103-08. Contribution to the problem of deepening research on minerals and ores via scattered gamma radiation techniques.

Geol. nefti i gaza No. 7 (1960)

N. A. Vasil'eva et al., 55-59. Experience in the use of tritium, the radioactive hydrogen isotope, to study the flow of injected water driven into an oil reservoir.

Zavod. lab. 26, No. 7 (1960)

T. M. Khrenkova, 833-35. Radiometric technique for measuring coating thicknesses.

I. A. Berman, S. A. Khaletskaya, 836-37. Determination of the thickness of zinc coating by the tracer method.

Izvestiya akad. nauk SSSR, seriya geograf. No. 4 (1960)

Yu. N. Agashkin, 117-21. Tracer studies of snow thawing and runoff.

Izvestiya vyssh. ucheb. zaved. Gornyi zhurn No. 6 (1960)

B. M. Barbin, 139-42. Study of flotation feasibility of copper by the null method and by the tracer method.

Izvestiya vyssh. ucheb. zaved., Lesnoi zhur. No. 2 (1960)

A. S. Freidin, I. G. Krapivina, 117-20. Sterilization of lumber by ionizing radiations.

Izvestiya vyssh. ucheb. zaved. Pishchevaya tekhnol. No. 2 (1960)

V. F. Oreshko, K. A. Korotchenko, 17-21. Gamma-ray techniques in the study of starch degradation.

Izvestiya vyssh. ucheb. zaved. Khimiya i khim. tekhnol. 3, No. 1 (1960)

M. M. Grudinina, E. M. Aleksandrova, 176-78. Some problems related to emulsion polymerization of styrene, using the tracer method.

Izvestiya vyssh. ucheb. zaved. Khimiya i khim., tekhnol. 3, No. 3 (1960)

G. B. Fedorov et al., 395-401. Tracer study of the mobility, interatomic coupling and element distribution in zirconium and zirconium alloys.

Koks i khimiya No. 7 (1960)

A. Z. Kulishenko, K. P. Medvedev, 5-10. Radiosulfur S^{35} as tracer in studying desulfurization of coals.

Neft. Khoz. No. 6 (1960)

I. G. Zhuvagin, Yu. A. Akchas'yanov, 7-12. A new method using radioactive isotopes for checking the results of hydraulicking operations.

Prikladnaya geofizika No. 26 (1960)

A. A. Korzhev, 137-48. Contribution to estimating the porosity of permeable rocks, by the tracer method.

Radiotekhnika i elektronika 5, No. 7 (1960)

G. N. Shuppe, V. P. Vasil'ev, 1135-44. Tracer application to the study of oxide cathode processes and other problems in cathode electronics.

Svarochnoe proizvodstvo No. 9 (1960)

G. V. Balabina, 16-17. Thulium-170 tracer monitors weldments.

Trudy vsesoyuz. nauchno-issled. inst. mekhanizatsii sel'sko-khoz. 28 (1960)

A. Khamidov, 94-107. Use of gamma radiation in studying the effects of wheels on soil.

Trudy vsesoyuz. neftegaz. nauchno-issled. inst. No. 29 (1960)

F. A. Akelseev, F. Ts. Denisik, 32-43. Radioactive techniques for monitoring the development and exploration of oil fields.

N. A. Vasil'eva et al., 266-77. Results of tritium tracer investigations of injected water movement in an oil reservoir.

Trudy naucho-isslef. inst. rezinov. prom., symp.#6 (1960)

L. A. Oksent'evich, E. V. Zhuravskaya, 102-110. Nuclear radiation effects on crude and finished rubber.

Khim. volokna No. 3 (1960)

S. A. Nechaeva et al., 7-9. Study of the possibility of enhancing the heat stability of polyolefin fibers by ionizing radiation processing.

Khimiya i khim. tekhnol. 3, No. 3 (1960)

A. D. Sotskov et al., 452-56. Tracer studies of diffusion processes accompanying chemical and phase transformations.

Atompraxis 6, No. 8 (1960)

N. Desrosier, 293-300. The present state of the art in radiation processing of foods.

Industr. Chemist 36, No. 427 (1960)

P. Connor, W. Hardwick, 427-33. Use of radioactive radiations for sizing particles.

Industries Atomiques IV, No. 7-8 (1960)

C. Kellershohn, P. Vernejoul, 52-61. Medical tracer applications.

J. Juillard, 75-78. A plasma diode thermocouple.

J. Brit. Nucl. Energy Conf. 5, No. 3 (1960)

M. Crowley-Milling, 207-25. Radiation applications in industry.

Nova Technika No. 6 (1960)[Czech].

Z. Spurný, 270-71. Opportunities for using radioactive wastes and high-level radiation sources in the national economy.

Nucl. Energy 14, No. 147 (1960)

---, 369-70. New Amersham hot isotope laboratories.

W. Huber, A. Klein, 371-72. The outlook for radiation processing of foods.

Nucleonics 18, No. 8,(1960)

---, 94, 96, 98. Review of papers heard on panels on hot isotopes and radiations at the 1960 ANS meeting

F. Jackson et al., 102-105. Efficient tritium labeling with an electric discharge.

R. Black, W. Kerwick, 106-108. Sealed millicurie floats detect pipe leaks.

Nucleonics 8, No. 10 (1960)

G. Eichholz, 116, 118-120. Industrial tracer techniques in Canada.

B. Schumacher, 106, 109-110, 112, 114. Gaging gas density with fast charged particles.

Nukleonika V. No. 5 (1960)

J. Domanus, B. Osuchowski, 281-300. High-level Co^{60} sources used in gamma radiography of metal products.

SIGNIFICANCE OF ABBREVIATIONS MOST FREQUENTLY ENCOUNTERED IN SOVIET PERIODICALS

FIAN	Phys. Inst. Acad. Sci. USSR.
GDI	Water Power Inst.
GITI	State Sci.-Tech. Press
GITTL	State Tech. and Theor. Lit. Press
GONTI	State United Sci.-Tech. Press
Gosenergoizdat	State Power Press
Goskhimizdat	State Chem. Press
GOST	All-Union State Standard
GTTI	State Tech. and Theor. Lit. Press
IL	Foreign Lit. Press
ISN (Izd. Sov. Nauk)	Soviet Science Press
Izd. AN SSSR	Acad. Sci. USSR Press
Izd. MGU	Moscow State Univ. Press
LEIIZhT	Leningrad Power Inst. of Railroad Engineering
LET	Leningrad Elec. Engr. School
LETI	Leningrad Electrotechnical Inst.
LETIIZhT	Leningrad Electrical Engineering Research Inst. of Railroad Engr.
Mashgiz	State Sci.-Tech. Press for Machine Construction Lit.
MEP	Ministry of Electrical Industry
MES	Ministry of Electrical Power Plants
MESEP	Ministry of Electrical Power Plants and the Electrical Industry
MGU	Moscow State Univ.
MKhTI	Moscow Inst. Chem. Tech.
MOPI	Moscow Regional Pedagogical Inst.
MSP	Ministry of Industrial Construction
NII ZVUKSZAPIOI	Scientific Research Inst. of Sound Recording
NIKFI	Sci. Inst. of Modern Motion Picture Photography
ONTI	United Sci.-Tech. Press
OTI	Division of Technical Information
OTN	Div. Tech. Sci.
Stroiizdat	Construction Press
TOE	Association of Power Engineers
TsKTI	Central Research Inst. for Boilers and Turbines
TsNIEL	Central Scientific Research Elec. Engr. Lab.
TsNIEL-MES	Central Scientific Research Elec. Engr. Lab.–Ministry of Electric Power Plants
TsVTI	Central Office of Economic Information
UF	Ural Branch
VIESKh	All-Union Inst. of Rural Elec. Power Stations
VNIIM	All-Union Scientific Research Inst. of Metrology
VNIIZhDT	All-Union Scientific Research Inst. of Railroad Engineering
VTI	All-Union Thermotech. Inst.
VZEI	All-Union Power Correspondence Inst.

Note: Abbreviations not on this list and not explained in the translation have been transliterated, no further information about their significance being available to us. – Publisher.

Soviet Journals Available in Cover-to-Cover Translation

ABBREVIATION	RUSSIAN TITLE	TITLE OF TRANSLATION	PUBLISHER	TRANSLATION BEGAN Vol.	Issue	Year
AÉ	Atomnaya énergiya	Soviet Journal of Atomic Energy	Consultants Bureau	1	1	1956
Akust. zh.	Akusticheskii zhurnal	Soviet Physics – Acoustics	American Institute of Physics	1	1	1955
	Antibiotiki	Antibiotics	Consultants Bureau	4	1	1959
Astr(on). zh(urn).	Astronomicheskii zhurnal	Soviet Astronomy–AJ	American Institute of Physics	34	1	1957
Avto(mat). svarka	Avtomaticheskaya svarka	Automatic Welding	British Welding Research Association (London)		1	1959
	Avtomatika i Telemekhanika	Automation and Remote Control	Instrument Society of America	27	1	1956
	Biofizika	Biophysics	National Institutes of Health*		1	1957
	Biokhimiya	Biochemistry	Consultants Bureau	21	1	1956
Byull. éksp(erim). biol. i med.	Byulleten' éksperimental'noi biologii i meditsiny	Bulletin of Experimental Biology and Medicine	Consultants Bureau	41	1	1959
DAN (SSSR) / Dokl(ady) AN SSSR	Doklady Akademii Nauk SSSR	The translation of this journal is published in sections, as follows:				
		Doklady Biochemistry Section	American Institute of Biological Sciences	106	1	1956
		Doklady Biological Sciences Sections (Includes: Anatomy, biophysics, cytology, ecology, embryology, endocrinology, evolutionary morphology, genetics, histology, hydrobiology microbiology, morphology, parasitology, physiology, zoology sections)	American Institute of Biological Sciences	112	1	1957
Life Sciences		Doklady Botanical Sciences Sections (Includes: Botany, phytopathology, plant anatomy, plant ecology, plant embryology, plant physiology, plant morphology sections)	American Institute of Biological Sciences	112	1	1957
		Proceedings of the Academy of Sciences of the USSR, Section: Chemical Technology	Consultants Bureau	106	1	1956
Chemical Sciences		Proceedings of the Academy of Sciences of the USSR, Section: Chemistry	Consultants Bureau	106	1	1956
		Proceedings of the Academy of Sciences of the USSR, Section: Physical Chemistry	Consultants Bureau	112	1	1957
		Doklady Earth Sciences Sections (Includes: Geochemistry, geology, geophysics, hydrogeology, mineralogy, paleontology, petrography, permafrost sections)	American Geological Institute	124	1	1959
Earth Sciences		Proceedings of the Academy of Sciences of the USSR, Section: Geochemistry	Consultants Bureau	106-123	1-6	1957-1958
		Proceedings of the Academy of Sciences of the USSR, Sections: Geology	Consultants Bureau	106-123	1-6	1957-1958
Mathematics		Doklady Soviet Mathematics	The American Mathematics Society	131	1	1961
		Soviet Physics–Doklady (Includes: Aerodynamics, astronomy, crystallography, cybernetics and control theory, electrical engineering, energetics, fluid mechanics, heat engineering, hydraulics, mathematical physics, mechanics, physics, technical physics, theory of elasticity sections)	American Institute of Physics	106	1	1956
Physics		Proceedings of the Academy of Sciences of the USSR, Applied Physics Sections (does not include mathematical physics or physics sections)	Consultants Bureau	106-117	1	1956-1957
Derevoobrabat. prom-st'.	Derevoobrabatyvayushchaya promyshlennost'	Wood Processing Industry	Timber Development Association (London)		9	1959
	Élecktrosvyaz	Telecommunications	Massachusetts Institute of Technology*		1	1957
Éntom(ol). oboz(renie)	Éntomologicheskoe obozrenie	Entomological Review	American Institute of Biological Sciences	38	1	1959
Farmakol. (i) toksikol(ogiya)	Farmakologiya i toksikologiya	Pharmacology and Toxicology	Consultants Bureau	20	1	1957
FMM	Fizika metallov i metallovedenie	Physics of Metals and Metallography	Acta Metallurgica*	5	1	1957
Fiziol. zhurn. SSSR (im. Sechenova)	Fiziologicheskii zhurnal im. I. M. Sechenova	Sechenov Physiological Journal USSR	National Institutes of Health*		1	1957
Fiziol(ogiya) rast.	Fiziologiya rastenii	Plant Physiology	American Institute of Biological Sciences	4	1	1957
	Geokhimiya	Geochemistry	The Geochemical Society		1	1958
FTT	Fizika tverdogo tela	Soviet Physics–Solid State	American Institute of Physics	1	1	1959
Izmerit. tekh(nika)	Izmeritel'naya tekhnika	Measurement Techniques	Instrument Society of America		1	1959
Izv. AN SSSR, O(td). Kh(im). N(auk)	Izvestiya Akademii Nauk SSSR: Otdelenie khimicheskikh nauk	Bulletin of the Academy of Sciences of the USSR: Division of Chemical Sciences	Consultants Bureau		1	1952

continued

Izv. AN SSSR, O(td). T(ekhn). N(auk): Met(all). i top.	(see Met. i top.)					
Izv. AN SSSR Ser. fiz(ich).	Izvestiya Akademii Nauk SSSR: Seriya fizicheskaya	Bulletin of the Academy of Sciences of the USSR: Physical Series	Columbia Technical Translations		1	1954
Izv. AN SSSR Ser. geofiz.	Izvestiya Akademii Nauk SSSR: Seriya geofizicheskaya	Bulletin (Izvestiya) of the Academy of Sciences USSR: Geophysics Series	American Geophysical Union		1	1954
Izv. AN SSSR Ser. geol.	Izvestiya Akademii Nauk SSSR: Seriya geologicheskaya	Izvestiya of the Academy of Sciences of the USSR: Geologic Series	American Geological Institute		1	1958
Kauch. i rez.	Kauchuk i rezina	Soviet Rubber Technology	Research Association of British Rubber Manufacturers	18	1	1959
	Kinetika i kataliz	Kinetics and Catalysis	Consultants Bureau	1	3	1960
	Koks i khimiya	Coke and Chemistry USSR	Coal Tar Research Association (Leeds, England)		1	1958
Kolloidn. zh(urn).	Kolloidnyi zhurnal	Colloid Journal	Consultants Bureau	14	1	1952
	Kristallografiya	Soviet Physics – Crystallography	American Institute of Physics	2	1	1957
Metalov. i term. obrabot. metal.	Metallovedenie i termicheskaya obrabotka metallov	Metal Science and Heat Treatment of Metals	Acta Metallurgica	6	1	1958
	Metallurg	Metallurgist	Acta Metallurgica		1	1957
Met. i top.	Metallurgiya i topliva	Russian Metallurgy and Fuels	Eagle Technical Publications		1	1960
Mikrobiol.	Mikrobiologiya	Microbiology	American Institute of Biological Sciences	26	1	1957
OS	Optika i spektroskopiya	Optics and Spectroscopy	American Institute of Physics		6	1959
	Pochvovedenie	Soviet Soil Science	American Institute of Biological Sciences		1	1958
	Priborostroenie	Instrument Construction	British Scientific Instrument Research Association		1	1959
Pribory i tekhn. éks(perimenta)	Pribory i tekhnika éksperimenta	Instruments and Experimental Techniques	Instrument Society of America		1	1957
Prikl. matem. i mekh.	Prikladnaya matematika i mekhanika	Applied Mathematics and Mechanics	American Society of Mechanical Engineers		1	1958
PTÉ	(see Pribory i tekhn. éks.)					
	Problemy Severa	Problems of the North	National Research Council of Canada			
Radiotekh.	Radiotekhnika	Radio Engineering	Massachusetts Institute of Technology*	12	1	1957
Radiotekh. i élektronika	Radiotekhnika i élektronika	Radio Engineering and Electronics	Massachusetts Institute of Technology*	2	1	1957
	Stanki i instrument	Machines and Tooling	Production Engineering Research Assoc.		1	1959
	Stal'	Stal (In English)	Iron and Steel Institute		1	1959
Stek. i keram.	Steklo i keramika	Glass and Ceramics	Consultants Bureau	13	1	1956
Svaroch. proiz-vo	Svarochnoe proizvodstvo	Welding Production	British Welding Research Association		4	1959
Teor. veroyat. i prim.	Teoriya veroyatnostei i ee primenenie	Theory of Probability and Its Applications	Society for Industrial and Applied Mathematics		1	1956
Tsvet. Metally	Tsvetnye metally	Nonferrous Metals	Primary Sources		1	1960
UFN	Uspekhi fizicheskikh Nauk	Soviet Physics – Uspekhi (partial translation)	American Institute of Physics	66	1	1958
UKh	Uspekhi khimii	Russian Chemical Reviews	The Chemical Society (London)		1	1960
UMN	Uspekhi matematicheskikh nauk	Russian Mathematical Surveys	London Mathematical Society	15	1	1960
Usp. fiz. nauk	(see UFN)					
Usp. khim(ii)	(see UKh)					
Usp. matem. nauk	(see UMN)					
Usp. sovr. biol.	Uspekhi sovremennoi biologii	Russian Review of Biology	Oliver and Boyd		48	1959
Vest. mashinostroeniya	Vestnik mashinostroeniya	Russian Engineering Journal	Production Engineering Research Assoc.		4	1959
Vop. gem. i per. krovi	Voprosy gematologii i perelivaniya krovi	Problems of Hematology and Blood Transfusion	National Institutes of Health*		1	1957
Vop. onk.	Voprosy onkologii	Problems of Oncology	National Institutes of Health*		1	1957
Vop. virusol.	Voprosy virusologii	Problems of Virology	National Institutes of Health*		1	1957
Zav(odsk). lab(oratoriya)	Zavodskaya laboratoriya	Industrial Laboratory	Instrument Society of America	25	1	1959
ZhAKh Zh. anal(it). khimii	Zhurnal analiticheskoi khimii	Journal of Analytical Chemistry USSR	Consultants Bureau	7	1	1952
ZhETF Zh. éksperim. i teor. fiz.	Zhurnal éksperimental'noi i theoreticheskoi fiziki	Soviet Physics–JETP	American Institute of Physics	28	1	1955
ZhFKh Zh. fiz. khimii	Zhurnal fizicheskoi khimii	Russian Journal of Physical Chemistry	The Chemical Society (London)		7	1959
ZhMÉI Zh(urn). mikrobiol. épidemiol. i immunobiol.	Zhurnal mikrobiologii, épidemiologii i immunobiologii	Journal of Microbiology, Epidemiology and Immunobiology	National Institutes of Health*		1	1957
ZhNKh Zh(urn). neorgan(ich). khim(ii)	Zhurnal neorganicheskoi khimii	The Russian Journal of Inorganic Chemistry	The Chemical Society (London)		1	1959
ZhOKh Zh(urn). obshch(ei) khimii	Zhurnal obshchei khimii	Journal of General Chemistry USSR	Consultants Bureau	19	1	1949
ZhPKh Zh(urn). prikl. khimii	Zhurnal prikladnoi khimli	Journal of Applied Chemistry USSR	Consultants Bureau	23	1	1950
ZhSKh Zh(urn). strukt. khimii	Zhurnal strukturnoi khimii	Journal of Structural Chemistry	Consultants Bureau	1	1	1960
ZhTF Zh(urn). tekhn. fiz.	Zhurnal teknicheskoi fiziki	Soviet Physics–Technical Physics	American Institute of Physics	26	1	1956
Zh(urn). vyssh. nervn. deyat. (im. Pavlova)	Zhurnal vysshei nervnoi deyatel'nosti (im. I. P. Pavlova)	Pavlov Journal of Higher Nervous Activity	National Institutes of Health*		1	1958

*Sponsoring organization. Translation through 1960 issues is a publication of Pergamon Press.

A Milestone in Scientific Communication...

Advances in Cryogenic Engineering

VOLUME 1
VOLUME 2
VOLUME 3
VOLUME 4
VOLUME 5

Edited by K. D. Timmerhaus

These 5 volumes, the proceedings of the Cryogenic Engineering Conferences held since 1954, form the only authoritative collection on the research and development to date in this new and exciting field.

A working tool for industry!

ROCKETRY • MISSILES • LIQUEFACTION OF GASES • FREE RADICALS SPECTROSCOPY • ELECTRONICS • MINIATURIZATION • AIR SEPARATION • PURIFICATION • INSULATION • ATOMIC ENERGY are all vitally affected by the rapid research progress in low-temperature technology.

In order to meet the growing demand for more information about cryogenics, Plenum Press has reprinted Volumes 1-4 in new hard-cover editions and presents

(Special rate of $35 for first four volumes)

VOLUME 5
(Proceedings of the Fifth National Conference on Cryogenic Engineering, 1959)

Foreign price
Volumes 1-5 $15.00
Volumes 1-4 (set) $40.00

for the first time.

cloth **illustrated** **over 350 pages in each volume** **$13.50 per volume**

PLENUM PRESS 227 WEST 17TH STREET, NEW YORK 11, N. Y.

A subsidiary of Consultants Bureau Enterprises, Inc.

RESEARCH by Soviet EXPERTS

Translated by Western Scientists

SPECTRA AND ANALYSIS

by A. A. Kharkevich

The first handbook directed toward acousticians and others working in those fields which require the analysis of oscillations—ultrasonics, electronics, shock and vibration engineering. This volume is devoted to the analysis of *spectral concepts* as they are applied to oscillations in acoustics and electronic engineering, and to a discussion of the methods of spectral analysis. Contents include KOTEL'NIKOV'S theorem for bounded spectra, the spectra and analysis of random processes, and (in connection with the latter) the statistical compression of spectra.

cloth **236 pages** **$8.75**

ULTRASONICS AND ITS INDUSTRIAL APPLICATIONS

by O. I. Babikov

This work is concerned with ultrasonic control methods which are applied in industry, and also with the action of high-intensity ultrasonic oscillations on various technological processes. Considerable attention is devoted to ultrasonic pulse methods of flaw detection and physicochemical research. It is an invaluable aid to scientific researchers, engineers, and technicians working in fields which make use of ultrasonic methods industrially, as well as being a convenient reference for a broad category of readers who might wish to become acquainted with the current state of ultrasonic instrumentation.

cloth **265 pages** **$9.75**

Tables of contents upon request

CONSULTANTS BUREAU

227 West 17th Street • New York 11, N.Y. • U.S.A.